ON DYNAMIC REPRESENTATION OF SYNCHRONOUS GENERATOR-EXCITER SYSTEM AND STUDY OF STABILIZING EXCITATION CONTROLS

BY

SAROJ KANTI BISWAS

A THESIS

SUBMITTED TO THE DEPARTMENT OF ELECTRICAL ENGINEERING
IN PARTIAL FULFILMENT OF THE REQUIREMENTS FOR THE DEGREE
OF MASTER OF SCIENCE IN ENGINEERING (ELECTRICAL)

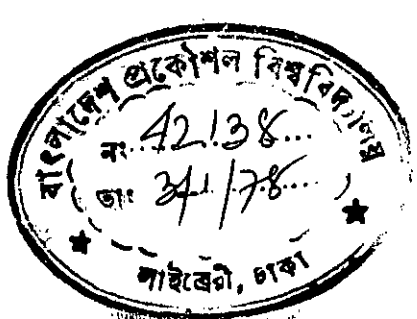

T.69

DEPARTMENT OF ELECTRICAL ENGINEERING
BANGLADESH UNIVERSITY OF ENGINEERING AND TECHNOLOGY
DACCA, BANGLADESH

DECEMBER, 1977.

C E R T I F I C A T E

This is to certify that this work has done by me and it has not been submitted elsewhere for the award of any degree or diploma.

Countersigned

A.H.M. Abdur Rahim

(Supervisor)

Signature of the Candidate

Saroj Kanti Biswas

Accepted as satisfactory for partial fulfilment of the requirements for the degree of M.Sc. Engg. in Electrical Engineering.

EXAMINERS

(i) A.H.M. Abdur Rahim

(Dr. A.H.M. Abdur Rahim)
Supervisor

(ii) _____

(Dr. A.B.M. Amanul Islam Chowdhury)
External Examiner

(iii) _____

(Dr. A.M. Zahoorul Huq)
Member

Dated-
2.12.77

(iv) _____

(Dr. Syed Fazle Rahman)
Member

ACKNOWLEDGEMENT

The author expresses his indebtness and deep sense of gratitude to Dr. A H.M. Abdur Rahim Associate Professor of Electrical Engineering, Bangladesh University of Engineering and Technology, for his valuable guidance, constant encouragement and numerous suggestions throughout the course of this work.

The author also wishes to express his sincere gratitude and thanks to Prof. A.M. Zahoorul Huq, Head of the Department of Electrical Engineering, Bangladesh University of Engineering and Technology for his scholarly advice and for rendering all possible help.

Thanks are due to the authority and members of the staff of the Computer Division, Bureau of Statistics, Govt. of the Peoples' Republic of Bangladesh, for their co-operation in using the Computer.

The author also wishes to thank the members of the teaching staff of the Department of Electrical Engineering for their kind help and suggestions.

ABSTRACT

A dynamic model of a synchronous generator infinite bus system with a solid state exciter system has been developed. To get an accurate machine representation precision measurement of different synchronous machine parameters have been attempted. The transfer function of the different blocks of the exciter viz. adding, rectifing, sensing circuits, comparators, inverters etc. has been determined.

A d.c. inductance bridge is used for measurement of machine inductances which eliminates possible errors in common a.c.bridge measurement. The inertia constant of the machine is measured by an all electric method — by retardation test rather than the usual dynamometer method of measurement. A comparative study of the different per unit systems has been made and the "unit voltage base" system is found to be relatively simple and easy from application viewpoint.

The single machine infinite bus system has been simulated on a digital computer and tested for different types of faults on it, both with and without additional stabilizing signals. Signals derived from different system states are fed to the exciter in addition to the normal voltage regulator action. It is observed that signals derived from field current and torque angle deviations control the transients effectively when applied in combination with rotor velocity deviation signal. With rotor velocity signal alone, the results obtained are in agreement with those obtained experimentally.

The effect of variation of different parameters of the exciter on power system stability are also investigated.

CONTENTS

LIST OF FIGURES

NOTATIONS

D	Damping coefficient
E_{fd}	Generator open circuit voltage
E_o	Operating value of E_{fd}
e_a, e_b, e_c	Generator phase voltage rms.
e_{ao}	Peak value of rated stator phase voltage
e_d, e_q	stator d and q axes voltages respectively
e_t	Generator terminal voltage
e_{tr}	Reference terminal voltage
f	Frequency
i_a, i_b, i_c	Generator phase currents
I_{ao}	Peak value of rated stator phase current
i_d, i_q	Stator currents in d and q axes respectively
i_{fd}	Per unit field current
I_{fdo}	Base value of field current
J	Moment of inertia of rotor mass
K_r	Regulator Gain
L_{ao}	Base inductance (stator)
L_{afd}	Stator field mutual inductance (direct axis)
L_{ffd}	Field coil self inductance
L_d, L_q	Stator d and q axes inductances respectively
L_e	Equivalent inductance from machine terminal to infinite bus.
L_{df}	Mutual inductance between field and damper winding
M	Generator inertia constant
n	Speed deviation
T_r	Regulator time constant, sec.

P_{in}	Net power input
P_o	Power output
Q_o	Reactive power output
R_{fd}	Field winding resistance
r_{fd}	per unit field resistance
R_a	Armature resistance per phase
r_a	Per unit armature resistance
r_e	Equivalent resistance from machine terminal to infinite bus
T_{in}	Net torque input
T_g	Air gap torque of generator
T_m	Inertia constant (2H) seconds
$u_s(t)$	Stabilizing signal
V	Bus bar voltage
V_d, V_q	Bus bar voltage in d and q axes respectively
V_{fd}	Applied field voltage
x_{afd}	Per unit stator field direct axis reactance
x_d, x_q	Per unit stator reactance in d and q axes respectively
x_{ffd}	Per unit reactance of field coil
X_{ao}	Base reactance (stator)
x_e	Equivalent reactance from machine terminal to infinite bus in per unit.
∂	Torque Angle
ω	Angular velocity rad/sec.
ω_o	Base angular velocity
Ψ_d, Ψ_q	Stator flux linkages in d and q axes respectively
Ψ_{fd}	Field coil flux linkage
Ψ_a, Ψ_b, Ψ_c	Flux linkage of stator phases

CHAPTER 1

INTRODUCTION

1.1 Representation of a Synchronous Generator in a Power System

Modern power systems are highly complex with large number of interconnected synchronous generators. This interconnection although ensures reliability of electric power supply, raises a serious problem that transient disturbances may propagate from any part of the system to the rest of the network resulting in loss of synchronism of some or all of the machines in absence of adequate safeguard. For reliability of power supply, the power system must be stable under both transient and steady state conditions of which transient stability is of major importance. Detailed and precision study of transient stability of the system needs complete and correct system representations which again requires an accurate mathematical model of the dynamic behavior of the synchronous machines. Moreover, in recent times some kind of control, mainly in the exciation system, are applied to increase the transient stability limit. To determine the effective control signals which may be applied, an accurate system representation is essential.

The conventional methods of system representation exclude the rotor circuits of the synchronous machines and obviously the results do not represent the exact characteristics. Modern trend is to include all the rotor circuits, including the damper winding and any other circuits on the rotor (if present),

in the system representation. Instead of representing the synchronous machine as simply a voltage behind transient reactance as in the conventional analysis, it is looked upon as a coupled assemblage of coils — three on the stator and two or more on the rotor.

The dynamics of a synchronous generator equipped with voltage regulator can be derived from the Park's equations[1,2,3], generator swing equation etc. and can be represented by a set of first order nonlinear differential equations:

$$\dot{\underline{X}} = \underline{f}[\underline{X}, u] \quad .... \quad (1.1)$$

The state vector $\underline{X}$ comprises of different flux linkages or currents, rotor angular position, velocity etc. and u is the excitation voltage. The vector function $\underline{f}$ depends, among other things, on the different parameters like resistance and inductances of rotor and stator circuits, machine inertia etc., all of them except the inertia constant being measured at the machine terminals when stationary. The accuracy of system representation will depend on the accuracy of measurement of different parameters.

Measurement of these parameters should be done under condition which are close to the actual system conditions in normal operation. Different types of bridge circuits which employ a.c. signals are available for measurement of inductances-both self and mutual. But the actual operating conditions of the machine can not be simulated in the a.c. bridge

methods. Another major problem in a.c. bridge methods is with the measurements in the short circuited damper winding which is physically inaccessable but acts as a short circuited secondary of a transformer. This causes appreciable error in the measured stator and rotor parameters also. But the damper windings are known to improve stability and so, for simplicity, it is often excluded in stability studies.

Power system computations are usually done in per unit rather than in actual volts, ohms etc. due to inherent advantages of per unit system. But unfortunately, like static system such as transformer there is no unique[4] system to convert the actual parameters of synchronous machine, mainly the rotor circuit quantities into per unit quantities. This is due to the fact that the "turns ratio" as commonly used in the case of transformers has no unique definition in the case of rotating machines. For simplicity and ease of computation, a suitable system of conversion should be selected.

1.2 Power System Stability and Methods to Improve Stability

Power system stability, as defined by Kimbark[1], is a term applied to alternating current electric power systems, denoting a condition in which the various synchronous machines of the system remain in synchronism or 'in step' with each other. Conversely, instability denotes a condition involving loss of synchronism or falling 'out of step'. Depending on the magnitude and type of disturbances, power system stability

may be classified into three types. These are described below:

Steady state stability is the ability of the power system to maintain power transfer over the system without loss of stability or synchronism when the magnitude of power transfer is changed gradually. It is assumed that the increase in power output occurs slowly enough to allow the regulating devices to respond with their steady state characteristics.

Transient stability is the ability of power system to maintain stability for a sudden large impact on the system. It is assumed that the regulating devices do not have time to function during the transient period.

For a machine with a continuously acting voltage regulator and governor, negative feedback is introduced so that the power and voltage differences which may cause machine instability are constantly monitored and corrected. In this way, the load can be increased beyond the ordinary steady state limit to a new power limit, called the dynamic stability limit. The dynamic stability limit depends primarily on the parameters of voltage regulator and governor.

The swing equation which governs the mechanical oscillation of synchronous machine can be written as

$$M \frac{d^2\delta}{dt^2} + D \frac{d\delta}{dt} = P_{in} - P_o \quad \ldots \quad (1.2)$$

where the output power P_o is a function of machine internal voltage and hence the excitation voltage and also transfer impedance between the machine and the receiving bus. The right handside of equation (1.2) represents the accelerating power

P_a. At steady state P_a must be zero while the rotor angle and machine currents are constant. The known methods of controlling the accelerating power P_a are changing the transfer admittance, controlling the mechanical input which is not very effective and controlling the field excitation of the synchronous generator. The last approach of stabilization will be considered in detail.

1.3 Historical Development of Excitation Control

The history of excitation control of synchronous machines dates back to 1924 when a group of engineers published a paper stating that excitation control is one of the ways to improve stability. Upto 1948 excitation was mostly provided by shaft coupled d.c. machine with an electromechanical device to control its field excitation so as to keep the terminal voltage constant. Amplidyne rotating amplifiers with a gain of as high as 10^6 was introduced during this period. Though the performance of ignitron tube exciter, introduced during this period, was good, it was not used widely due to its higher capital and maintenance cost. Brushless exciter consisting of a.c. generator with rotating armature and silicon rectifiers were used in small installations in the fifties. All these exciters had the drawback of low ceiling voltage (1.3 - 1.5 p.u.) and slow speed of response (about 200 V/Sec) and were of limited effectiveness in improving the stability of power system.

In the sixties newly developed silicon controlled rectifiers were used to develop static exciters, operated from terminal voltage of the synchronous machine. These exciters were very fast in response, have high ceiling voltage (4-8 p.u.) and high rate of voltage rise (2000-3000 V/Sec). These high speed voltage regulators have two major effects[6,7]. The first is the increase in the restoring synchronizing forces by varying excitation in such a way as to reduce the rotor angle excursion, thus increasing transient stability. The second is the deterioration[8,9] of machine damping resulting in dynamic instability. In certain situations combined characteristics of of load, generator, exciter prime mover result in significantly reduced damping causing sustained oscillations that cease when the voltage regulator is switched to manual.

Fortunately, the excitation system can be used to increase damping rather than reduce it and this requires an additional stabilizing signal to the voltage regulator. The use of rotor velocity[7,10] and a "continuous judicious combination" of velocity and acceleration[11] has been suggested as the stabilizing signal. A signal derived from electric power output[12] of the machine has been used successfully to improve transient stability. Jones[13] and Smith[14] considered the problem of transient removal with bang bang excitation control. A quasi-optimal excitation scheme is also searched[15] for "online" excitation control for power system stabilization.

1.4 Scope of Thesis

In a previous study[16], the performance of a solid state excitation scheme for stabilization of a single machine infinite bus system was studied. The introduction of high gain exciter with the synchronous generator reduces the effective damping of the system, requiring additional stabilizing signals. Because of limited facilities, only feedback signal derived from rotor velocity of the generator was employed for stabilization. Evaluation of the scheme with other stabilizing signals need a correct and precise determination of the synchronous generator - excitation system dynamics.

To determine the dynamic model of the synchronous generator the different parameters of the synchronous generator such as resistances, inductances and inertia constants were measured as precisely as possible. The input output relations of the different blocks of the excitation scheme designed were determined and were incorporated with the machine equations to give the overall system dynamic equations (1.1). The system was then simulated on a digital computer and different types of stabilizing controls were investigated for a number of simulated faults on the single machine infinite bus system. It was observed that feedback signals derived from suitable combination of rotor velocity and torque angle was very effective in removing the power system transients.

CHAPTER 2

SYNCHRONOUS GENERATOR AND TRANSMISSION SYSTEM MODEL

In this chapter the voltage and flux linkage relations of a synchronous generator derived from Park's equations are given in a state space form. The various machine quantities are expressed in terms of per unit stator quantities by a suitable "turns ratio" discussed later. The generator swing equations and flux linkage relations are then combined with the transmission line equations to arrive at the dynamic model of the synchronous generator infinite bus system. This in addition to the excitation system model developed in next chapter gives the complete system model.

2.1 Synchronous Generator Voltage and Flux Relations

An apprach to the analysis of electrical machines is to regard every machine as a coupled assemblage of coils, some of which are in relative motion. In this coupled circuit apprach, the three phase synchronous machine is represented by three stator coils, the field coil and the amortisseur windings. The formulation of the machine equations for the prediction of its performance characteristics under any condition of operation requires the determination of its parameters. These parameters are determined either by solving the electromagnetic field problems of the machine by using Maxwell's equations or from various measurements at the machine terminals.

The most basic equations for a synchronous machine are the differential equations for the stator phases and rotor coils relating voltages, currents and fluxes. But unfortunately these equations contain parameters which depend

on rotor position and solution of the equations poses a great problem. The use of Park's transformation eliminates much of the difficulty and the set of equations can be replaced by another set of time invariant relations.

In the Park's transformation all the armature currents, voltages and flux linkages are resolved onto a two axis reference frame which rotate in synchronism with the rotor. They are commonly known as direct axis and quadrature axis, the former being along the pole axis and the later at 90^{o} out of phase from the former. The relationship between the d and q axes and the phase axes are shown in Fig. 2.1.

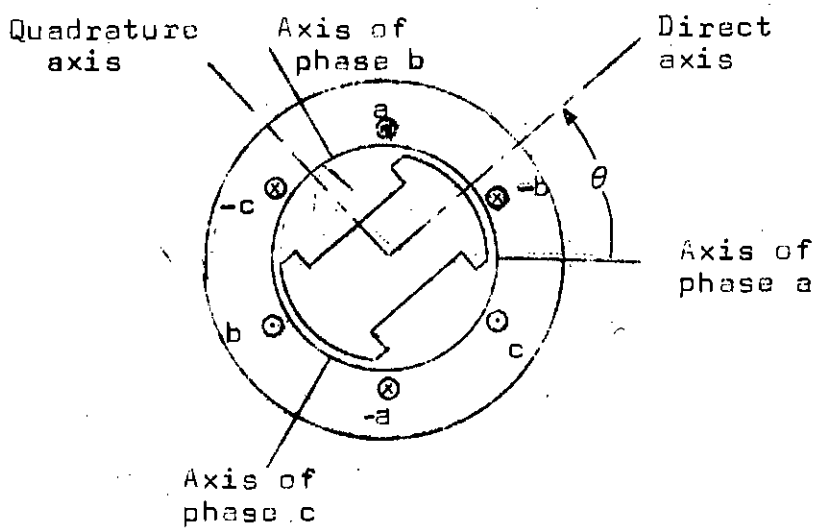

Fig. 2.1 Idealized Synchronous Machine.

The Park's transformations and the inverse relations are

$$\begin{bmatrix} K_d \\ K_q \\ K_o \end{bmatrix} = \frac{2}{3} \begin{bmatrix} \text{Cos } \theta & \text{Cos } (\theta - 120) & \text{Cos } (\theta + 120) \\ -\text{Sin } \theta & -\text{Sin } (\theta - 120) & -\text{Sin } (\theta + 120) \\ \frac{1}{2} & \frac{1}{2} & \frac{1}{2} \end{bmatrix} \begin{bmatrix} K_a \\ K_b \\ K_c \end{bmatrix} \qquad (2.1)$$

$$\begin{bmatrix} K_a \\ K_b \\ K_c \end{bmatrix} = \begin{bmatrix} \text{Cos } \theta & -\text{Sin } \theta & 1 \\ \text{Cos } (\theta-120) & -\text{Sin}(\theta-120) & 1 \\ \text{Cos}(\theta+120) & -\text{Sin}(\theta+120) & 1 \end{bmatrix} \begin{bmatrix} K_d \\ K_q \\ K_o \end{bmatrix}$$

where K symbolizes currents, voltage or flux linkages. The subscripts abc denote phase quantities and dqo denotes direct axis, quadrature axis quantities and zero sequence components. For the purpose of developing a mathematical model of the synchronous machine the following assumptions are made [2,3] :

1) The distributed windings may be adequately represented by lumped windings.

2) All self and mutual inductances may be represented as constants plus a simple sine variation of rotor angle of θ or 2θ as shown below:

Rotor field self inductance $\quad \mathcal{L}_{ff} = L_{ffd}$

Stator field mutual inductance $\quad \mathcal{L}_{af} = L_{afd} \text{ Cos } \theta$

$$\mathcal{L}_{bf} = L_{afd} \text{ Cos}(\theta-120)$$

$$\mathcal{L}_{cf} = L_{afd} \text{ Cos}(\theta+120)$$

Self inductance of stator phases

$$\mathcal{L}_{aa} = L_{aao} + L_{g2} \text{ Cos } 2\theta$$

$$\mathcal{L}_{bb} = L_{aao} + L_{g2} \text{ Cos } (2\theta+120)$$

$$\mathcal{L}_{cc} = L_{aao} + L_{g2} \text{ Cos}(2\theta-120)$$

where $L_{aao} = L_{al} + L_{go}$

Mutual inductance between stator phases

$$\mathcal{L}_{ab} = -.5L_{go} + L_{g2}\ \text{Cos}\ (2\theta-120)$$
$$\mathcal{L}_{bc} = -.5L_{go} + L_{g2}\ \text{Cos}\ 2\theta$$
$$\mathcal{L}_{ca} = -.5L_{go} + L_{g2}\ \text{Cos}\ (2\theta+120)$$

3) Magnetic saturation and hysteresis are neglected.

4) The amortissieur winding and all other rotor circuits are neglected for simplicity.

The starting point of the analysis is the set of flux linkage and voltage equations for the set of stator and rotor windings of the idealized synchronous generator:

$$\begin{bmatrix}\Psi_a\\ \Psi_b\\ \Psi_c\\ \Psi_{fd}\end{bmatrix} = \begin{bmatrix}\mathcal{L}_{aa} & \mathcal{L}_{ab} & \mathcal{L}_{ac} & \mathcal{L}_{af}\\ \mathcal{L}_{ba} & \mathcal{L}_{bb} & \mathcal{L}_{bc} & \mathcal{L}_{bf}\\ \mathcal{L}_{ca} & \mathcal{L}_{cb} & \mathcal{L}_{cc} & \mathcal{L}_{cf}\\ \mathcal{L}_{fa} & \mathcal{L}_{fb} & \mathcal{L}_{fc} & \mathcal{L}_{ff}\end{bmatrix} \begin{bmatrix}-i_a\\ -i_b\\ -i_c\\ i_{fd}\end{bmatrix} \quad ..(2.2)$$

$$\begin{bmatrix}e_a\\ e_b\\ e_c\end{bmatrix} = p\begin{bmatrix}\Psi_a\\ \Psi_b\\ \Psi_c\end{bmatrix} - R_a\begin{bmatrix}i_a\\ i_b\\ i_c\end{bmatrix} \quad \ldots \quad (2.3)$$

$$V_{fd} = p\Psi_{fd} + R_{fd}\, i_{fd}$$

where e's represent terminal voltages and i's are currents flowing out of the generates. Applying Park's transformation these equations can be reduced to:

$$\Psi_{fd} = L_{ffd} i_{fd} - \frac{3}{2} L_{afd} i_d$$

$$\Psi_d = L_{afd} i_{fd} - L_d i_d \qquad \ldots \qquad (2.4)$$

$$\Psi_q = - L_q i_q$$

$$\Psi_o = - L_o i_o$$

$$V_{fd} = R_{fd} i_{fd} + p \Psi_{fd}$$

$$e_d = - R_a i_d + p \Psi_d - \omega \Psi_q \qquad \ldots \qquad (2.5)$$

$$e_q = - R_a i_q + p \Psi_q + \omega \Psi_d$$

$$e_o = - R_a i_o + p \Psi_o$$

where $L_d = L_{al} + \frac{3}{2} (L_{go} + L_{g2})$

$$L_q = L_{al} + \frac{3}{2} (L_{go} - L_{g2})$$

$$L_o = L_{al}$$

L_d and L_q are called the direct and quadrature axis synchronous inductances respectively and L_{al} is the leakage inductance.

The excitation voltage of the synchronous generator is given by[2]:

$$E_{fd} = \frac{X_{afd}}{R_{fd}} \Psi_{fd} \qquad \ldots \qquad (2.6)$$

Equations (2.4), (2.5) and (2.6) give the current, voltage and flux linkage relations of a synchronous machine completely under any conditions of operation. However for balanced three phase operation, zero sequence terms will be zero.

2.2 Per Unit System

In power system analysis, general practice is to express different variables in per unit rather than in actual volts, ohms etc. In conventional analysis with interconnected transmission networks, transformers etc. per unit quantities of the whole system are referred to one side of transformer. In modern analysis, since the synchronous machine is considered as a coupled assemblage of coils, rotor circuits come into consideration. Obviously the rotor circuit quantities should be referred to the stator side and then expressed in per unit. It is also possible to refer the stator quantities to the rotor side. But with interconnected machines, two stage transfer will be necessary to refer some of the system parameters to the rotor side of a particular machine. Furthermore, in case of machines with more than one rotor circuits, referring the quantities to rotor field coil will be very complicated. In view of all these difficulties, it is preferred to refer all the rotor quantities to stator side.

Conversion of stator quantities to per unit poses no problem at all. The stator currents, voltages, inductances etc. are just divided by base value — generally the name plate value of the machine. The peak values of currents, voltages are usually selected as base. This is due to the reason that under balanced operation the direct and quadrature axis armature currents are proportional to peak armature current as

$$i_d = I \cos \alpha$$

$$i_q = I \sin \alpha \qquad \ldots \qquad (2.7)$$

where I is the peak armature current; α is the phase angle of armature current with respect to time axis.

To refer the rotor circuit quantities to the stator side a suitable "turns ratio" is required by which rotor quantities must be multiplied. But unfortunately there is no unique value of this turns ratio. For instance, one may define turns ratio as the ratio of number of turns per stator phase to number of turns per field pole. A second definition may be given as the ratio of effective turns per stator phase, considering the pitch factor, distribution factor etc. to number of turns per field pole. Other definition of turns ratio could be the ratio with mathematical turns per field pole for fundamental component of stator flux etc. In fact various authors have advocated for various turns ratios for synchronous machine. It is not surprising, therefore, that the published formulae for referring rotor quantities to stator and the corresponding values are not in accord since they use different turns ratios. However the per unit quantities of a machine are consistent for a particular analysis.

The mutual reactance is defined[2] as the voltage induced in each stator phase per unit field current or in otherwords:

$$E_{fd} = X_{afd} I_{fd} \qquad \ldots \qquad (2.8)$$

Since normal stator voltage is universally taken as unity, the product $X_{afd}\ I_{fd}$ must be unity at normal open circuit air gap line voltage. Therefore, it is evident that once the turns ratio is selected, the base rotor current cannot be selected arbitrarily. But it is preferable to select the unit field current first, since an arbitrary selection of turns ratio may yield a unit field current which is inconsistent with actual field current at normal open circuit operation. Once the unit field current is defined, the ratio of this current with proper stator current will give the required turns ratio. The term "current ratio" which is defined later is physically more meaningful and will be used in the following discussions instead of "turns ratio".

With the selection of base current ratio, the next thing to do is to convert the actual rotor quantities to per unit values. The flux linkage and voltage equations for the synchronous generator as deduced in previous section are

$$\begin{aligned} \psi_{fd} &= L_{ffd}\, i_{fd} - \tfrac{3}{2} L_{afd}\, i_d \\ \psi_d &= L_{afd}\, i_{fd} - L_d\, i_d \qquad \ldots \qquad (2.4) \\ \psi_q &= - L_q\, i_q \end{aligned}$$

$$\begin{aligned} v_{fd} &= R_{fd}\, i_{fd} + p\,\psi_{fd} \\ e_d &= -R_a\, i_d + p\,\psi_d - \omega\,\psi_q \qquad \ldots \qquad (2.5) \\ e_q &= - R_a\, i_q + p\,\psi_q + \omega\,\psi_d \end{aligned}$$

The direct and quadrature axes fluxes may be thought of as fluxes which, although rotate with rotor at synchronous speed, are centered over d and q axes respectively. This suggests that the d and q axis circuits could be represented by some sort of static equivalent circuit. But an essential condition for the existance of static equivalent circuit, is the reciprocity of mutual inductance coefficient and this is not satisfied by equation (2.4). For reciprocity of mutual inductance coefficient the currents, inductances etc. are defined in the following way:

$$
\begin{aligned}
L'_{afd} &= \frac{3}{2} L_{afd} \\
R'_{fd} &= \frac{3}{2} R_{fd} \qquad \ldots \qquad (2.9) \\
L'_{ffd} &= \frac{3}{2} L_{ffd} \\
i'_{fd} &= \frac{2}{3} i_{fd}
\end{aligned}
$$

These newly defined coefficients are used for per unit conversion. The formulae for the per unit conversion are given below [4]:

$$
\begin{aligned}
x_d &= \frac{L_d}{L_{ao}} \\
x_q &= \frac{L_q}{L_{ao}} \\
x_{afd} &= \frac{3}{2} \frac{L_{afd}}{L_{ao}} \left[\frac{I_{fdo}}{\frac{3}{2} i_{ao}} \right] \\
x_{ffd} &= \frac{3}{2} \frac{L_{ffd}}{L_{ao}} \left[\frac{I_{fdo}}{\frac{3}{2} i_{ao}} \right]^2 \qquad \ldots \qquad (2.10) \\
r_{fd} &= \frac{3}{2} \frac{R_{fd}}{X_{ao}} \left[\frac{I_{fdo}}{\frac{3}{2} i_{ao}} \right]^2
\end{aligned}
$$

$$r_a = \frac{R_a}{X_{ao}}$$

$$v_{fd} = \frac{V_{fd}}{e_{ao}} \qquad \left[\frac{I_{fdo}}{\frac{3}{2} i_{ao}} \right]$$

$$\text{Base current ratio} = \frac{I_{fdo}}{\frac{3}{2} i_{ao}}$$

Similarly per unit conversion formulae can be written for other rotor circuits also.

The selection of the rotor base current is a major problem. However it is clear from (2.10) that no unique value of base current ratio is demanded by the general per unit system. Most commonly used methods of defining the base rotor current and hence the base current ratio are[5]

1. X_{ad} base system: The base field current is that current which will induce in each stator phase a peak voltage equal to $x_{ad}\, i_{ao}$.
2. Unit voltage base system: The base field current is the current required to induce normal, open circuit, airgap line stator voltage.
3. Magnetomotive force base system: The base field current will give a magnetomotive force per pole equal to the flat topped armature reaction at normal stator current.
4. Equal mutual base system: The base rotor currents are defined so that the mutual impedances for a machine with one additional rotor circuit are all equal.

Each system has its own advantage. The X_{ad} base system makes all the mutual inductance terms to be numerically equal to X_{ad}. However, determination of base current ratio requires the determination of X_{ad}. In the mmf method the current ratio may be calculated from number of turns per field pole and stator phase, pitch factor, distribution factor etc. which require some design data of the machine. In equal mutual method all the mutual inductances are equal and the base current ratio may be calculated from design data. The unit voltage base system is the simplest one in which the base field current may easily be determined from machine open circuit characteristics. Another major advantage of unit voltage system is that the stator rotor mutual inductance coefficients are unity for field circuit and other rotor circuits. The unit voltage base system will be used in this study.

To express the machine equations in per unit system, time and rotor angle must also be expressed in p.u. The base time t_o is defined as

$$t_o = \frac{1}{\omega_o} \qquad \ldots \qquad (2.11)$$

which is the time required for the rotor to move one electrical radian at synchronous speed. The differential operator p ($\frac{d}{dt}$) is replaced by $\frac{p}{\omega_o}$ in per unit since

$$p_{p.u.} = \frac{d}{dt/t_o} = t_o \frac{d}{dt} = \frac{1}{\omega_o} \frac{d}{dt} = \frac{p}{\omega_o} \qquad .. \quad (2.12)$$

To express the rotor angle θ in p.u., base rotor angle is defined as

$$\theta_o = 1 \text{ rad.} = \omega_o t_o$$

Then any rotor angle $\theta' = \omega t + \partial$ in p.u. is

$$\theta_{p.u.} = \frac{\omega t + \partial}{\theta_o} = \frac{\omega t + \partial}{1} = \omega t + \partial \qquad (2.13)$$

which implies that rotor angle in p.u. is equal to the actual rotor angle.

2.3 Equations of Synchronous Generator Infinite Bus System

The mathematical relations of a simple power system — a synchronous generator feeding an infinite bus through a transmission line is developed in this section. The equation relating voltages and currents of the system is

$$\begin{bmatrix} e_a \\ e_b \\ e_c \end{bmatrix} = R_e \begin{bmatrix} i_a \\ i_b \\ i_c \end{bmatrix} + L_e p \begin{bmatrix} i_a \\ i_b \\ i_c \end{bmatrix} + \begin{bmatrix} V_a \\ V_b \\ V_c \end{bmatrix} \qquad (2.14)$$

where V's are bus voltages and R_e and L_e are transmission line resistance and inductances respectively. Using Park's transformation this equation can be reduced to

$$\begin{aligned} e_d &= R_e i_d + L_e p i_d - \omega L_e i_q + V_d \\ e_q &= R_e i_q + L_e p i_q + \omega L_e i_d + V_q \\ e_o &= r_o i_o + L_e p i_o + V_o \end{aligned} \qquad (2.15)$$

For symmetrical three phase operation the zero sequence terms will be zero. V_d and V_q are direct and quadrature axis bus voltages respectively where

$$V_d = V \text{ Sin } \delta$$
$$V_q = V \text{ Cos } \delta \qquad (2.16)$$

where δ is the torque angle - the angle between the rotor of the generator and infinite bus reference axis; the generator being ahead of infinite bus.

The power output of synchronous generator is given by

$$T_g = \frac{E_{fd}V}{(x_d+x_e)} \text{Sin } \delta + \frac{V^2(x_d-x_q)}{2(x_d+x_e)(x_q+x_e)} \text{ Sin } 2\delta \qquad (2.17)$$

The basic swing equation describing the mechanical oscillations of synchronous machine is

$$\frac{H}{\pi f} \quad \frac{d^2\delta}{dt^2} = T_{in} - T_g \qquad (2.18)$$

Defining the per unit speed deviation as

$$n = \frac{\omega - \omega_o}{\omega_o} \qquad (2.19)$$

equation (2.18) may be expressed as

$$p\delta = \omega_o n$$
$$pn = \frac{1}{T_m}\left[T_{in} - T_g\right] \qquad (2.20)$$

where $T_m = 2H$, is the inertia constant of the machine.

The voltage and flux linkage relations of the synchronous machine developed in section (2.1) and the transmission line equation (2.15) are expressed in the following normalized forms with the help of conversion formulae suggested in the previous section.

$$\begin{aligned} \Psi_{fd} &= x_{ffd} i_{fd} - x_{afd} i_d \\ \Psi_d &= x_{afd} i_{fd} - x_d i_d \\ \Psi_q &= - x_q i_q \end{aligned} \tag{2.21}$$

$$\begin{aligned} v_{fd} &= r_{fd} i_{fd} + \frac{1}{\omega_o} p \Psi_{fd} \\ e_d &= - \frac{\omega}{\omega_o} \Psi_q - r_a i_d + \frac{1}{\omega_o} p \Psi_d \\ e_q &= \frac{\omega}{\omega_o} \Psi_d - r_a i_q + \frac{1}{\omega_o} p \Psi_q \end{aligned} \tag{2.22}$$

$$\begin{aligned} e_d &= r_e i_d - \frac{\omega}{\omega_o} x_e i_q + \frac{x_e}{\omega_o} p i_d + V \sin \delta \\ e_q &= r_e i_q + \frac{\omega}{\omega_o} x_e i_d + \frac{x_e}{\omega_o} p i_q + V \cos \delta \end{aligned} \tag{2.23}$$

$$e_t = \sqrt{e_d^2 + e_q^2}$$

$$E_{fd} = \frac{x_{afd}}{r_{fd}} v_{fd}$$

Expressing field voltage v_{fd} in terms of excitation voltage E_{fd} and substituting the flux linkages of equation (2.21) to voltage equations (2.22) and equating with (2.23) the following equations can be obtained:

$$p\Psi_{fd} = E_{fd}\frac{\omega_o r_{fd}}{x_{afd}} - \omega_o r_{fd} i_{fd}$$

$$p\Psi_d = \omega_o\left[\frac{x_e}{\omega_o} pi_d + r_e i_d - \frac{\omega}{\omega_o} x_e i_q + V \sin\delta\right]$$

$$+\omega_o r_a i_d - \omega x_q i_q \qquad (2.24)$$

$$p\Psi_q = \omega_o\left[\frac{x_e}{o} pi_q + r_e i_q + \frac{\omega}{\omega_o} x_e i_d + V \cos\delta\right]$$

$$+\omega_o r_a i_q - \omega\left[x_{afd} i_{fd} - x_d i_d\right]$$

Differentiating equations (2.21)

$$p\Psi_{fd} = x_{ffd} pi_{fd} - x_{afd} pi_d$$

$$p\Psi_d = x_{afd} pi_{fd} - x_d pi_d \qquad (2.25)$$

$$p\Psi_q = - x_q pi_q$$

Equating the above two equations the derivatives of currents may be expressed in the following matrix form:

$$\begin{bmatrix} x_{ffd} - x_{afd} & 0 & 0 \\ x_{afd} - (x_d + x_e) & 0 & 0 \\ 0 & 0 & -(x_e + x_q) \end{bmatrix} \begin{bmatrix} pi_{fd} \\ pi_d \\ pi_q \end{bmatrix} = \begin{bmatrix} -\omega_o r_{fd} i_{fd} + E_{fd}\frac{\omega_o r_{fd}}{x_{afd}} \\ \omega_o(r_e + r_a) i_d - x_e i_q + \omega_o V \sin\delta - \omega x_q i_q \\ \omega_o(r_e + r_a) i_q + \omega x_e i_d + \omega_o V \cos\delta \\ + \omega x_d i_d - \omega x_{afd} i_{fd} \end{bmatrix} \qquad (2.26$$

Solving this equation for the derivatives of the currents and combining them with the swing equations (2.20) gives a set of 5 nonlinear first order differential equations for the single machine infinite bus system having no governor and exciter dynamics and in the absence of amortisseur windings:

$$\begin{bmatrix} pi_{fd} \\ pi_d \\ pi_q \\ pn \\ p\delta \end{bmatrix} = \begin{bmatrix} a_1 i_{fd} + a_2 i_d + a_3(1+n) i_q + a_4 \sin\delta + a_5 E_{fd} \\ a_6 i_{fd} + a_7 i_d + a_8(1+n) i_q + a_9 \sin\delta + a_{10} E_{fd} \\ a_{11}(1+n) i_{fd} + a_{12}(1+n) i_d + a_{13} i_q + a_{14} \cos\delta \\ a_{15} E_{fd} \sin\delta + a_{16} \sin 2\delta + a_{17} \\ a_{18} n \end{bmatrix} \qquad (2.27)$$

The direct and quadrature axis voltage equations are

$$e_d = a_{19} i_{fd} + a_{20} i_d + a_{21} i_q (1+n) + a_{22} E_{fd} + a_{23} \sin\delta$$

$$e_q = a_{24} i_{fd} (1+n) + a_{25} i_d (1+n) + a_{26} i_q + a_{27} \cos\delta \qquad (2.28)$$

where

$$a_1 = \frac{r_{fd}(x_d + x_e)}{\Delta d} \qquad a_2 = \frac{(r_e + r_a) x_{afd}}{\Delta d}$$

$$a_3 = \frac{-x_{afd}(x_e + x_q)}{\Delta d} \qquad a_4 = \frac{V x_{afd}}{\Delta d}$$

$$a_5 = \frac{- r_{fd}(x_d + x_e)}{x_{afd} \Delta d} \qquad a_6 = \frac{r_{fd} x_{afd}}{\Delta d}$$

$$a_7 = \frac{(r_e + r_a) x_{ffd}}{\Delta d} \qquad a_8 = \frac{- x_{ffd}(x_e + x_q)}{\Delta d}$$

$$a_9 = \frac{V\, x_{ffd}}{\Delta d} \qquad a_{10} = \frac{-\, r_{fd}}{\Delta d}$$

$$a_{11} = \frac{x_{afd}}{\Delta q} \qquad a_{12} = \frac{-\,(x_d + x_e)}{\Delta q}$$

$$a_{13} = \frac{-(r_e + r_a)}{\Delta q} \qquad a_{14} = \frac{-\, V}{\Delta q}$$

$$a_{15} = \frac{-\, V}{T_m (x_d + x_e)} \qquad a_{16} = \frac{-\, V^2 (x_d - x_q)}{2(x_d + x_e)(x_q + x_e) T_m}$$

$$a_{17} = \frac{T_{in}}{T_m} \qquad a_{18} = \omega_o$$

$$a_{19} = \frac{x_e r_{fd} x_{afd}}{\omega_o \Delta d} \qquad a_{20} = r_e + \frac{x_e x_{ffd} (r_e + r_a)}{\omega_o \Delta d}$$

$$a_{21} = -\, x_e - \frac{x_e x_{ffd} (x_e + x_q)}{\omega_o \Delta d} \qquad a_{22} = -\, \frac{x_e r_{fd}}{\omega_o \Delta d}$$

$$a_{23} = V + \frac{x_e\, x_{ffd} V}{\omega_o \Delta d} \qquad a_{24} = \frac{x_e\, x_{afd}}{\omega_o \Delta q}$$

$$a_{25} = x_e - \frac{x_e (x_d + x_e)}{\omega_o \Delta q} \qquad a_{26} = r_e - \frac{x_e (r_e + r_a)}{\omega_o \Delta q}$$

$$a_{27} = V - \frac{x_e\, V}{\omega_o \Delta q}$$

$$\Delta d = \frac{x_{afd}^2 - x_{ffd} (x_d + x_e)}{\omega_o}$$

$$\Delta q = \frac{(x_e + x_q)}{\omega_o}$$

CHAPTER 3

THE EXCITER MODEL

3.1 Introduction

An electronic exciter, designed and constructed in a previous study[16] is considered. The exciter comprises of sawtooth, adder, comparator, inverter circuits and a set of rectifiers. An analog computer was used to provide the operational amplifiers for the comparators and adders. A set of three controlled and three uncontrolled rectifiers rectify the three phase ac voltage obtained from a constant voltage source and feed the field of the generator. By changing the firing angles of the controlled rectifiers, the excitation voltage may be varied from nearly zero to maximum value. The firing angle of the SCR was controlled by a reference dc voltage and provision was kept for use of auxiliary signals. Two circuits, one for sensing and recording the change in terminal voltage and another for sensing the deviation in rotor velocity were constructed. Figure 3.1 shows the block diagram of the exciter and Fig. 3.2 shows the details of the excitation system. The input output relations of different blocks of the excitation system, namely the different sensing circuits, the SCR control circuits etc. are deduced. A simplified block diagram and transfer function is presented in the last section.

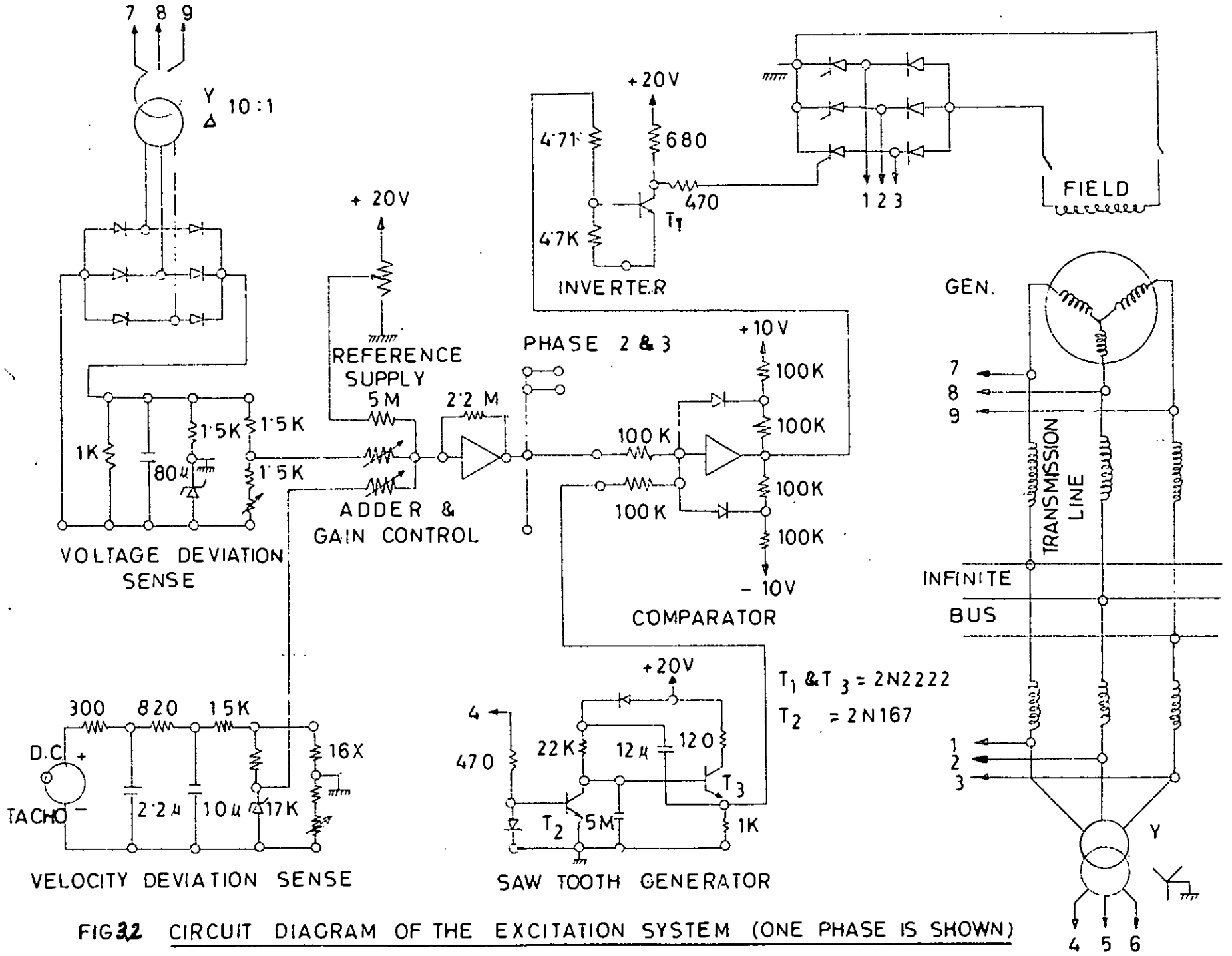

FIG 3.2 CIRCUIT DIAGRAM OF THE EXCITATION SYSTEM (ONE PHASE IS SHOWN)

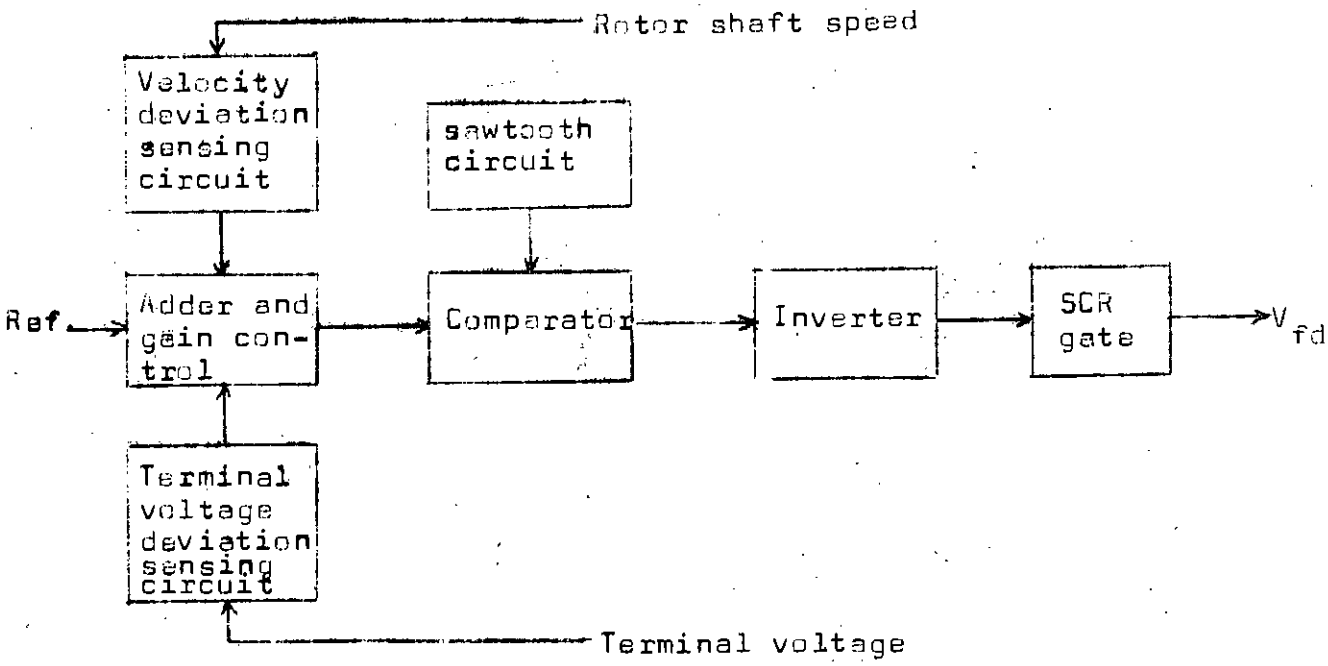

Fig.3.1 Block Diagram of Excitation System.

3.2 Voltage Deviation Sensing Circuit

The circuit for sensing the terminal voltage deviation of the generator consists of a step down transformer, a set of rectifiers and a bridge network. The d.c. voltage proportional to the terminal voltage is compared with a reference signal (from a Zener diode) and the bridge network is adjusted such that the output signal of the network is zero at steady state but whenever there is a change in terminal voltage a signal appears at the output. Fig. 3.3 shows the terminal voltage deviation sensing network.

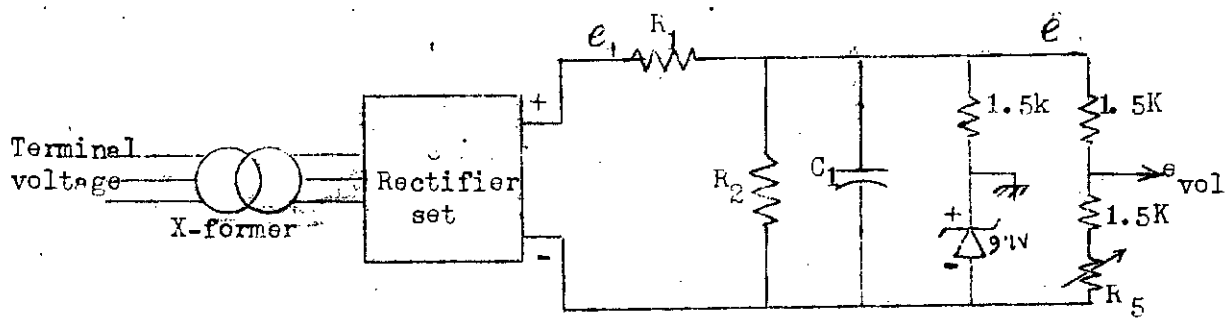

Fig. 3.3 Terminal Voltage Sensing Circuit.

In the circuit R_1 represents the diode forward resistance and the winding resistance of transformer. The voltage deviation signal is obtained at the terminal marked e_{vol}. The Zener diode operates in the breakdown region so that its voltage can be treated as a d.c. reference voltage. The output of the bridge network can be expressed as

$$e_{vol} = \frac{1.5 + R_5}{3.0 + R_5} e - 9.1 \qquad (3.1)$$

Defining percentage change of e as

$$e_{dev} = \frac{e - e_o}{e_o} \qquad (3.2)$$

where e_o is the steady state voltage across bridge, equation (3.1) becomes

$$e_{vol} = \frac{1.5 + R_5}{3.0 + R_5} e_o(1 + e_{dev}) - 9.1$$

R_5 is adjusted so that at steady state e_{vol} is zero. Therefore the steady state relation is

$$\frac{1.5 + R_5}{3.0 + R_5} e_o = 9.1$$

Hence at a changed voltage condition the output of the voltage deviation circuit is

$$e_{vol} = 9.1\ e_{dev} \qquad (3.3)$$

It is to be noted here that due to the presence of series resistance R_1 percentage change of e_1 is not equal to percentage change of e. In addition, due to the capacitor C_1 there will be a time lag. Considering the Zener diode as a d.c. voltage source the following node equation can be written in terms of Laplace operator S.

$$\frac{e - e_1}{R_1} + \frac{e}{R_2} + eCS + \frac{e - 9.1}{1500} + \frac{e}{3000+R_5} = 0 \qquad (3.4)$$

Substituting $e_{1dev} = \frac{e_1 - e_{10}}{e_{10}}$ it reduces to

$$e_o\ (1 + e_{dev}) = \frac{\left[0.006067 + e_{10}(1+e_{1dev})/R_1\right] R}{1 + RCS} \qquad (3.5)$$

where $\frac{1}{R} = \frac{1}{R_1} + \frac{1}{R_2} + \frac{1}{1500} + \frac{1}{3000+R_5}$

Equations for steady state and transient conditions can be obtained from equation (3.5) as:

$$e_o = \left[.006067 + \frac{e_{10}}{R_1}\right] R$$

$$e_{dev} = \frac{\left[1 + .006067 \times R/e_o\right] e_{1dev}}{1 + RCS}$$

Substituting the available data e_o = 17 volts, $R_1 = 120\,\Omega$ $R_2 = 1\ K\Omega$, $C_1 = 80\,\mu f$, $R_5 = 223\,\Omega$

$$e_{dev} = \frac{0.966\ e_{1dev}}{1 + 0.0077S} \qquad (3.6)$$

Since transformer winding resistance and diode resistance is included in R_1, percentage change of machine terminal voltage will be equal to percentage change of e_1. Therefore the output signal from the voltage deviation sensing circuit can be obtained by combining equations (3.3) and (3.6).

$$e_{vol} = \frac{8.8}{1+.0077S}\ V_{dev} \qquad (3.7)$$

where $V_{dev} = \frac{e_t - e_{tr}}{e_{tr}}$ is the percentage change of machine terminal voltage. Equation (3.7) may be expressed in another form, putting e_{tr} = .74 p.u., which was the voltage during the performance test(with the machine floating)

$$e_{vol} = -11.9 \left[e_{tr} - \frac{e_t}{1 + .0077S} \right] \qquad (3.8)$$

Experimental study shows that gain of the voltage sensing network is 9.2 and the time constant is about 12 m Sec. which are close to theoretical results.

3.3 Velocity Deviation Sensing Network

The circuit which senses the deviation in velocity consists of a d.c. tachogenerator which produces a constant voltage when the generator is running at synchronous speed. The output of the tachogenerator is compared with a reference voltage to produce zero output at steady state. The circuit diagram is shown in Fig. 3.4.

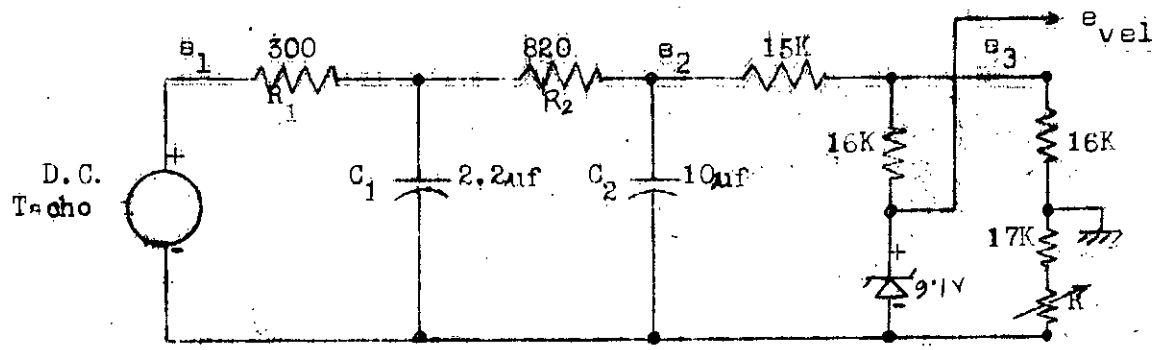

Fig. 3.4 Velocity Deviation Sensing Network.

The velocity deviation signal is obtained at the terminal marked e_{vel}.

$$e_{vel} = 9.1 - \frac{17 + R}{33 + R} e_3 \qquad (3.9)$$

Percentage deviation of voltage e_3 across the bridge is defined as

$$e_{3dev} = \frac{e_3 - e_{30}}{e_{30}}$$

where e_{30} is the voltage when the machine is running at steady state and e_3 is the voltage for any speed. Then equation (3.9) reduces to

$$e_{vel} = - 9.1\ e_{3dev} \qquad (3.10)$$

Substituting the experiemental values of e_{30} = 17.1 volts and R = 1.2 KΩ.

Due to the presence of large series resistance 15 K the percentage change of e_3 will not be equal to the percentage of e_2. But since the other two series resistance are small and also current through these resistance is also small (about 1 mA)

the percentage change of e_1 and percentage change of e_2 will be almost equal. In other words the loading effect can be neglected for the $R_1C_1R_2C_2$ lag network. Considering the Zener diode as a d.c. source the node equation can be written as

$$e_2 = e_3 + 15\left(\frac{e_3 - 9.1}{16} + \frac{e_3}{34.2}\right) \qquad (3.11)$$

$$= 2.3761\ e_3 - 8.53125$$

Substituting $e_{2dev} = \frac{e_2 - e_{20}}{e_{20}}$, the followings may be obtained

$$e_{20} = 2.3761\ e_{30} - 8.53125$$

$$e_{3dev} = \frac{e_{20}}{2.3761\ e_{30}}\ e_{2dev} = 0.788\ e_{2dev} \qquad (3.12)$$

The transfer function of the $R_1C_1R_2C_2$ lag network is

$$\frac{e_2}{e_1} = \frac{1}{R_1R_2C_1C_2S^2 + (R_1C_1+R_2C_2)S + 1}$$

$$\simeq \frac{1}{1 + 0.00886S} \qquad (3.13)$$

Therefore $e_{2dev} = \frac{e_{1dev}}{1 + .00886\ S}$ (3.14)

The voltage e_1 of the tachogenerator is proportional to speed N.

$$e_1 = KN$$

so that $e_{1dev} = n$ (3.15)

where e_{1dev} and n are percentage changes in e_1 and speed respectively. Combining equations (3.10), (3.12), (3.14) and

(3.15) the velocity deviation signal from the sensing network is

$$e_{vel} = \frac{-7.16\ n}{1 + .00886\ S} \qquad (3.16)$$

Experimental study gives a gain of -4.0 for the velocity sensing network. The time constant was not determined experimentally.

3.4 The SCR Exciter

A set of three SCRs and three uncontrolled rectifiers were arranged in a bridge circuit to rectify the three phase a.c. voltage obtained from a constant voltage source. The firing angle α of the SCR is controlled by a control circuit which is discussed in the next section. The d.c. voltage output of the bridge depends on the firing angle α of SCR. For $\alpha = 0$, each SCR conducts from 30° to 150° of the voltage wave. For the range of firing angle $0 < \alpha < 60^\circ$, the SCR starts conduction at $30 + \alpha$ and continues upto $150 + \alpha$. For α above 60° conduction starts at $30 + \alpha$ and continues upto 210°. The bridge rectifier and the rectified voltage wave are shown in Fig.3.5 and 3.6 respectively.

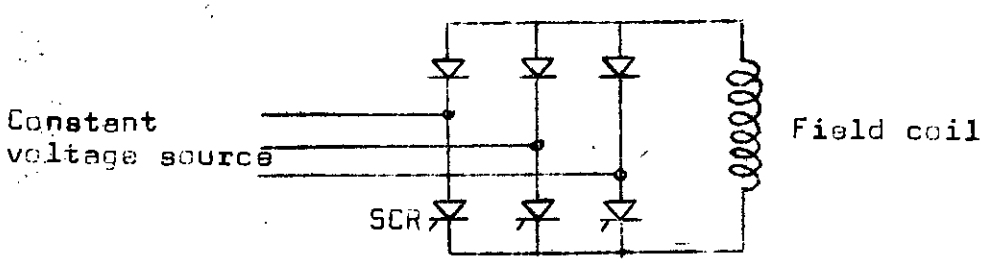

Fig. 3.5 Three Phase Bridge Rectifier.

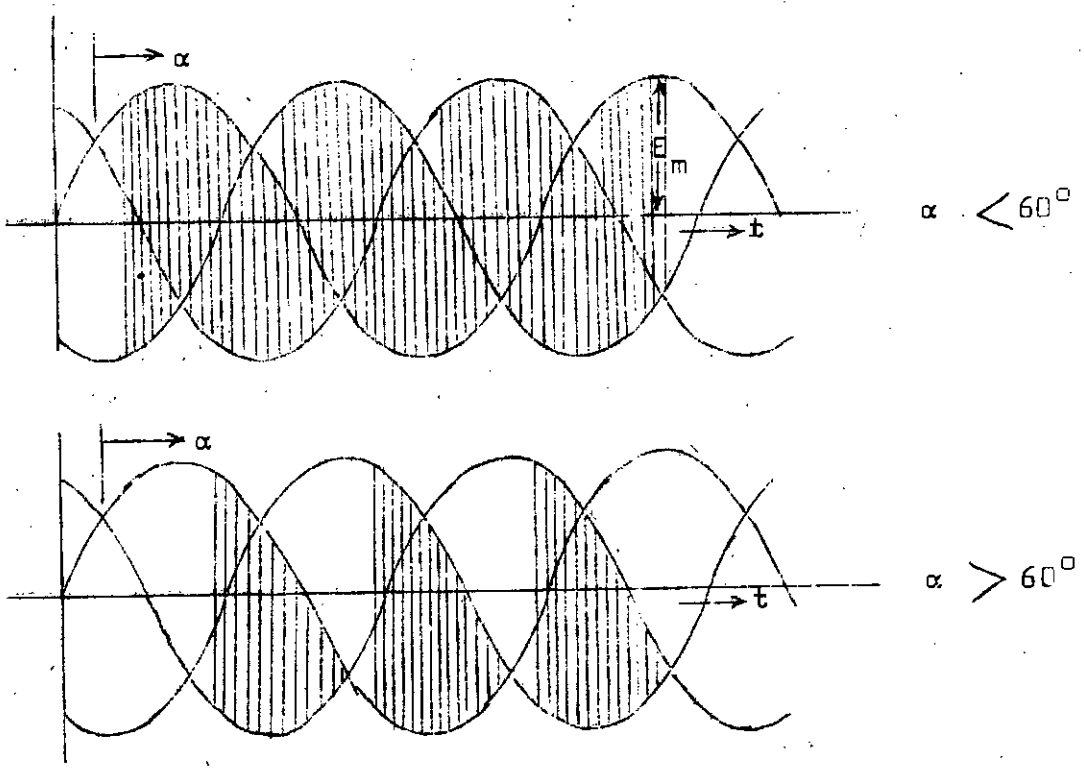

Fig. 3.6 Rectified Voltage of the Bridge Network.

The d.c. voltage of the bridge can be calculated from the Fig. 3.6. For α below 60°, the d.c. voltage is

$$E_{d.c} = \frac{3}{2\pi}\left[\int_{30+\alpha}^{90}\left[E_m \operatorname{Sin}\omega t - E_m \operatorname{Sin}(\omega t - 120)\right] d\omega t + \int_{90}^{150+\alpha}\left[E_m \operatorname{Sin}\omega t - E_m \operatorname{Sin}(\omega t - 240)\right] d\omega t\right]$$

$$= \frac{3E_L}{\sqrt{2}\,\pi}\,(1 + \operatorname{Cos}\alpha) \text{ volts} \qquad (3.17)$$

where E_L is the line to line a.c. voltage. For the firing angle α above 60°, the d.c. voltage is

$$E_{d.c} = \frac{1}{\pi - \alpha}\left[\int_{30+\alpha}^{210}\left[E_m \operatorname{Sin}\omega t - E_m \operatorname{Sin}(\omega t - 240)\right] d\omega t\right]$$

$$= \frac{\sqrt{2}\,E_L}{\pi - \alpha}\,(1 + \operatorname{Cos}\alpha) \text{ Volts} \qquad (3.18)$$

Expressing the field voltage V_{fd} in terms of excitation voltage E_{fd} $(=\frac{x_{afd}}{r_{fd}} v_{fd})$ and substituting the experimental values of x_{afd}, r_{fd} and E_L = 170 volts = .74 p.u.

$$\begin{aligned} E_{fd} &= 1.865\ (1 + \text{Cos}\ \alpha) && , \alpha < 60^{o} \\ &= 3.904(1+\text{Cos}\ \alpha)/(\pi - \alpha) && , \alpha > 60^{o} \end{aligned} \qquad (3.19)$$

where α is in radians and E_{fd} in p.u. Fig. 3.7 shows the SCR characteristics. The nonlinear SCR characteristics is linearized using least square curve fitting technique by a computer program which is given in appendix.

The equation of the linearized curve is

$$E_{fd} = 4.0929 - 1.1664\ \alpha$$

from which $$\Delta E_{fd} = - 1.1664 \Delta\alpha \qquad (3.20)$$

for small deviations about the operating point.

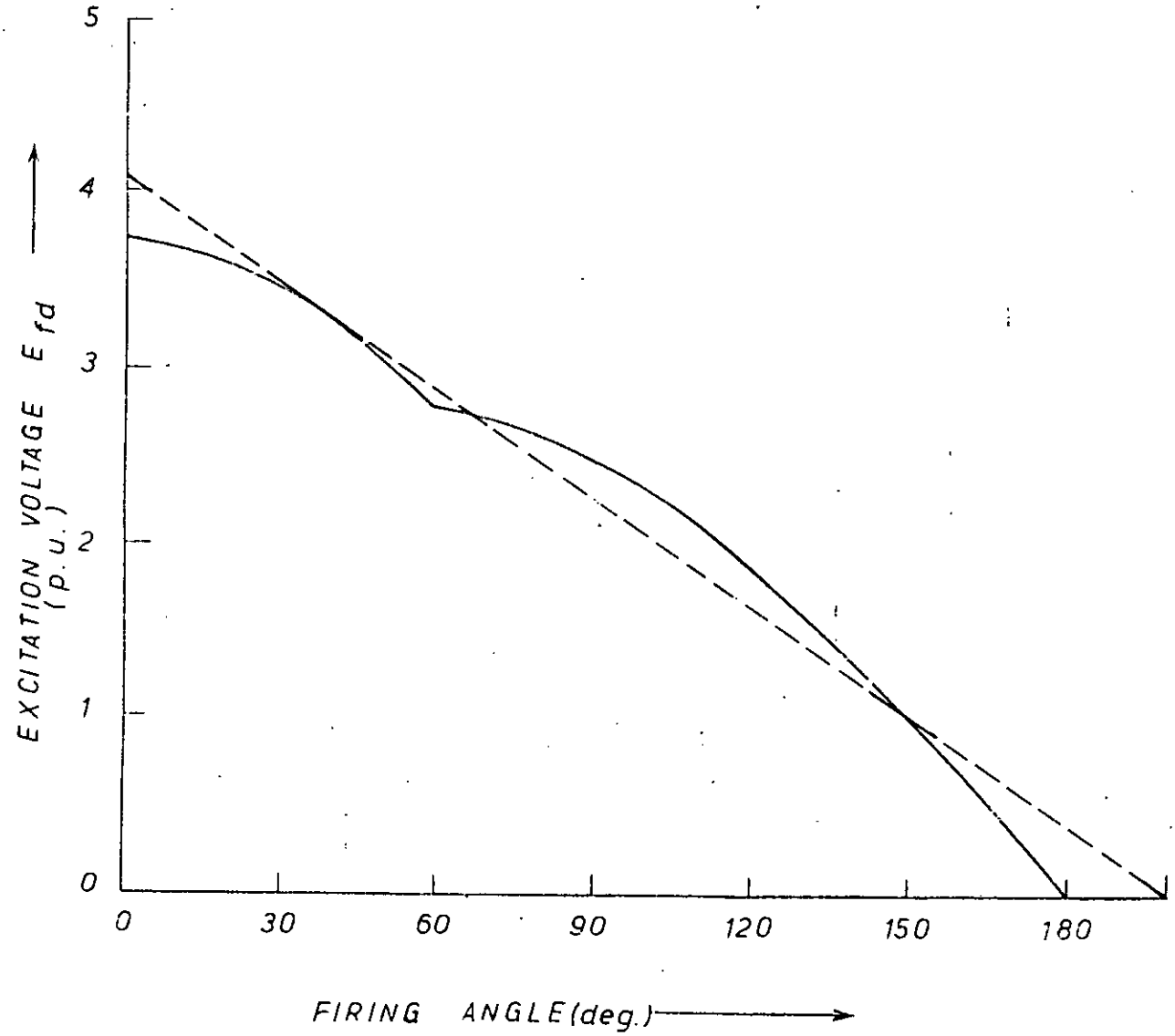

FIG. 3·7 THE SCR CHARACTERISTIC AND THE LINEARIZED CURVE.

3.5 SCR Control Circuits

The heart of the SCR firing control circuit consists of a set of three comparators (one for each phase). The comparator compares two input voltages. When the two voltages are exactly equal and opposite, the output voltage of the comparator switches its mode. The switched signal is used to fire the SCR's. One of the two voltages used for comparison is a voltage time base signal (or a saw). The other is a d.c. signal which is the algebric summation of reference signal, voltage deviation signal and velocity deviation signal. Since the switching of the comparator is in the direction of positive to negative voltage, the output of the comparator can not be used directly to fire the SCR's. To invert the polarity of this signal an inverter is used. The simplified block diagram of SCR firing control circuit is shown in Fig. 3.8.

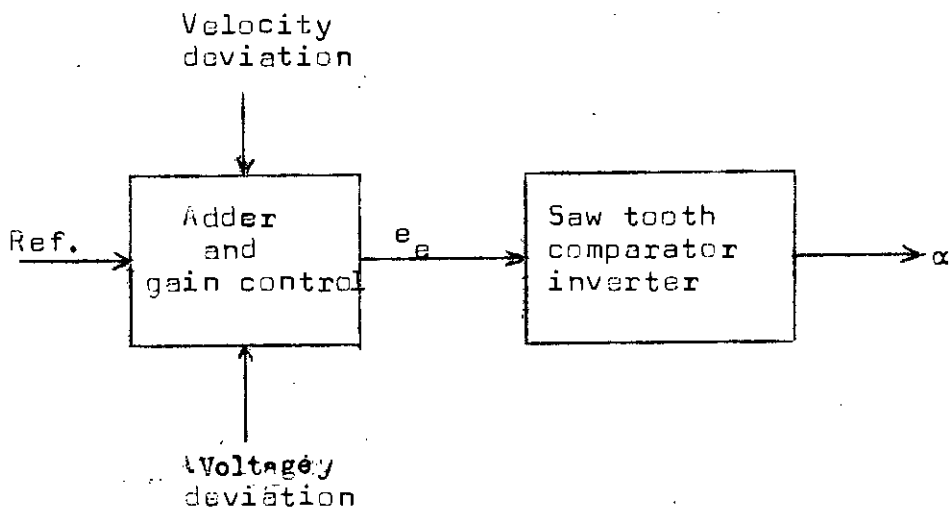

Fig. 3.8 Simplified Block Diagram of SCR Firing Circuit.

The adder in the excitation system is used to add velocity deviation signal, voltage deviation signal and the reference signal to produce a controlling d.c. voltage for the comparator. This circuit also serves the purpose of gain control for individual feedback signals. The adder circuit is shown in Fig. 3.9.

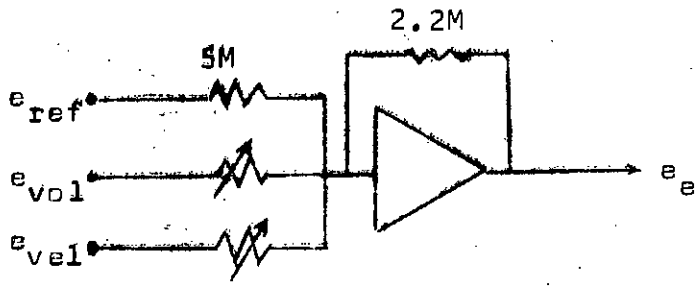

Fig. 3.9 Adder Circuit.

The output of the adder circuit is

$$e_e = 0.44\ e_{ref} + K_{vol}\ e_{vol} + K_{vel}\ e_{vel} \qquad (3.21)$$

where K_{vol} and K_{vel} are gain of voltage and velocity deviation signals respectively. The adder circuit output e_e is applied to the comparator and is compared with the saw tooth voltage. The combined effect of the comparator, inverter and saw tooth circuit is that whenever there is an increase in e_e, the firing angle α increases i.e. firing is delayed. Since the adder signal is d.c, the firing angle α will follow the saw tooth wave as shown in Fig. 3.10 which may be redrawn in another way to show the relation between adder voltage e_e and the firing angle α as shown in Fig. 3.11.

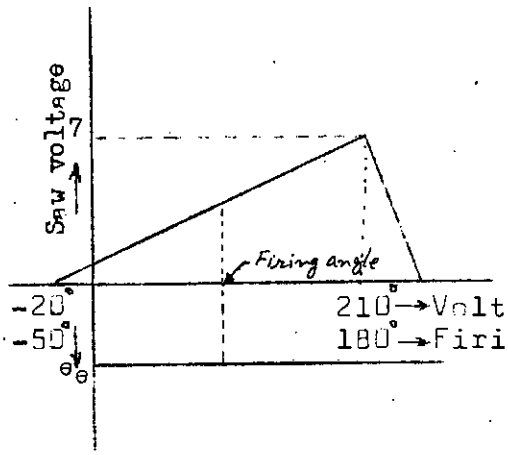

Fig. 3.10 Comparator input Signals.

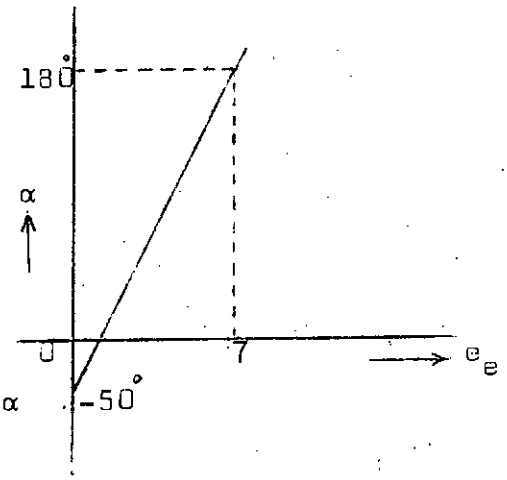

Fig. 3.11 Comparator Inverter Characteristics.

The equation of the line of Fig. 3.11 is

$$\alpha = 0.575\ e_e - 0.8749 \qquad (3.22)$$

For small deviation about the operating point equations (3.21) and (3.22) becomes

$$\Delta e_e = K_{vol}\ e_{vol} + K_{vel}\ e_{vel}$$
$$\Delta\alpha = 0.575\ \Delta e_e \qquad (3.23)$$

From experimental data it is found that for $E_{fd} = 170$ volts, with the machine floating, $e_{ref} = 8$ volts, α is about 66^o which is also obtained from equations (3.21) and (3.22). The corresponding d.c. voltage is 165 volts. This requires a voltage divider of ratio 0.268 at the d.c. output of SCR so that required voltage of 45.4 volts is applied to the field to give $E_{fd} = 170$ volts. Small time constants associated with the

electronic circuits such as comparator, inverter adder etc. and a time lag in SCR firing may be combined to one time constant for the exciter which is taken to be about 20 mSec.

3.6 Simplified Representation of Excitation System

The transfer function of each of the blocks of the excitation system has been developed in the previous sections. Combining them the overall block diagram of the excitation system can be redrawn as shown in Fig. 3.12.

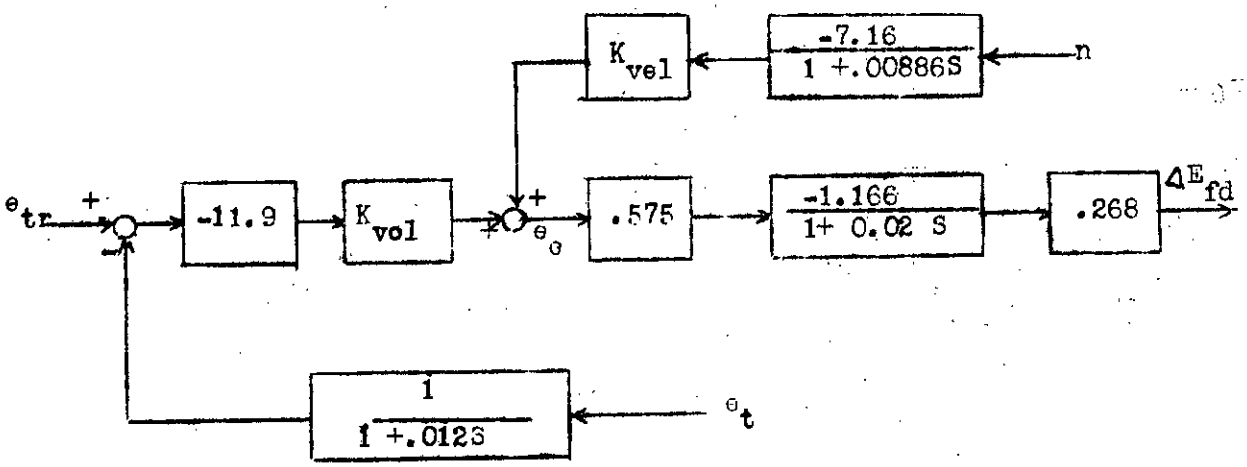

Fig. 3.12 Detailed Block Diagram of Excitation System.

The excitation system block diagram of Fig. 3.12 can be reduced to a simpler form as shown in Fig. 3.13. The calculated gains of the exciter and velocity feedback circuit are 2.2 K_{vol} and 0.612 K_{vel}/K_{vol} respectively which may be compared with respective experimental gains 2.0 K_{vol} and 0.4 K_{vel}/K_{vol}. The time constants of exciter and voltage sensing circuit are 20 mSec and 12 m Sec respectively and that of velocity sensing circuit may be neglected.

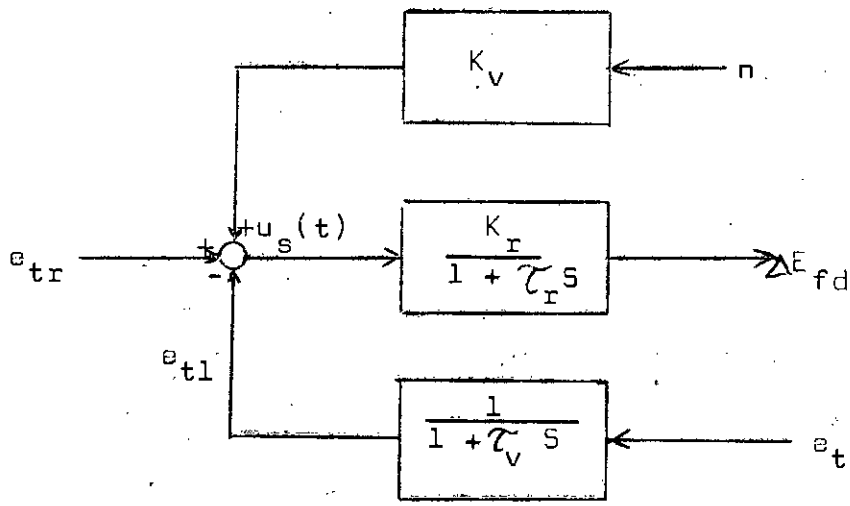

Fig. 3.13 Simplified Block Diagram of Excitation System.

The excitation system can now be represented by the following equations.

$$pe_{tl} = (e_t - e_{tl})/\tau_v \tag{3.24}$$

$$\Delta E_{fd} = \frac{K_r}{1 + \tau_r p} \left[e_{tl} - e_{tr} - u_s(t) \right] \tag{3.25}$$

where K_r is negative. The nonlinear form of equation (4.25) is

$$pE_{fd} = \frac{K_r}{\tau_r} e_{tl} - \frac{1}{\tau_r} E_{fd} + (E_o - K_r e_{tr})/\tau_r - \frac{K_r}{\tau_r} u_s(t) \tag{3.26}$$

If the time constant in the velocity sensing network is considered another differential equation would be necessary to represent it. The excitation system thus can be represented by a series of gains and time constants.

CHAPTER 4

MEASUREMENT OF GENERATOR PARAMETERS

4.1 Measurement of Inductances

As stated, the measurement of different synchronous machine inductances by d.c. bridge method gives more accurate results. Under normal steady state balanced operation, the resultant mmf of three armature coils is constant in magnitude and stationary with respect to rotor poles in direction. The resultant airgap mmf is, therefore, a vector sum of armature and rotor mmf's which is constant in magnitude and direction with respect to the pole axis. Therefore, the inductances which govern the performance of synchronous machine are inductances to direct current (and since airgap mmf wave is rotating at synchronous speed, these are called synchronous inductances). They must, therefore, be measured with direct current.

Any attempt to measure inductances at stand still with 50 c/s alternating current will fail completely due to the presence of damper winding which acts as a short circuited secondary of a transformer. Moreover the core loss will become appreciable so that there will be large error in measured quantities. The d.c. bridge method eliminates these difficulties. The procedure [18] followed for the measurement are given below.

a) Measurement of Self Inductance of Field Coil:-

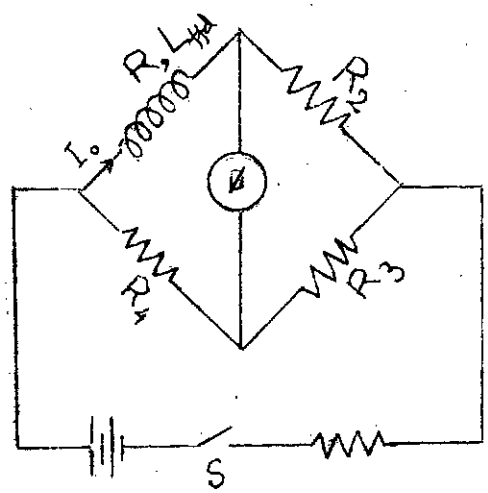

$R = 162$
$R_2 = 44.4$
$R_3 = 44.9$
$R_4 = 164$

Fig. 4.1 Wheatstone Bridge Arrangement for Measuring Self Inductance.

Figure 4.1 shows the Wheatstone bridge arrangement where R,L represents the field coil of the machine. $R_2 R_3, R_4$ are non inductive resistances. Using a d.c. source the bridge was balanced and let I_o be the current in the field coil. When switch S is opended, the current in the inductor falls exponentially to zero from the initial value I_o, given by the relation

$$i = I_o \, e^{-\left(\frac{L_{ffd}}{R + R_2 + R_3 + R_4}\right)t} \qquad (4.1)$$

The voltage across the detector is

$$v = i \, (R_2 + R_3) \qquad (4.2)$$

Let the detctor be such that it indicates the time integral of voltage across it, that is

$$\phi = \int_0^\infty v\,dt$$

$$= \frac{R_2 + R_3}{R + R_2 + R_3 + R_4} L_{ffd} I_o$$

$$= \frac{R_2}{R + R_2} L_{ffd} I_o \qquad (4.3)$$

(The bridge is balanced so that $\frac{R}{R_2} = \frac{R_4}{R_3}$)

Knowing ϕ from the detector self inductance can be calculated.

$$L_{ffd} = \frac{R + R_2}{R_2} \frac{\phi}{I_o} \qquad (4.4)$$

Generally, the voltage integrator may be either a ballistic galvanometer with a series resistor or a fluxmeter. However due to nonavailability of ballistic galvanometer and fluxmeter, an oscillosscope was used as the detector. The oscilloscope has an advantage over the ballistic galvanometer or fluxmeter detector. The creep of meter needle due to slight unbalance of bridge introduces some error in measurement which is eliminated in oscilloscope measurement. The oscillogram of the transient pulse was taken and integrated by planimeter and also checked by calculating area. One of the oscillograms is reproduced in Fig. 4.2. Measurements are carried out with different values of initial currents. Fig. 4.3 shows variation of self inductance with current.

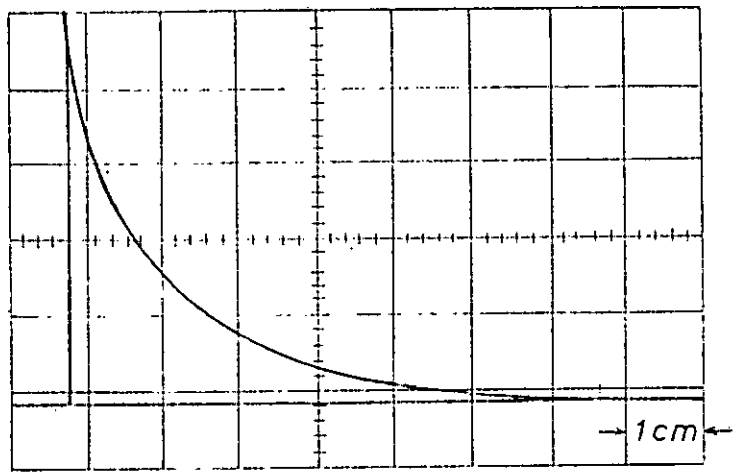

Scale: ·1 Sec/cm.
5 V/cm.

FIG. 4·2 TRANSIENT VOLTAGE PULSE ACROSS THE DETCTOR.

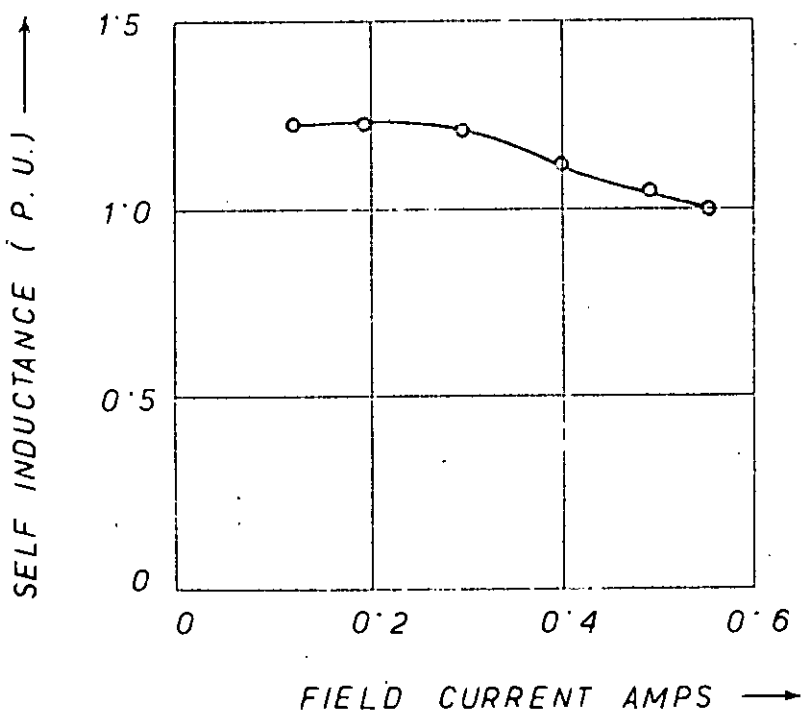

FIG. 4·3 VARIATION OF SELF INDUCTANCE OF FIELD COIL WITH CURRENT.

The presence of damper winding does not affect the measurement of self inductance. This is shown as follows:

Let L_{df} be the mutual inductance between field and damper winding. Then the voltage induced in the field circuit due to the presence of induced current in the damper winding is $L_{df} \frac{di_{kd}}{dt}$. The time integral of this induced voltage

$$\int_0^{\infty} \left[L_{df} \frac{di_{kd}}{dt} \right] dt \qquad (4.5)$$

as given in equation (4.5) is zero, because the initial and final values of the induced damper current are zero.

b) Measurement of Mutual Inductance:-

The method discussed above can be applied for measuring mutual inductance also. Figure 4.4 shows the necessary bridge arrangement.

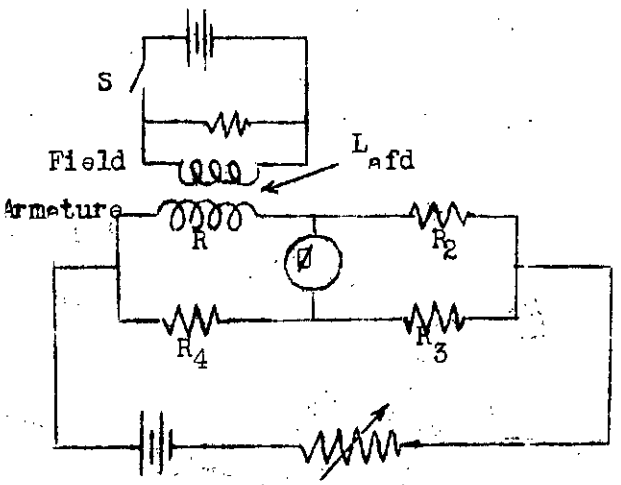

Fig. 4.4 Bridge Arrangement for Measurement of Mutual Inductance.

The bridge was balanced initially with rated current in the field and armature coil. Then the switch S is opened which causes a transient current in field circuit and a corresponding induced voltage $L_{afd} \frac{di_{fd}}{dt}$ in the armature coil. The transient voltage pulse across the detector was recorded by an oscilloscope and time integral of voltage was calculated. It can be shown that the mutual inductance can be expressed as

$$L_{afd} = \frac{R + R_2}{R_2} \frac{\phi}{I_{fdo}} \qquad (4.6)$$

where I_{fdo} is the initial field current and ϕ is the time integral of voltage across the detector.

It is to be noted here that mutual inductance varies sinusoidally with rotor position. The maximum value of mutual inductance is required for machine representation. Measurement of maximum mutual inductance requires an initial setting of field pole along the same axis with armature phase. Figure 4.5 shows variation of mutual inductance with field current.

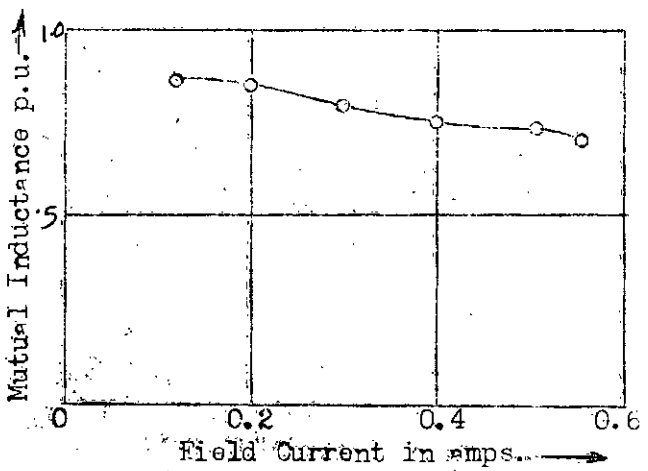

Fig. 4.5 Field Current Versus Mutual Inductance Plot.

In the bridge circuit considered above, the conditions are almost similar to actual operating conditions with both windings carrying currents. The currents may be adjusted for desired saturation. The mutual inductance measured by this method will correspond more closely to actual values than those obtained by other methods.

Ideally in the unit voltage base system mutual inductance between stator phase and field winding will be unity. The inductance bridge measurement of mutual inductance gives a slightly lower value. Mutual inductance can also be measured from open circuit characteristics of the machine using the relation

$$E_{fd} = \frac{X_{afd}}{R_{fd}} V_{fd}$$

Fig. 4.6 shows the open circuit characteristics of the machine. As defined in section 2.3, the base field current is found from the curve to be 0.376 amps. which is the field current necessary to give rated open circuit voltage. The calculated mutual reactance is 500 Ω at 50 c/s or in other words per unit mutual inductance is unity by equation 2.10.

c) Measurement of Direct and Quadrature Axis Synchronous Inductance:

The d.c. inductance bridge discussed earlier may also be applied for measuring d and q axis synchronous inductances. But these inductances are much smaller compared to mutual

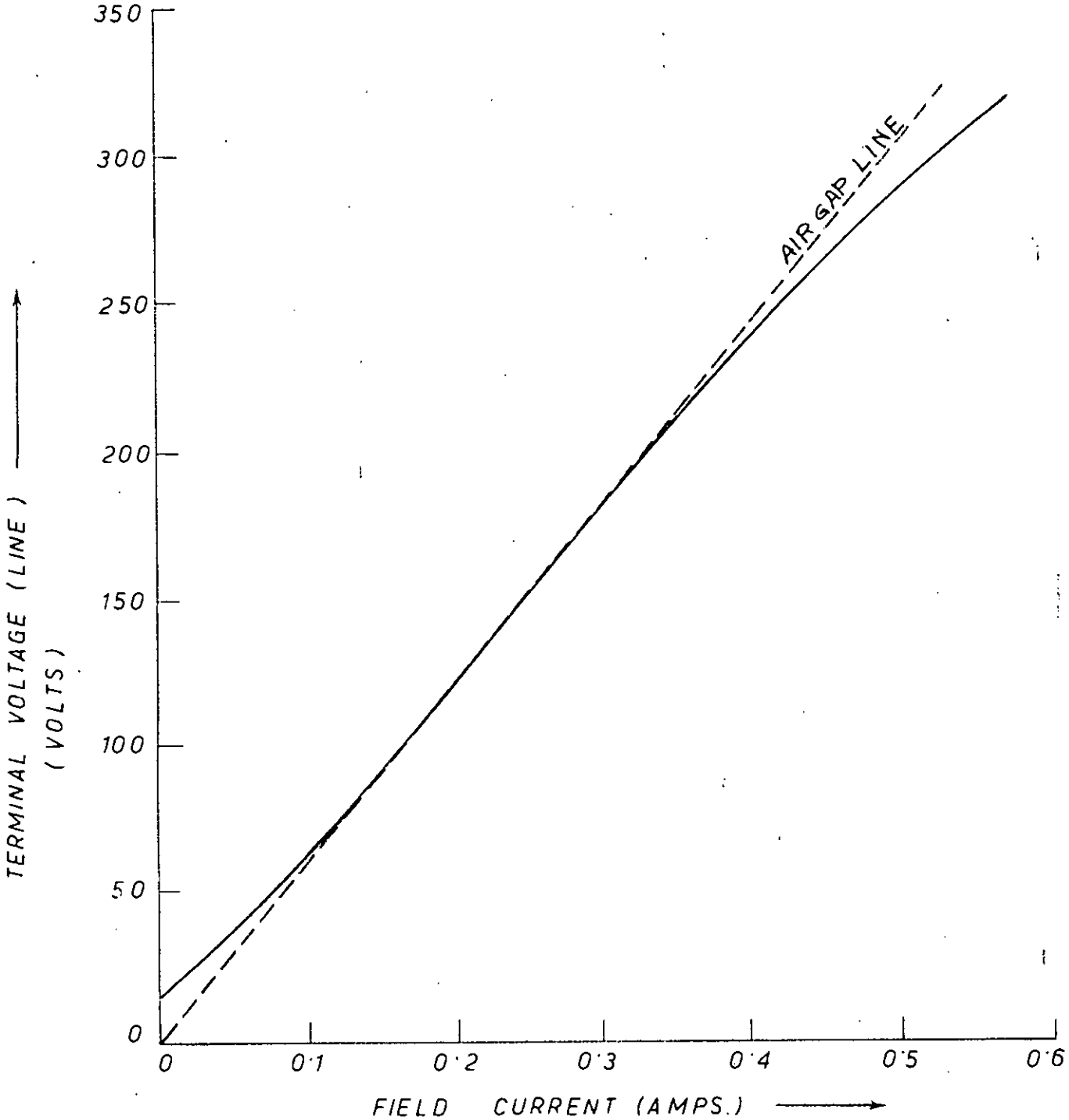

FIG. 4·6 OPEN CIRCUIT CHARACTERISTICS OF THE ALTERNATOR.

inductances. Measurement of these inductances by the same process requires very fast triggering of oscilloscope to get a good oscillogram, since the transient pulse is of very short duration. At the same time triggering must be synchronized with switching of bridge circuit. Because of the difficulties faced with the bridge method, the synchronous inductances of the machine were determined by slip test.

4.2 Measurement of Inertia Constant

The inertia constant is determined from the retardation test. The basic idea behind retardation method is that when the driving power of a rotating mass is interrupted it will decelerate and finally come to rest. The time required to decelerate is directly proportional to kinetic energy of the rotating mass and inversely upon friction, windage and other losses which dissipates energy.

The Kinetic energy of a rotating mass is given by

$$K.E = \tfrac{1}{2} J\omega^2 \qquad (4.7)$$

Any decrease in Kinetic energy would be equal to the work done in overcoming the losses during any interval of time. Let W be the loss due to friction windage etc. Then

$$Wdt = d\left(\tfrac{1}{2} J\omega^2\right) \qquad (4.8)$$

or $$W = J\omega \frac{d\omega}{dt}$$

$$= - M\alpha \qquad (4.9)$$

where retardation $\alpha = -\frac{d\omega}{dt}$ and M is the inertia constant.

Exact determination of retardation characteristics posses a problem. Tachometer measurement of speed is not satisfactory since it will introduce large error. With field excitation constant, the generated voltage of a d.c. generator is directly proportional to speed. Therefore, the speed time characteristics may be obtained from a simple record of voltage.

However instead of measuring the generated voltage directly the arrangement shown in Fig. 4.7 was made. The differential voltage E_D was recorded with a pen recorder. The pen recorder plot is shown in Fig. 4.8. The speed is proportional to sum of battery voltage and the differential voltage.

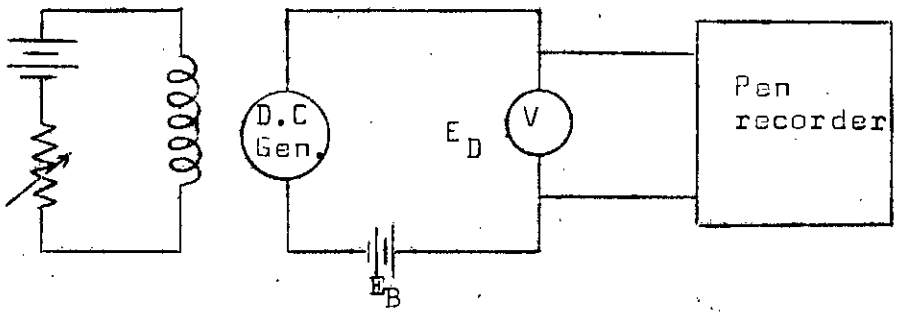

Fig. 4.7 Set up for Measurement of Inertia.

If the voltmeter is calibrated by some standard speed measuring instrument, the speed can be directly read from the differential voltage. The speed N for any differential voltage E_D will be given by

$$N = N_c \frac{E_D + E_B}{E_{DC} + E_B} \qquad (4.10)$$

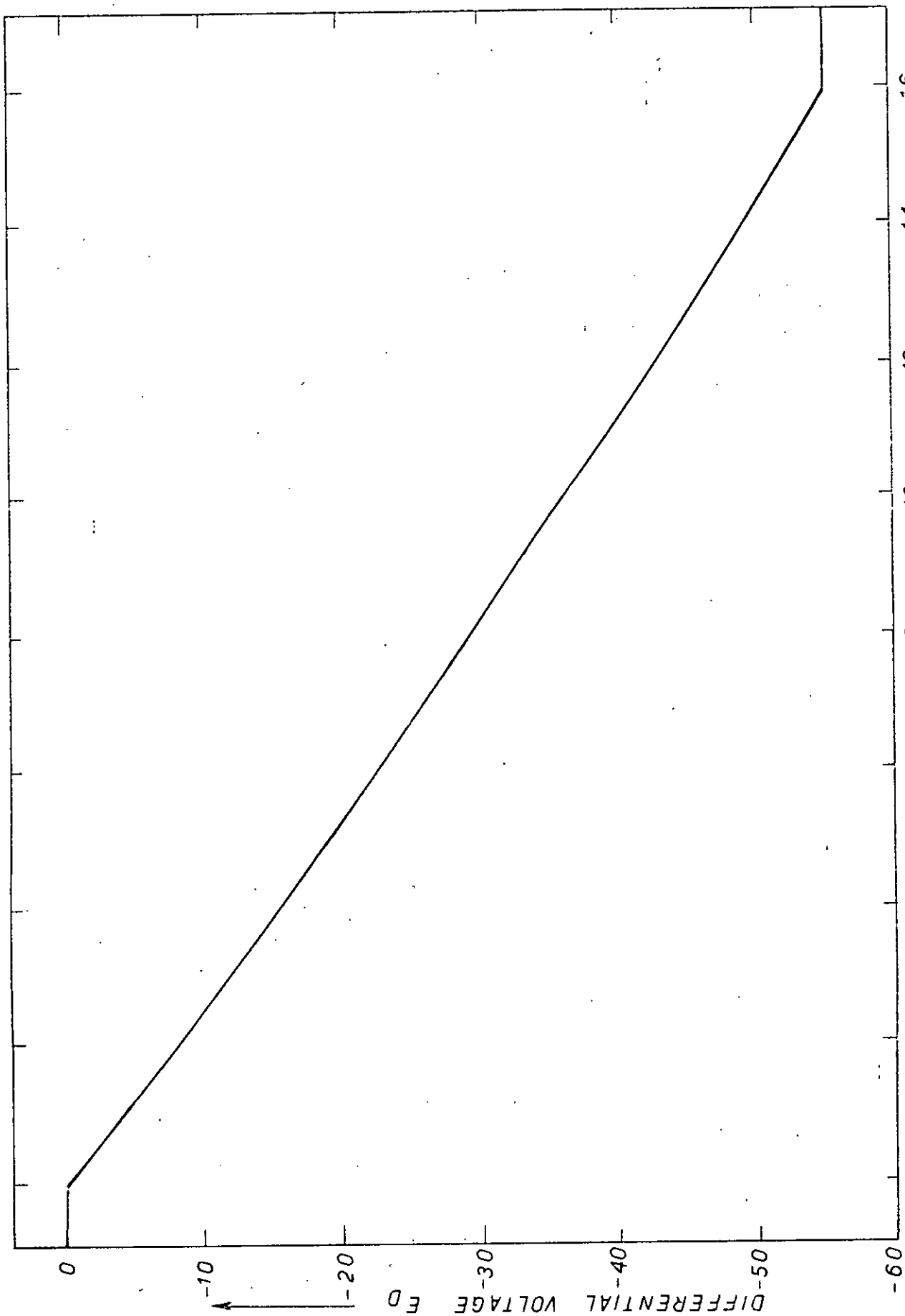

FIG. 4·8 DIFFERENTIAL VOLTAGE VS. TIME FROM SET UP OF FIG. 4·7.

where E_{DC} is the differential voltage at some known speed N_c. The known speed in the experimental set up was 1500 rpm and E_{DC} was zero. The speed time curve can be calculated using equation (4.10) which is shown in Fig. 4.9. The no load input power at rated speed which is nothing but friction, windage and I^2R loss was measured.

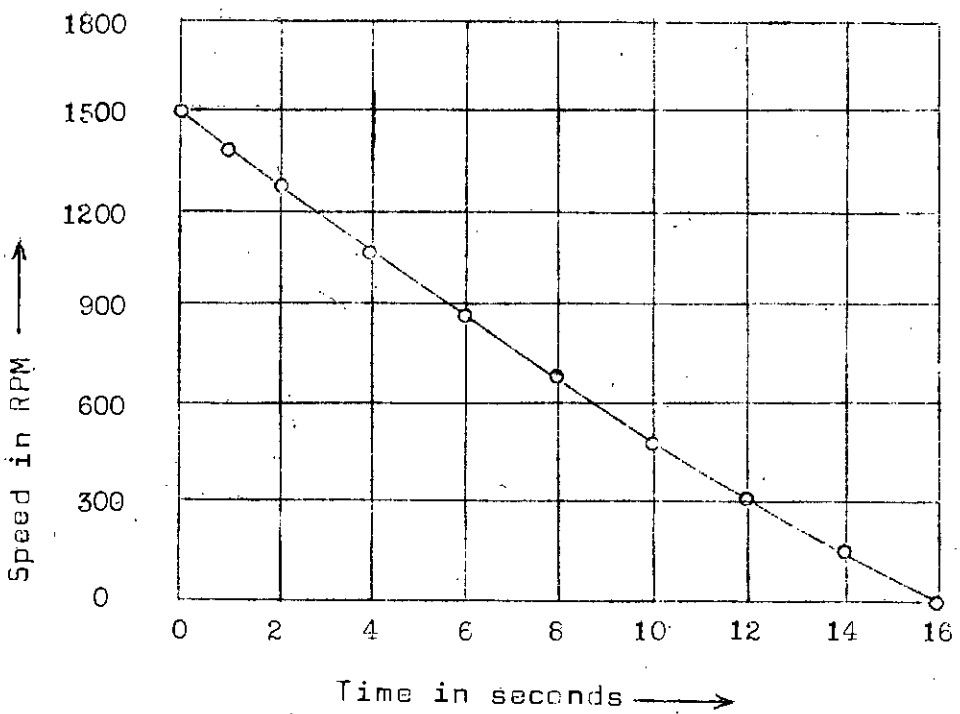

Fig. 4.9 Speed Time Characteristics Obtained from Setup of Fig. 4.7.

For the machine under test the following data were obtained:

No load input power	382 watt.
Armature copper loss	20.7 watt.
Friction, windage loss	361.3 watt.
Retardation	150 rpm/sec (from Fig.4.9) or 15.7 rad/sec^2.

The inertia constant M is calculatec from equation (4.9) and the value obtained is 0.4 Joule sec/elect. deg.

4.3 Results

A 1.5KW, 230V synchronous machine driven by a d.c. motor on an AEG generalized machine set was considered. The values of the various parameters obtained are listed here. A Wheatstone bridge arrangement with a precision of 10^{-4} was used to measure different resistances.

Base voltage (stator) = 187.8 volts

Base current (stator) = 5.325 amps.

Base impedance = 35.3 ohms

Base field current = 0.376 amps

Base current ratio = 0.04702

Parameters	Actual values	Per unit values
1. Armature Resistance	4.812 ohms	0.1134 p.u.
2. Field Resistance	162.12 ohms	0.01542
3. Field coil self inductance	40.4 Henry	1.195
4. Direct axis synchronous inductance	0.108 "	1.05
5. Quadrature axis synchronous inductance	0.0627 "	0.558
6. Stator field mutual inductance	1.35 " 1.59 "	0.85 (by bridge) 1.0 (by O.C.C.)
7. Inertia constant of rotor mass	0.4 Joule Sec/ elect.deg. (M)	2.4 (H)

Table 4.1

Inductances in the above table represent values at rated operating conditions.

CHAPTER 5

EFFECT OF EXCITER PARAMETERS AND STABILIZING CONTROLS

5.1 Introduction

The power system considered for study consists of a 1.5 KW, 230 V alternator on an AEG four machine set which is connected to a power system bus through a simulated transmission line. The generator is equipped with controlled rectifier excitation system having the provision of applying different stabilizing signals. The block diagram of the overall system is shown in Fig. 5.1.

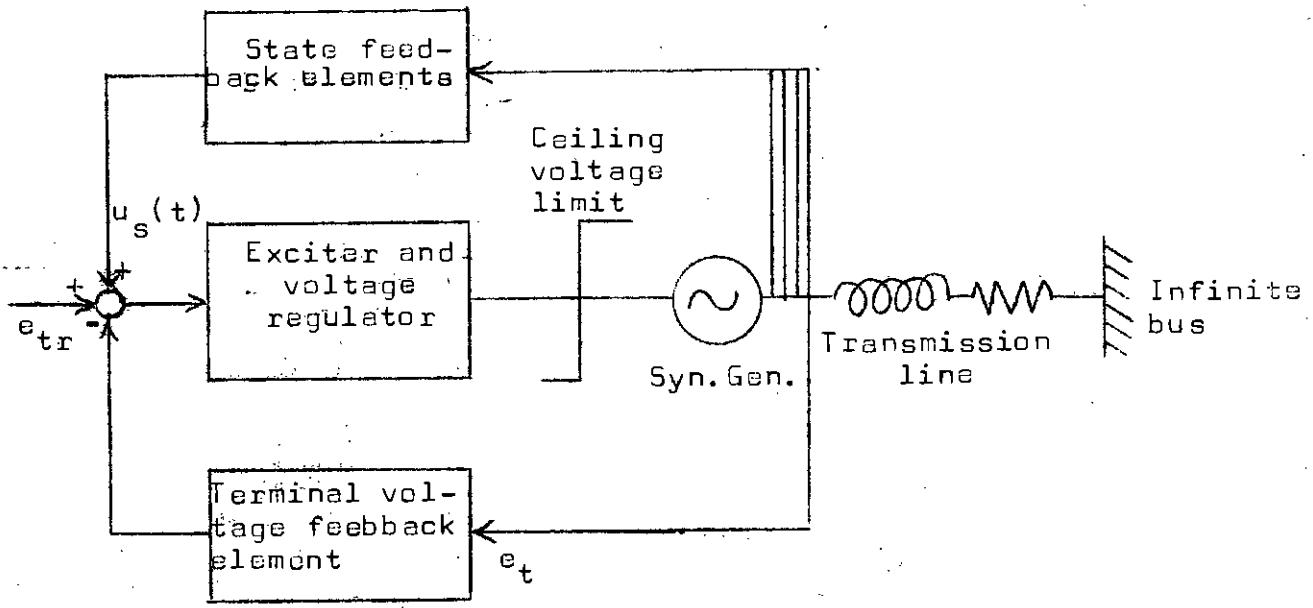

Fig. 5.1 System Configuration.

The state space representation of the synchronous generator and excitation system as deduced in Chapter 2 and 3 are given as:

$$\begin{bmatrix} pi_{fd} \\ pi_d \\ pi_q \\ p\eta \\ p\partial \\ pE_{fd} \\ pe_{t1} \end{bmatrix} = \begin{bmatrix} a_1 i_{fd} + a_2 i_d + a_3(1+\eta) i_q + a_4 \sin \partial + a_5 E_{fd} \\ a_6 i_{fd} + a_7 i_d + a_8(1+\eta) i_q + a_9 \sin \partial + a_{10} E_{fd} \\ a_{11}(1+\eta) i_{fd} + a_{12}(1+\eta) i_d + a_{13} i_q + a_{14} \cos \partial \\ a_{15} E_{fd} \sin \partial + a_{16} \sin 2\partial + a_{17} \\ a_{18}\, \eta \\ \frac{K_r}{\tau_r} e_{t1} - \frac{1}{\tau_r} E_{fd} + (E_o - K_r e_{tr})/\tau_r - \frac{K_r}{\tau_r} u_s(t) \\ (e_t - e_{t1})/\tau_v \end{bmatrix} \quad (5.1)$$

or written in the form (1.1) is

$$\dot{X} = f[X,\ u]$$

The coefficients a_i are functions of synchronous machine parameters which have been determined and presented in Chapter 4.

Under steady state conditions the right hand side of equation (5.1) equals zero. Solution of this equation yields the steady state operating points. The computer program for the steady state solution is given in appendix II. The operating points considered for the study and the values of the parameters are also listed in appendix I.

To simulate a disturbance or fault on the power system represented by the set of equations (5.1), functions or the parameters in the right hand side of the equation are modified accordingly. The set of differential equations (5.1) are solved

by a fourth order Runge Kutta integration method. The computer program developed for solution of the differential equations is given in appendix II. The solution of the differential equations which are the different states of the system such as current, rotor angular position, velocity etc. are recorded. For accuracy of result the step size must be much smaller than the smallest time constant in the system. But the smaller the step size the larger is the computing time. A step size of 5 m Sec has been found to be a satisfactory compromise.

Effect of different parameters of excitation system such as exciter gain, time constant etc. have been studied. Determination of the exciter gain for best performance was attempted. The term "best performance" is used to mean minimum first rotor excursion due to a disturbance and maximum damping of rotor angle oscillation subsequent to this first swing.

A high speed voltage regulator is known to reduce stability rather than increasing it. But it is possible to increase damping by excitation control and this requires an additional stabilizing signal in addition to the normal voltage error signal. Search for suitable stabilizing signals derived from the system states have been carried out. An "optimum" combination of the different system quantities for best transient removal has been attempted.

5.2 Effect of Regulator Gain

In order to investigate the effect of regulator gain on the stability of the power system a three phase short circuit for a duration of 120 m Sec (6 c/s) was considered at the generator terminals. The operating point was at 60° of the underexcited machine when the output power was 31.5%. (The maximum power that can be delivered by the machine under this excitation is 37%). The power difference or the accelerating power due to short circuit causes the machine to accelerate and the voltage regulator reacts accordingly by varying the voltage applied to the field. For the operating point under consideration the machine in absence of voltage regulator can not survive the three phase fault and for low values of regulator gain also the system becomes unstable. For small values of gain, the oscillations grow gradually and the system becomes unstable. This is a case of dynamic instability. With increase in regulator gain the first swing stability improves but damping is poor. Too large a regulator gain again deteriorates the system response and for a gain of 800 and over it has been observed that the machine goes completely out of step. The system behaves almost in a similar manner with an additional stabilizing signal derived from rotor velocity. Figures 5.2 and 5.3 show the effect of regulator gain in absence of additional stabilizing signal. Fig. 5.2 shows the rotor angle variation of the synchronous generator for different values of exciter gain with normal voltage regulator action and no additional stabilizing

signal. The maximum rotor excursion for different values of gain are plotted for a three phase short circuit at the machine terminals. It can be clearly seen that the generator becomes unstable for too small and again too large values of gain even with auxiliary velocity feedback signal.

So far as rotor first swing is concerned a regulator gain of 40 seems to be preferable. A higher gain cause oscillatory response. Fig. 5.4 shows that settling time at a gain of 20 is much smaller than that at a gain of 40 in which case low level oscillation continues for a larger period. However, the first rotor swing for a gain of 20 is not too large compared to that for 40. So regulator gain of 20 seems to be the best choice considering two important figures of merit of a system — the peak overshoot (first swing) and the settling time.

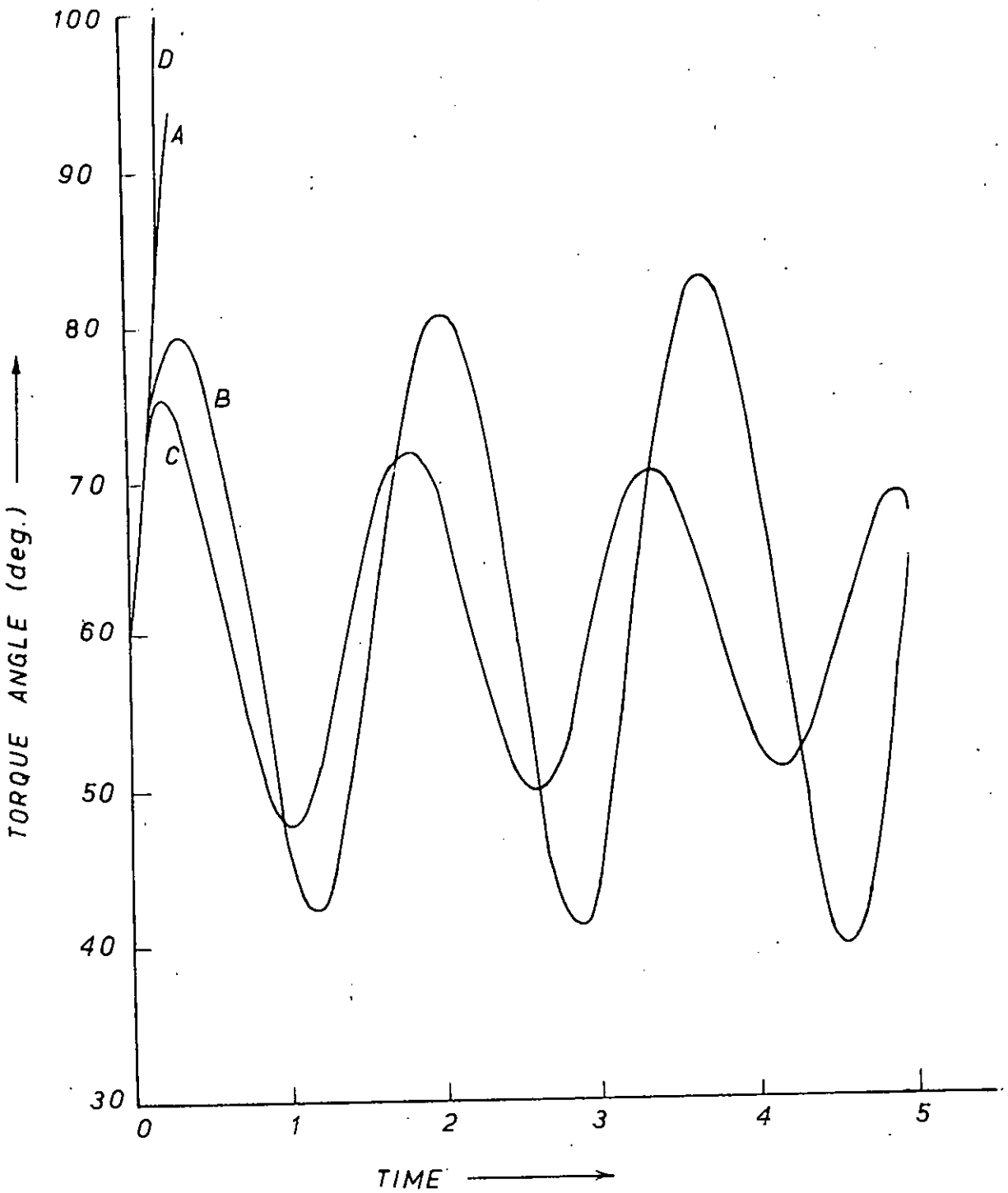

FIG. 5·2. SWING CURVES FOR A THREE PHASE FAULT SHOWING EFFECT OF REGULATOR GAIN WITHOUT STABILIZING SIGNAL.

A — UNREGULATED SYSTEM

B — REGULATOR GAIN, $K_r = -4$

C — " " , $K_r = -20$

D — " " , $K_r = -800$

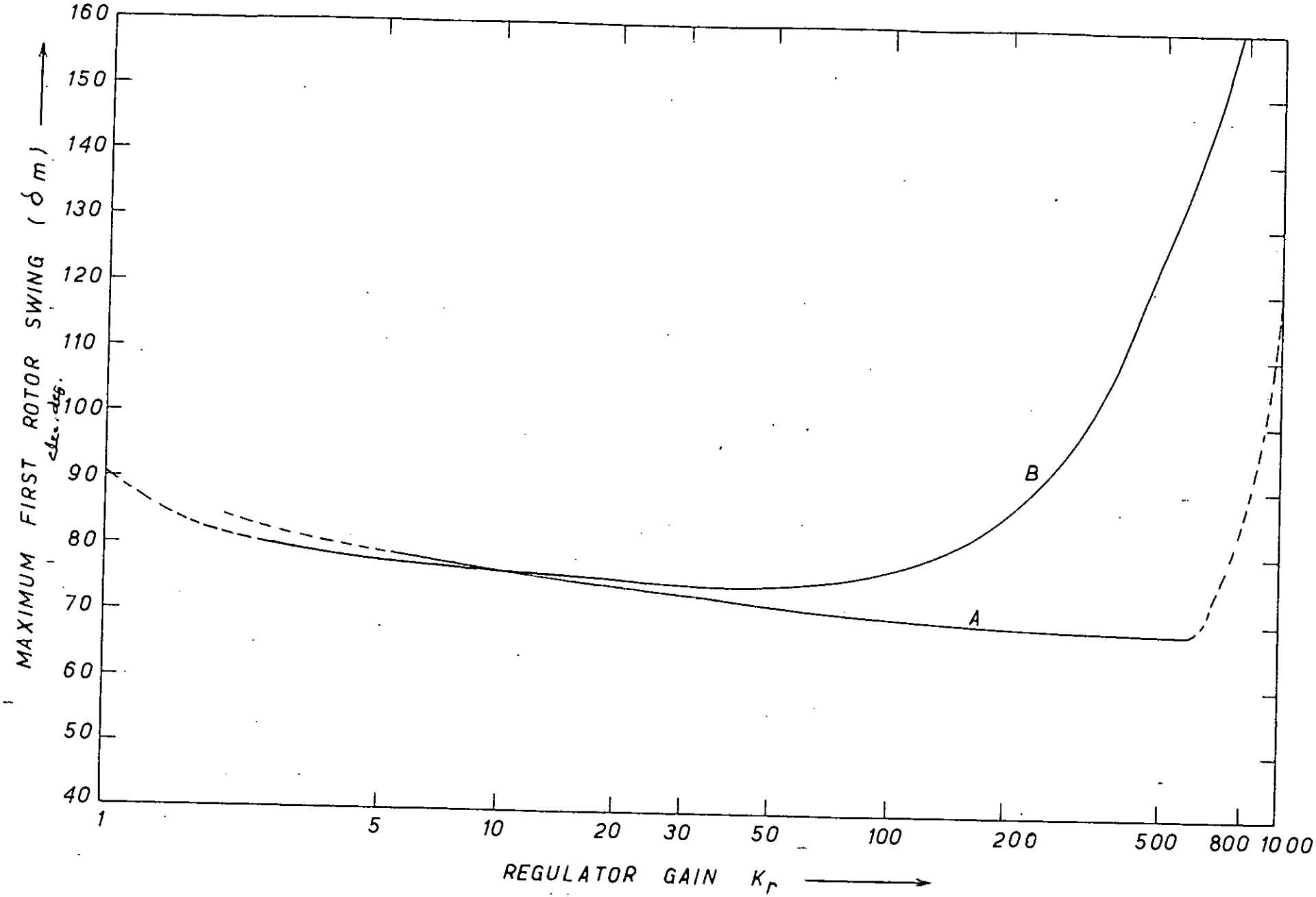

FIG. 5.3 VARIATION OF MAXIMUM ROTOR SWING WITH REGULATOR GAIN (FOR 3 Ø FAULT)
A – WITH VOLTAGE REGULATOR ONLY, B — WITH VOLTAGE REGULATOR & VELOCITY FEEDBACK.
DOTTED PORTION INDICATES LOSS OF STABILITY BY GROWING OSCILLATIONS

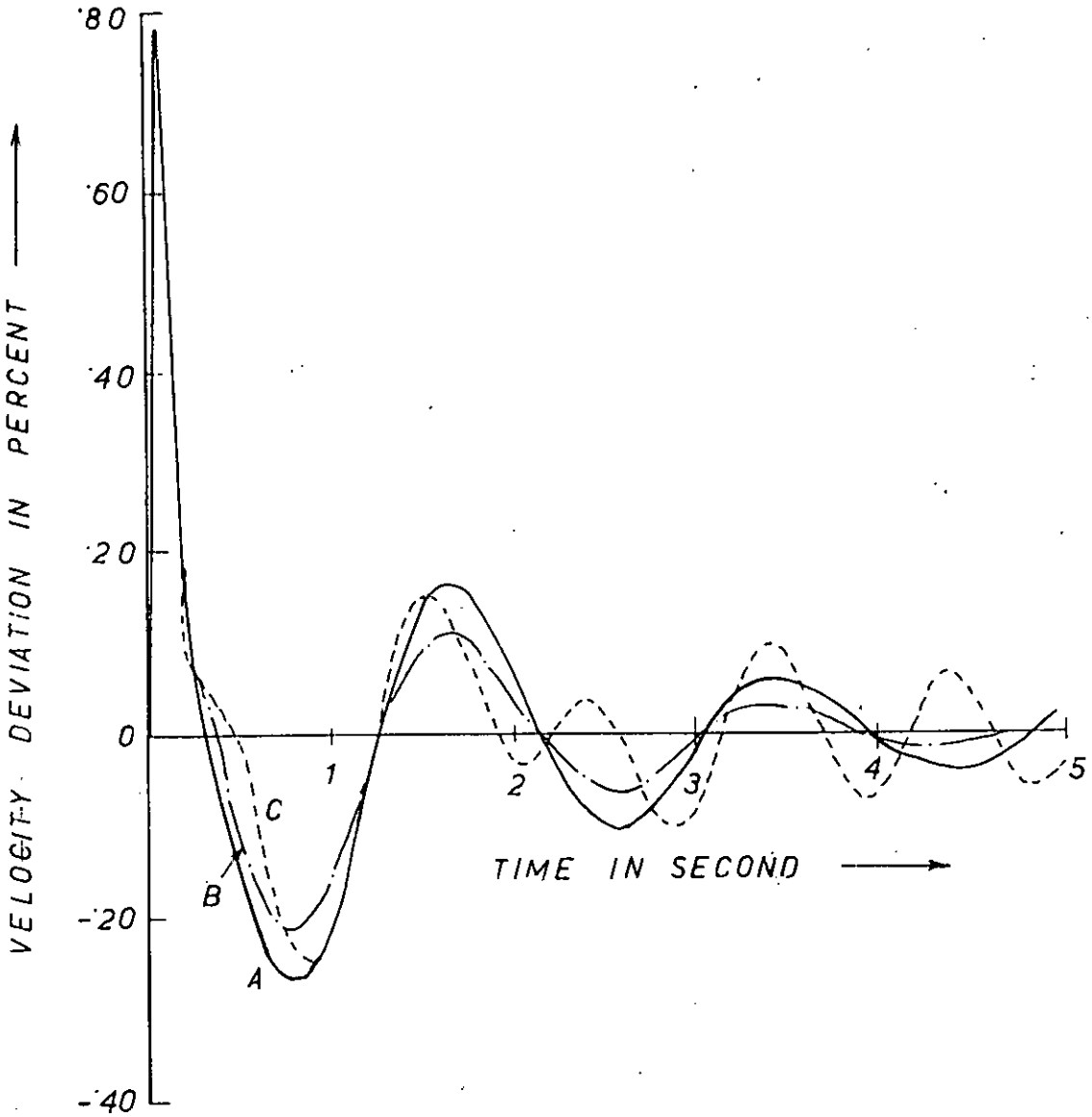

FIG. 5·4 VELOCITY DEVIATION FOR DIFFERENT REGULATOR GAIN FOR 3 Ø FAULT.

A — WITH REGULATOR GAIN = -4
B — " " " = -20
C — " " " = -40

5.3 Velocity Feedback Signal

A signal derived from rotor speed deviation is very effective in damping out system oscillations following a disturbance in the power system. Fig. 5.5 and 5.6 demonstrates this. A three phase short circuit at the terminals of an underexcited synchronous generator carrying a load of 31.5% at an operating angle of 60^{o} was applied. The swing curves and trajectories in velocity angle plane show that in absence of velocity feedback signal the system requires significantly large time to return to the steady operating point. With velocity signal the system returns to the equilibrium point after only a few oscillations.

The effect of different amounts of rotor velocity feedback signal has also been investigated. It is observed that, though the amount of velocity signal has no significant effect upon the magnitude of first rotor excursion, its effect upon the second and subsequent oscillations is considerable. A gain of about 20 has been found to be satisfactory. Too large a gain in the velocity feedback circuit causes an oscillatory response and the generator may even lose synchronism. A gain of 20 was used for the response shown in Fig. 5.5. Figure 5.7 show the variation of different rotor and stator voltages and currents for the 3 phase short circuit. A time constant of 20 m Sec was considered in the velocity feedback circuit and no significant change in transient performance was observed.

The effect of velocity signal on other types of system disturbance such as different amounts of torque step, torque

pulse for 6 cycles, a six cycle three phase fault at middle of transmission line and switching a parallel transmission line was studied. Swing curves of Fig. 5.8 - 5.12 show that in all types of system disturbances the velocity feedback signal has a satisfactory contribution in damping out the system oscillations. Different figures of merit such as settling time, peak overshoot etc. are listed at the end of the chapter.

As mentioned earlier, the effectiveness of a solid state excitation scheme, designed and constructed in a previous work [16] was studied for power system stabilization. Since a high speed voltage regulator reduces effective damping auxiliary stabilizing signals are required. Because of limited facilities only a signal derived from rotor velocity of the machine could be used with the exciter. A number of test cases such as momentary three phase short circuit, different amounts of torque steps were considered. Results obtained in that study showed that an excitation system equipped with terminal voltage feedback and also auxiliary velocity signal were helpful in controlling transients effectively.

The system considered in this study is exactly the same as in the previous one. Though the types of faults considered in that study could not be exactly simulated for obvious reasons, the results obtained in this study indicate response similar to those of the previous ones with terminal voltage and velocity feedback signals.

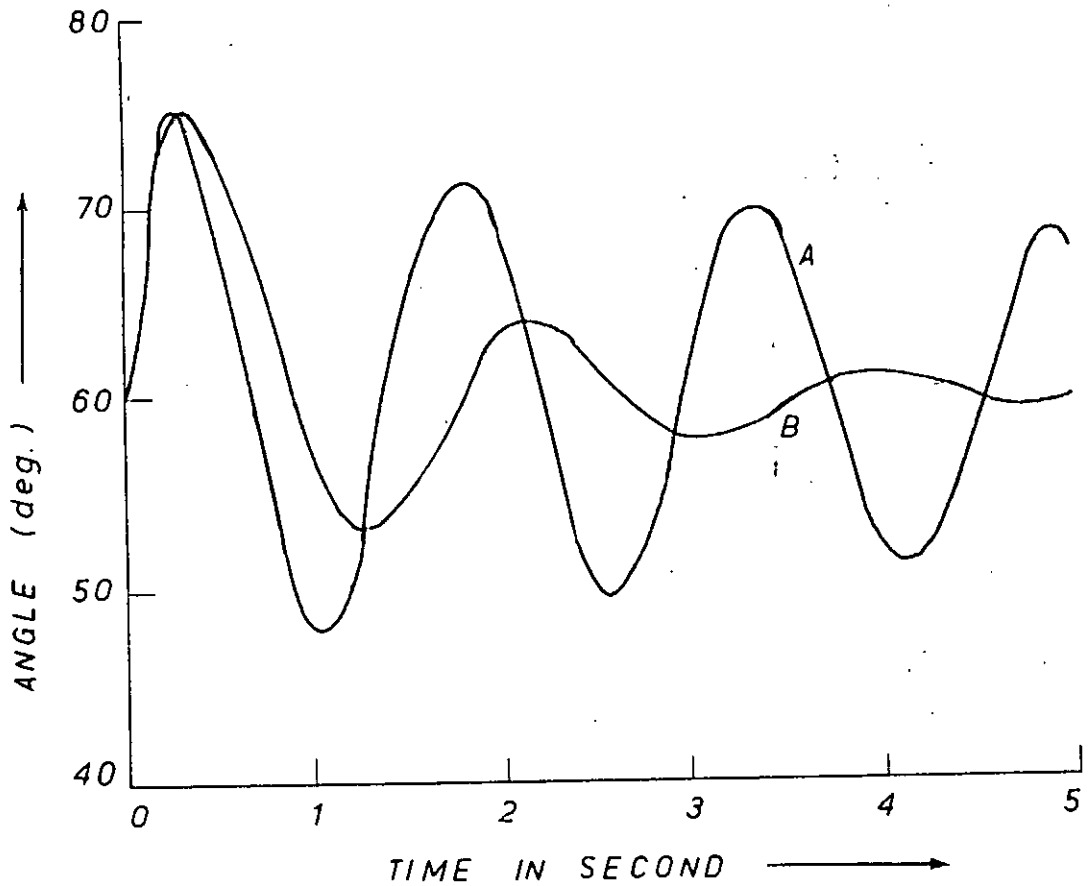

FIG. 5·5 SWING CURVES SHOWING EFFECT OF VELOCITY GAIN (THREE PHASE FAULT.).

A — WITH VOLTAGE FEEDBACK ONLY.

B — WITH VOLTAGE AND VELOCITY FEEDBACK ONLY.

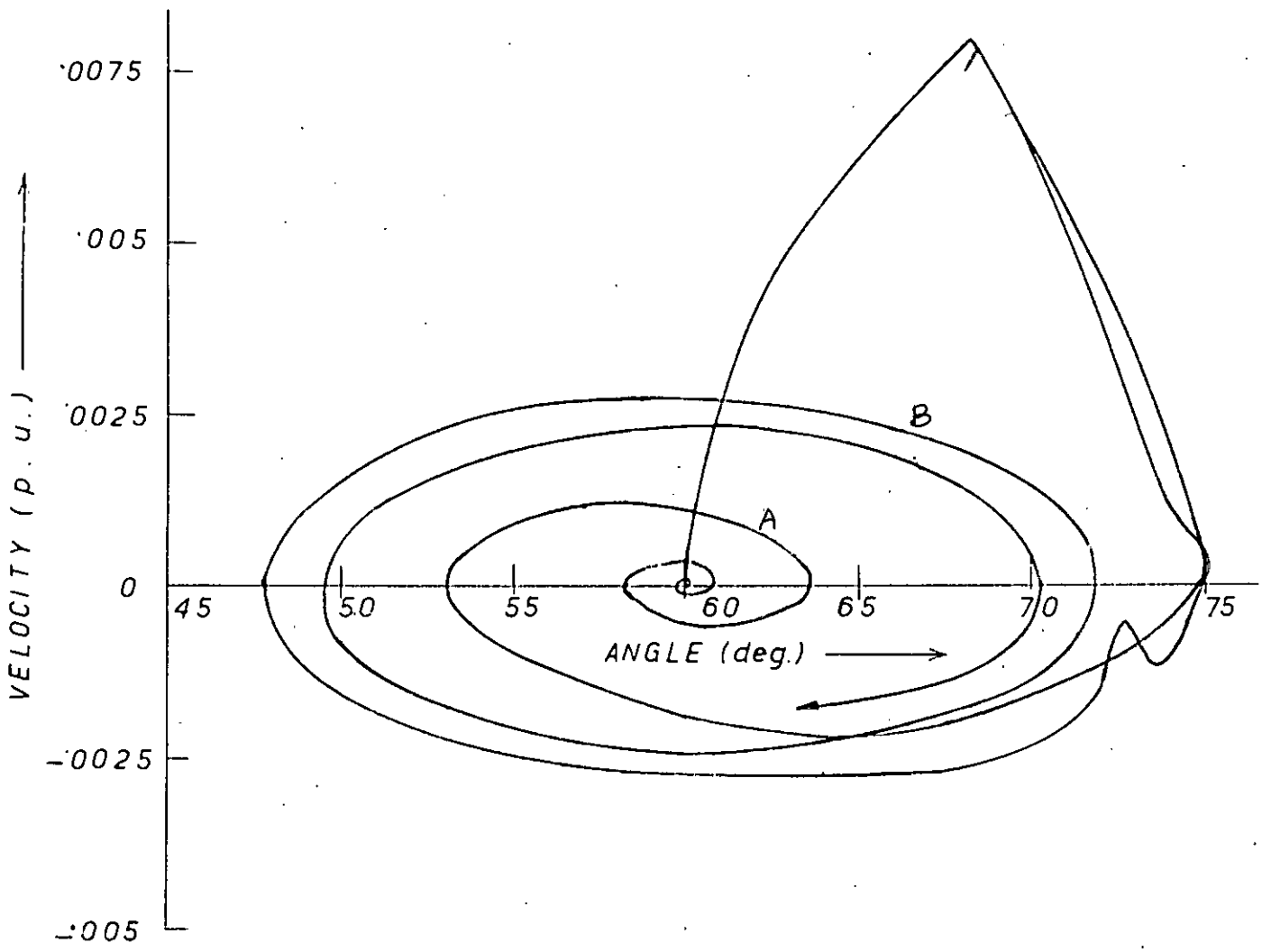

FIG. 5·6. VELOCITY ANGLE DIAGRAM FOR THREE PHASE FAULT,

A —— WITH VELOCITY SIGNAL.

B —— WITHOUT VELOCITY SIGNAL.

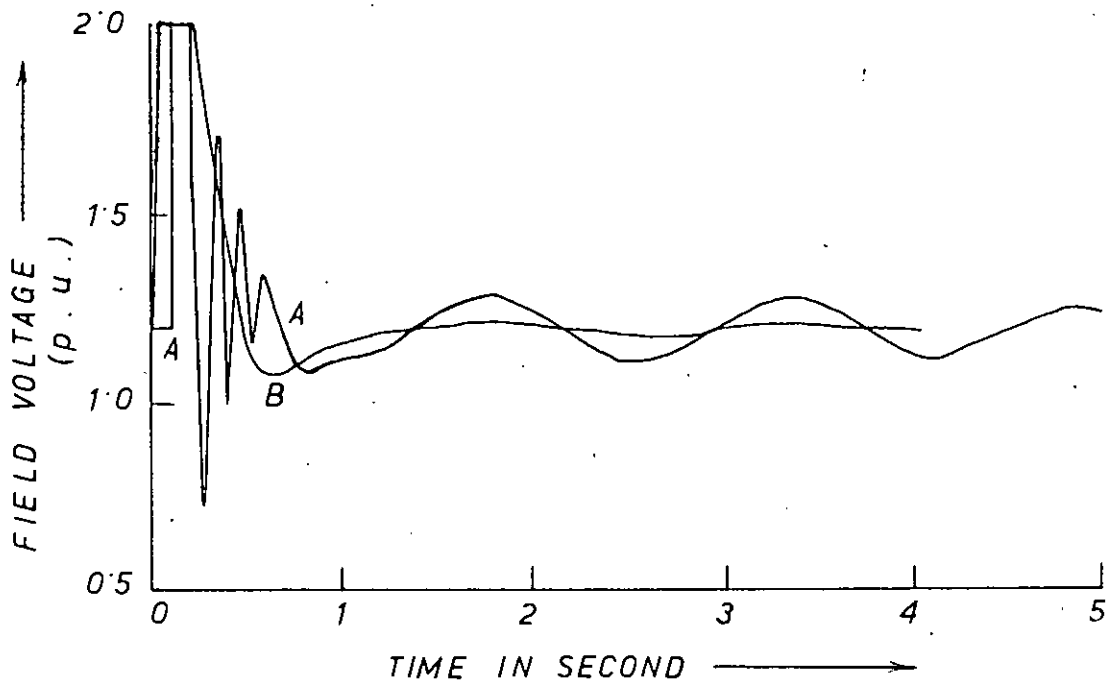

FIG. 5·7 (a) FIELD VOLTAGE CHARACTERISTICS FOR THREE PHASE FAULT.

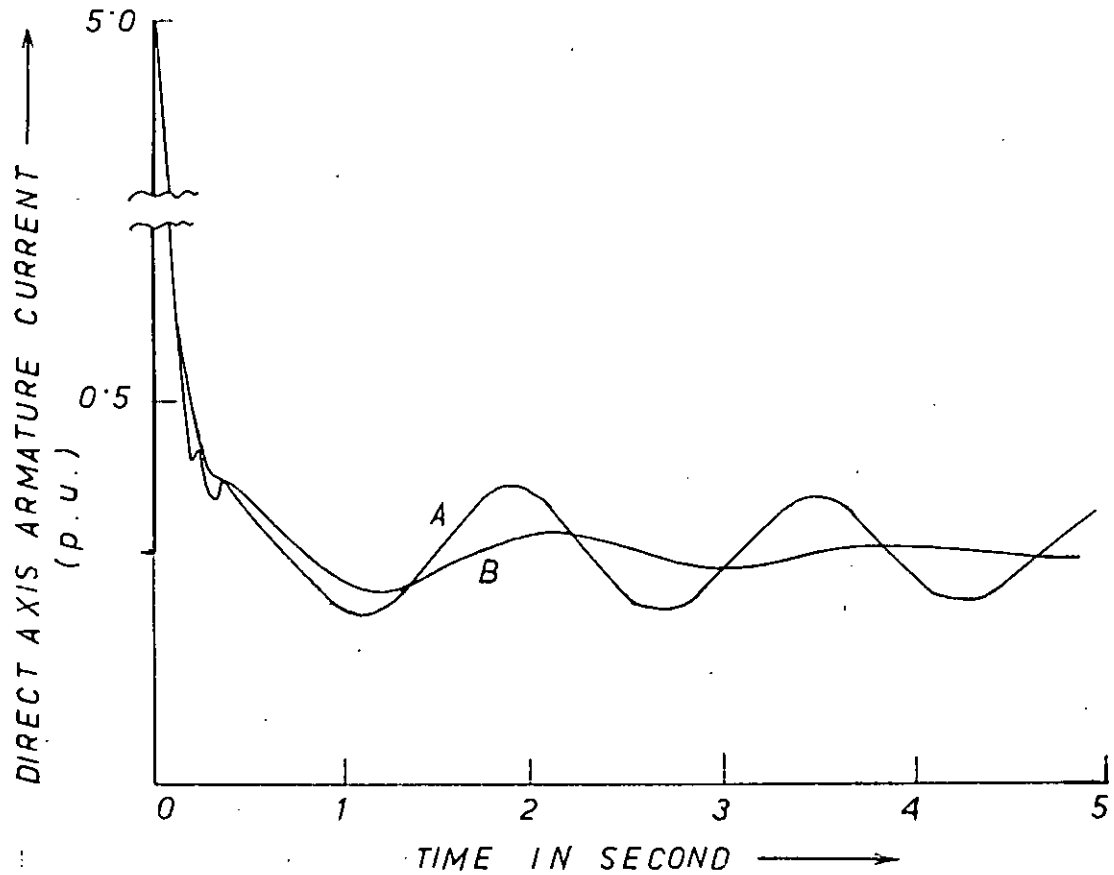

FIG. 5·7 (b) DIRECT AXIS ARMATURE CURRENT CHARACTERISTICS.

A — WITH VOLTAGE FEEDBACK ONLY.

B — WITH VOLTAGE AND VELOCITY FEEDBACK.

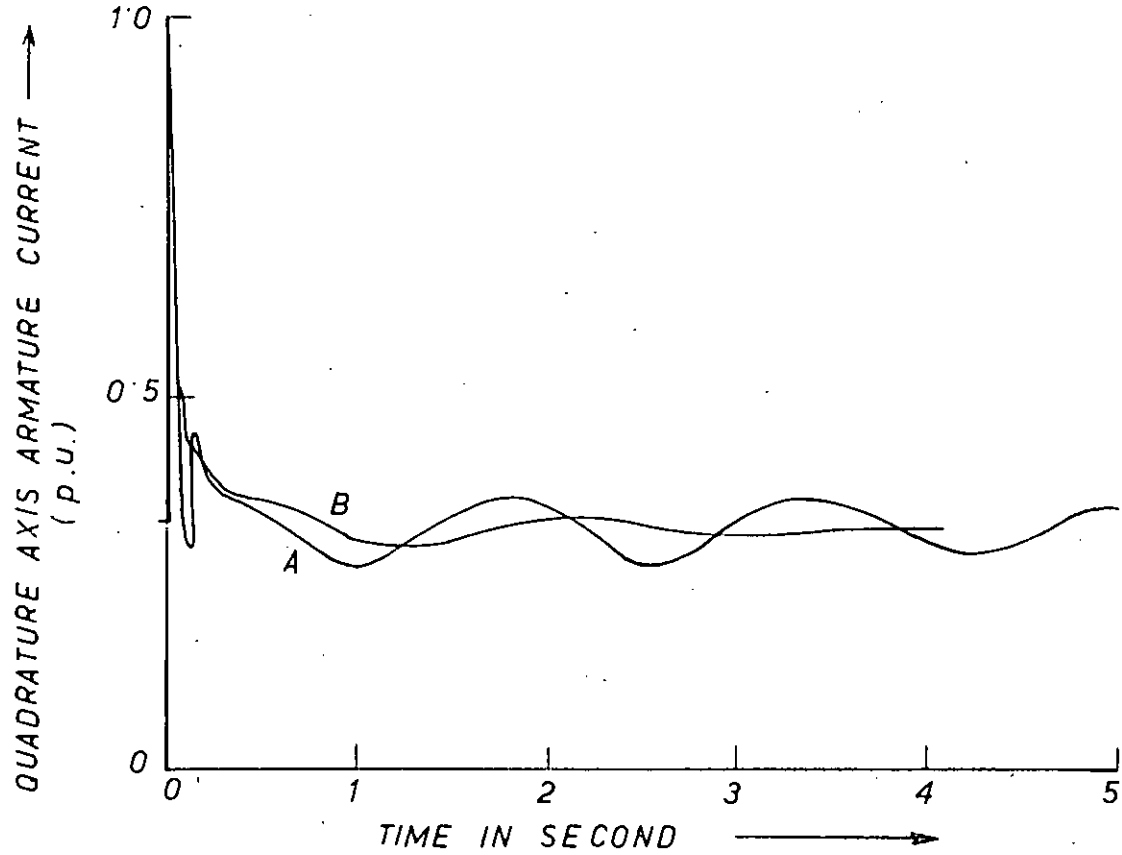

FIG. 57 (c) QUADRATURE AXIS ARMATURE CURRENT CHARACTERISTICS.

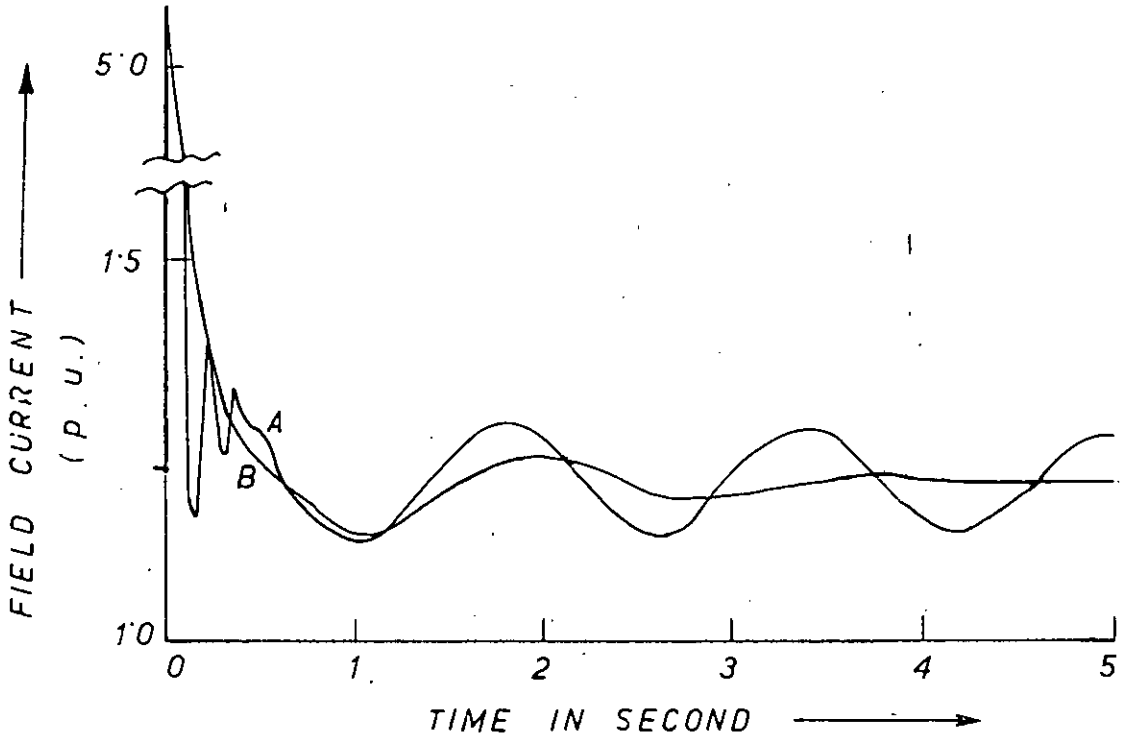

FIG. 5·7 (d) FIELD CURRENT VARIATION WITH TIME.

A — WITH VOLTAGE FEEDBACK ONLY

B — WITH VOLTAGE AND VELOCITY FEEDBACK.

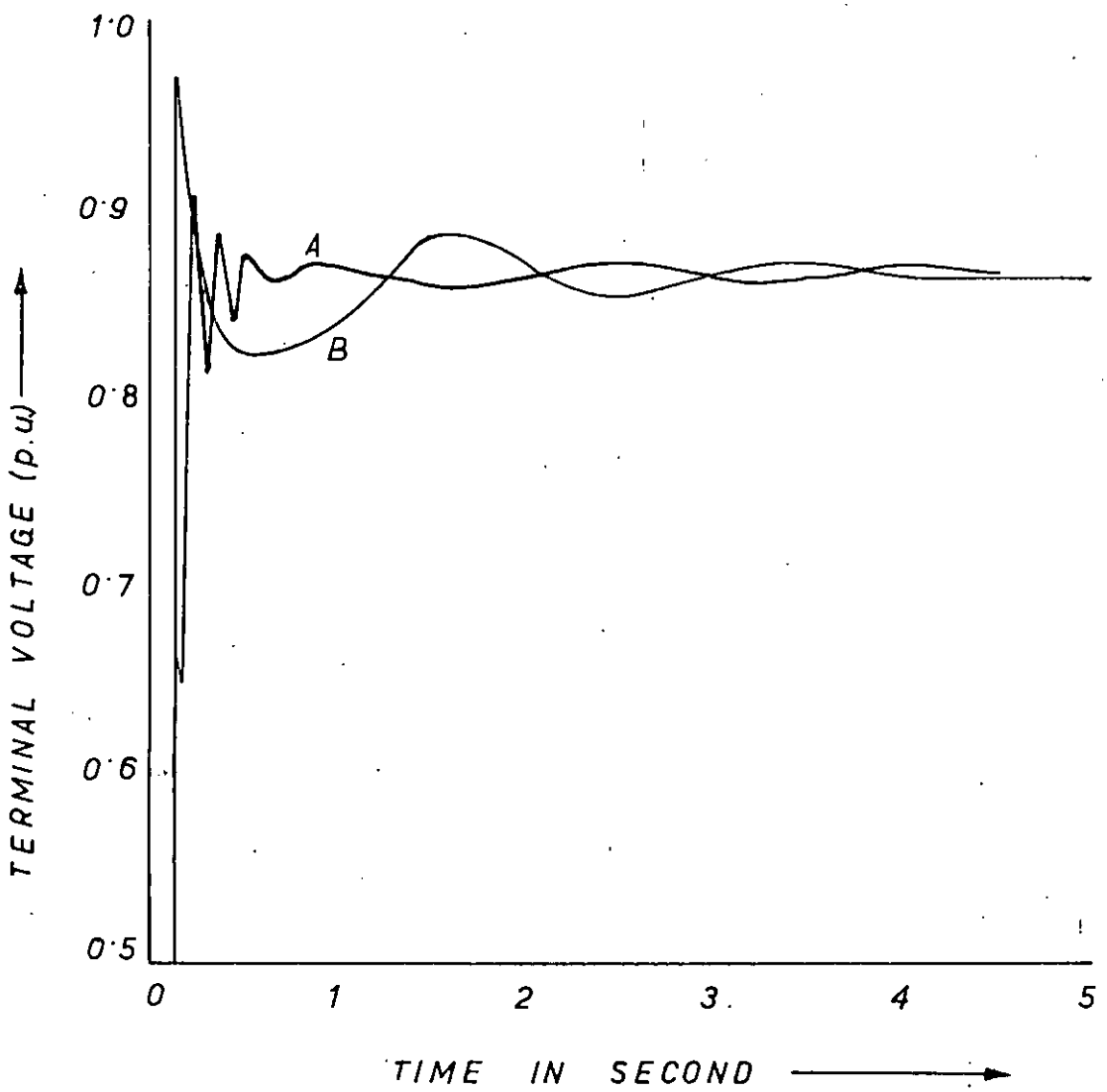

FIG. 5·7 (e) TERMINAL VOLTAGE VARIATION WITH TIME.

A —— WITH VOLTAGE FEEDBACK ONLY.

B —— WITH VOLTAGE AND VELOCITY FEEDBACK.

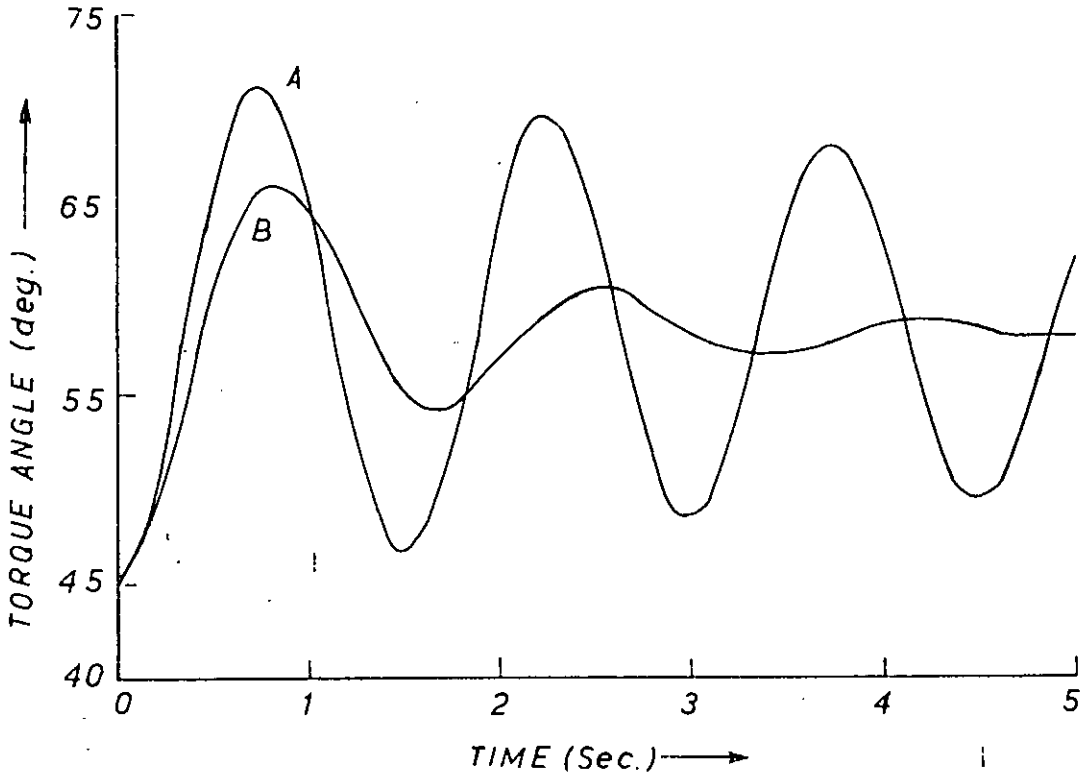

FIG. 5·8 TORQUE ANGLE CHARACTERISTICS FOR 25% TORQUE STEP.

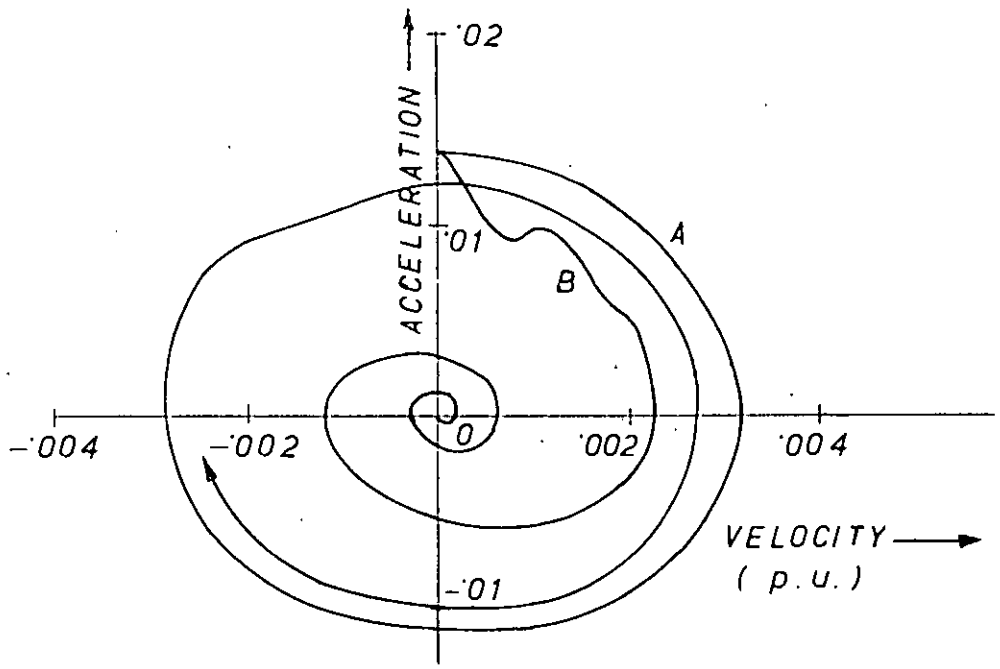

FIG. 5·9 ACCELERATION VS. VELOCITY FOR 25% TORQUE STEP.

A — WITH VOLTAGE FEEDBACK ONLY

B — WITH VOLTAGE AND VELOCITY FEEDBACK

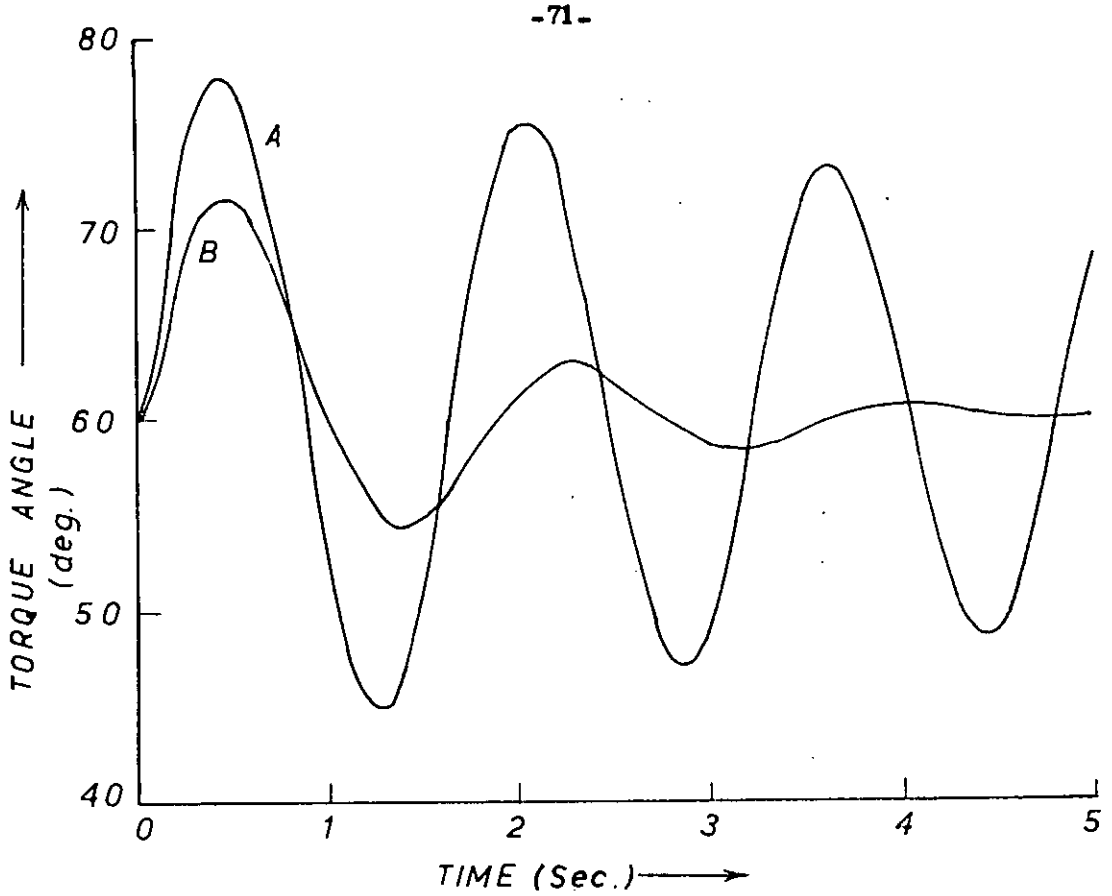

FIG. 5·10 TORQUE ANGLE VS. TIME FOR 50% TORQUE PULSE.

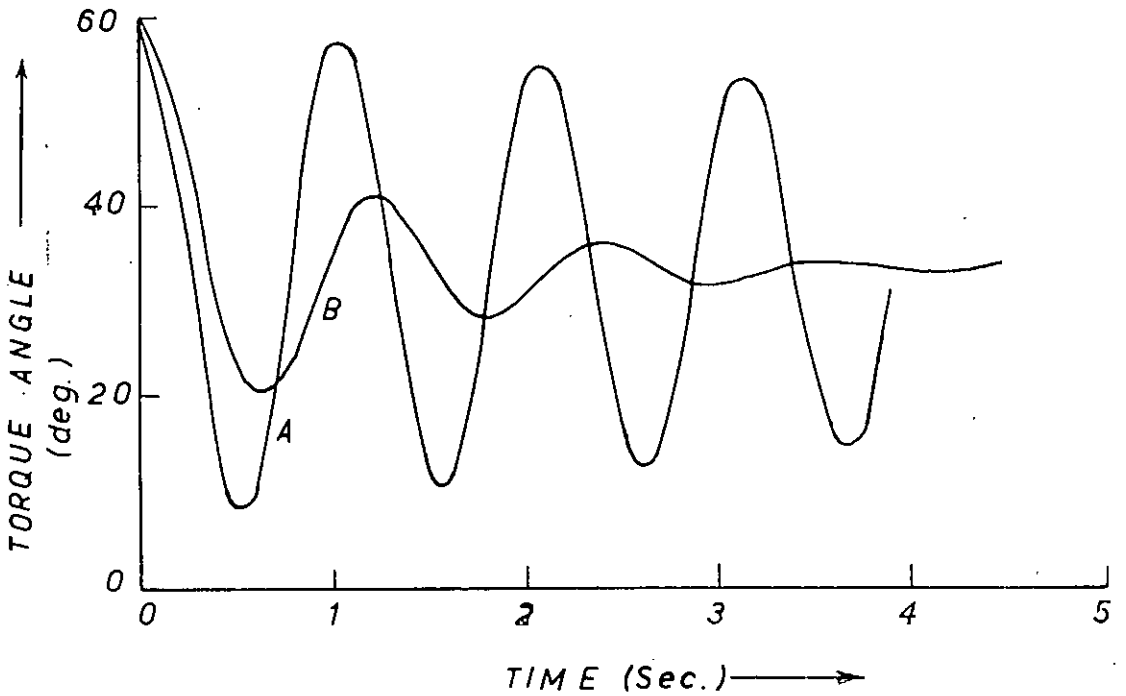

FIG. 5·11 ROTOR ANGLE VS. TIME FOR SWITCHING-ON OF A PARALLEL TRANSMISSION LINE.

A — WITH VOLTAGE FEEDBACK ONLY
B — WITH VOLTAGE AND VELOCITY FEEDBACK.

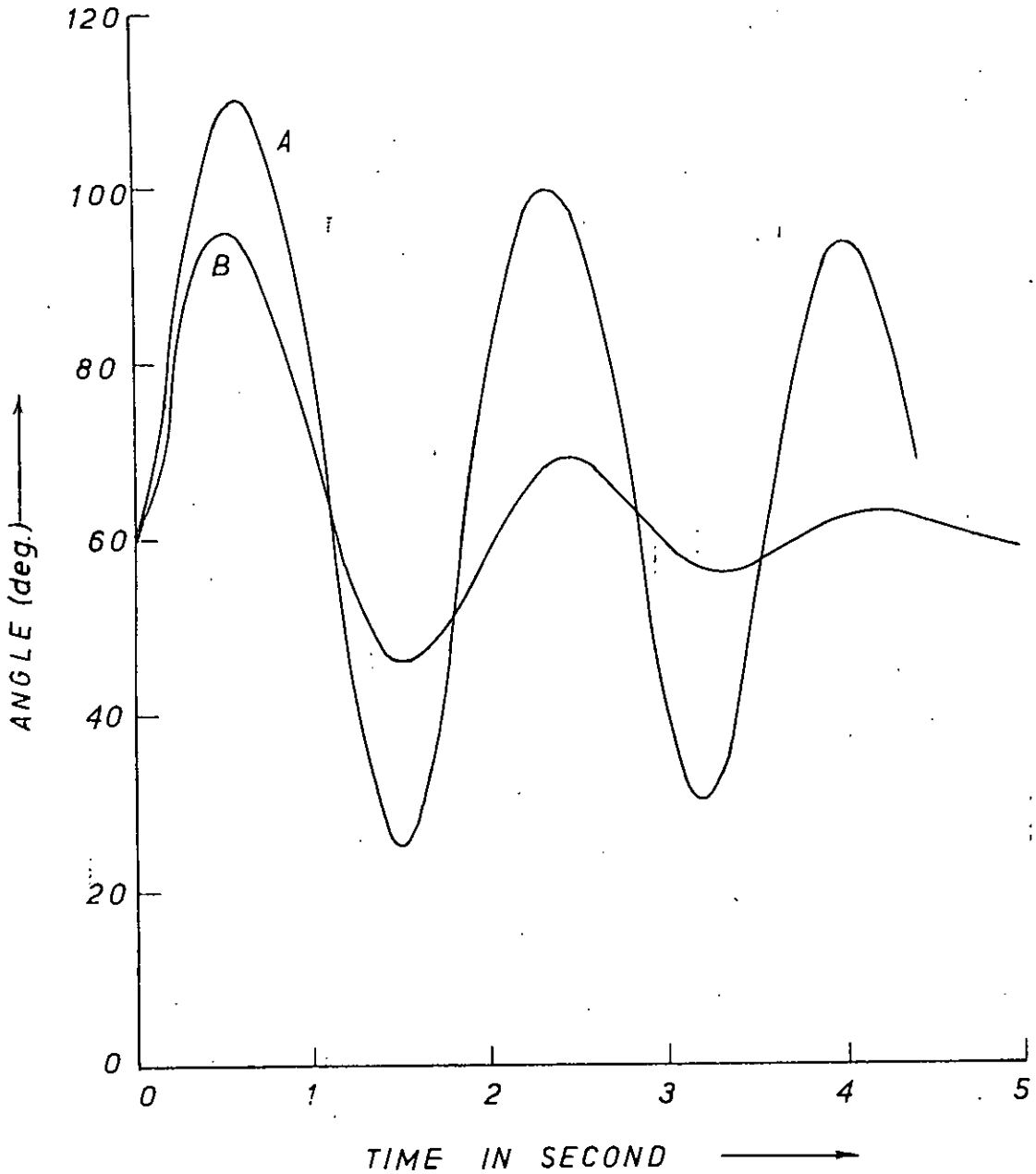

FIG. 5.12 ROTOR ANGLE VARIATION FOR THREE PHASE FAULT AT THE MIDDLE OF TRANSMISSION LINE.

A — WITH VOLTAGE FEEDBACK ONLY.

B — WITH VOLTAGE & VELOCITY FEEDBACK.

5.4 Field Current

In conjunction with normal voltage regulator action, a signal proportional to the field current deviation from steady state operating point was tried as a stabilizing signal. It was observed that a suitable combination of velocity and magnitude of field current deviation signal provided enough positive damping for the system. The field current signal alone and a combination of velocity and field current deviation (not magnitude) did not show at all any improvement in transient stability.

Different combinations of velocity and field current signals were considered for a 3 phase short circuit at the generator terminals. Fig. 5.13 is a comparative study of the different amount of combinations of velocity and field current signals. It was observed that the best gain for field current deviation with 20 times rotor velocity was - 0.5. Too large a gain makes the response oscillatory and may even make the system unstable. But this combination deteriorates transient stability for all type of disturbances except a three phase fault at the machine terminals. For other types of disturbances the first rotor excussion increases and settling time becomes greater than that with velocity signal only. But a gain of + 0.5 was seen to improve transient stability for all types of disturbance except that for a three phase fault the above gain gives a larger first rotor excussion withoutdetrimenting other quantities like settling time etc. This is quite apparent from fig. 5.13.

Fig. 5.15 - 5.18 show the effect of field current deviation signal on different types of system disturbances. The disturbances considered are 25% torque step, 50% torque pulse for 6 cycles, a three phase fault at middle of transmission line and a switching-in a parallel transmission line. The results for these different cases are tabulated at the end of the chapter.

A combination of velocity signal and magnitude of field current deviation signal showed sufficient improvement of transient stability over velocity signal alone. Since disturbances like torque steps etc. effect a shift in the steady field current it is quite expected, that this additional signal in the exciter forces the system to settle at a point different from the expected stable equilibrium state.

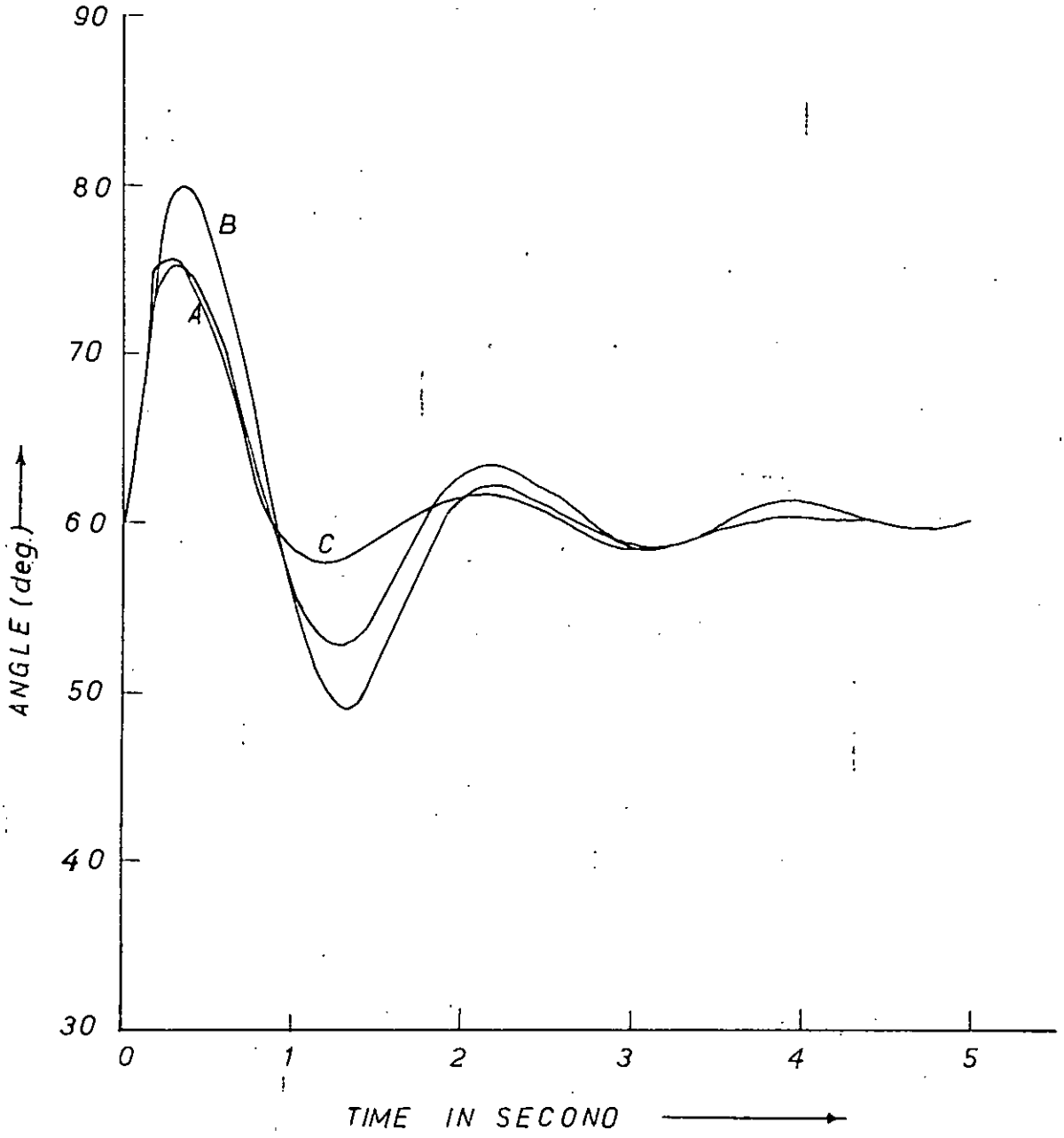

FIG. 5·13 SWING CURVE FOR A THREE PHASE FAULT

A — WITH VELOCITY SIGNAL ONLY
B — WITH VELOCITY AND + $|\Delta i_{fd}|$ SIGNAL
C — WITH VELOCITY AND − $|\Delta i_{fd}|$ SIGNAL

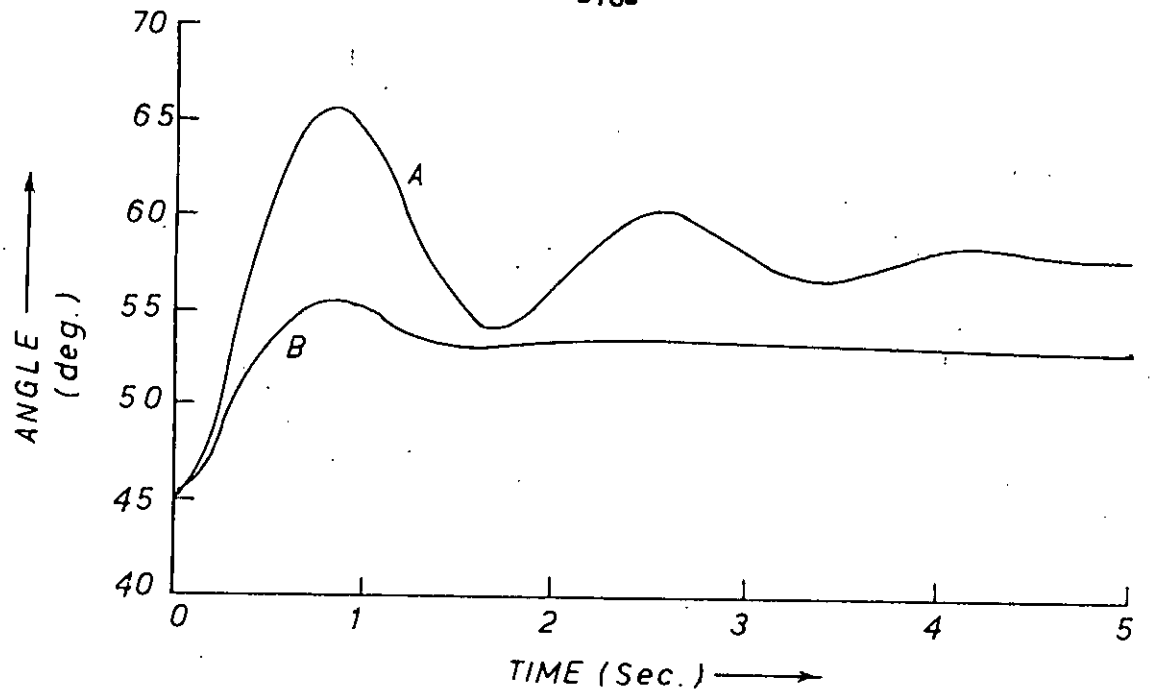

FIG. 5·14 TORQUE ANGLE CHARACTERISTICS FOR 25% TORQUE STEP.

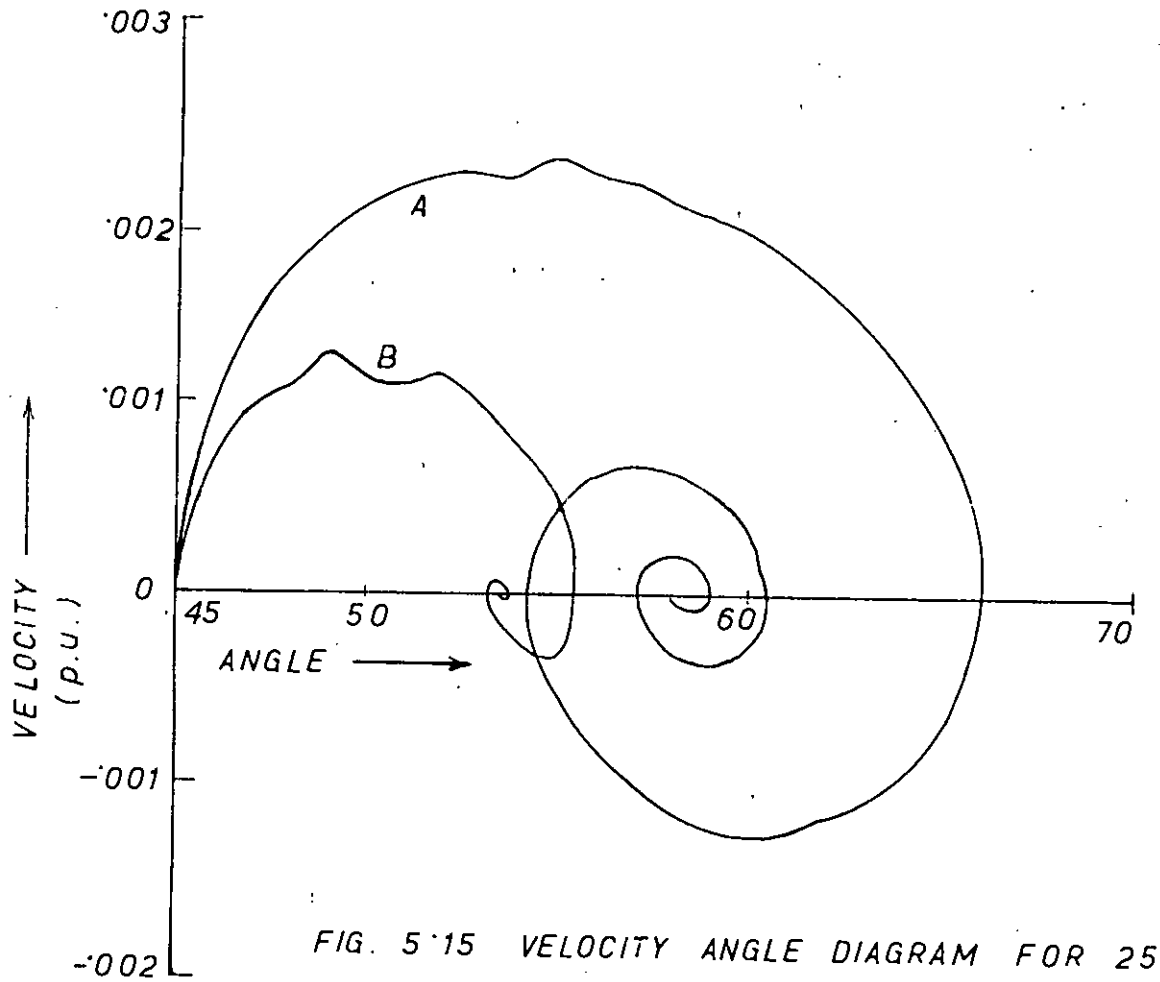

FIG. 5·15 VELOCITY ANGLE DIAGRAM FOR 25% TORQUE STEP.

A — WITH VELOCITY SIGNAL

B — WITH VELOCITY AND FIELD CURRENT SIGNAL.

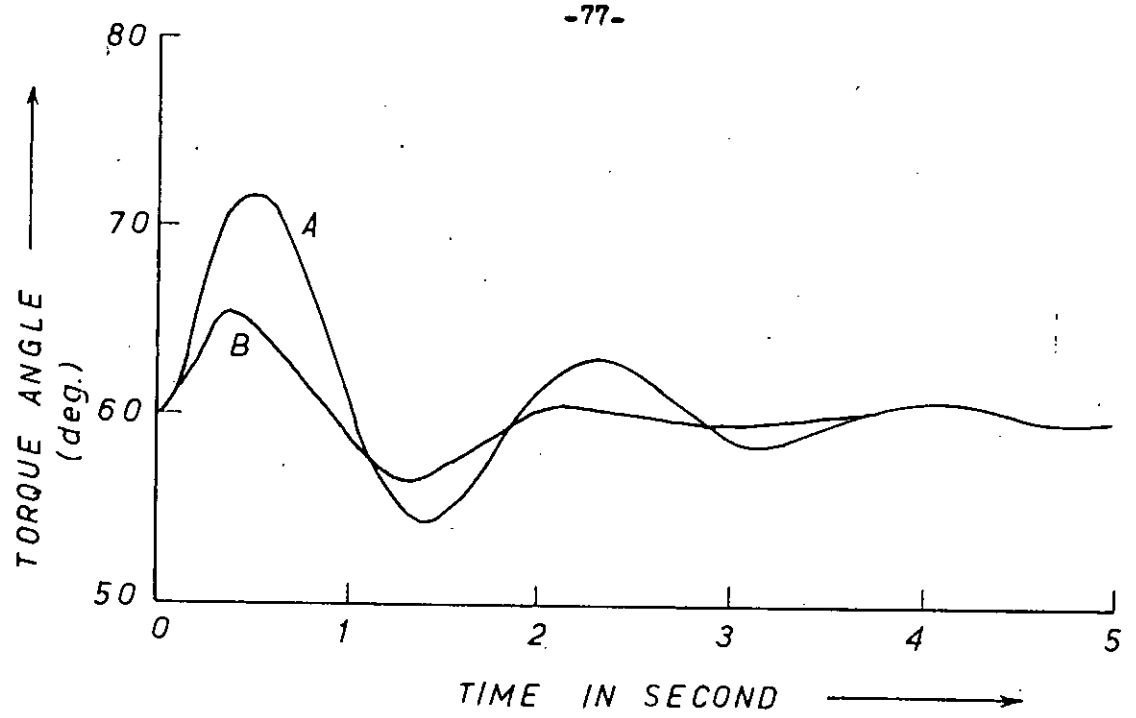

FIG. 5·16 ROTOR ANGLE VS. TIME FOR 50% TORQUE PULSE.

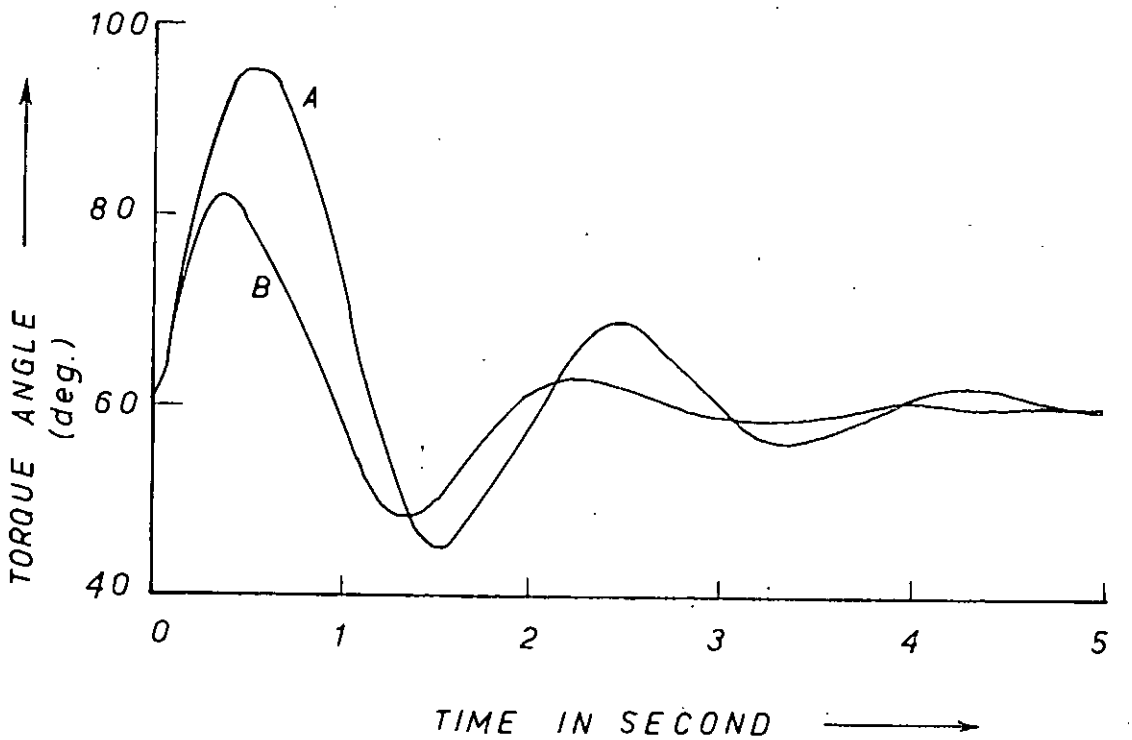

FIG. 5·17 ROTOR ANGLE OSCILLATION FOR A THREE PHASE FAULT AT MIDDLE OF TRANSMISSION LINE.

A — WITH VELOCITY SIGNAL.
B — WITH VELOCITY AND FIELD CURRENT SIGNAL.

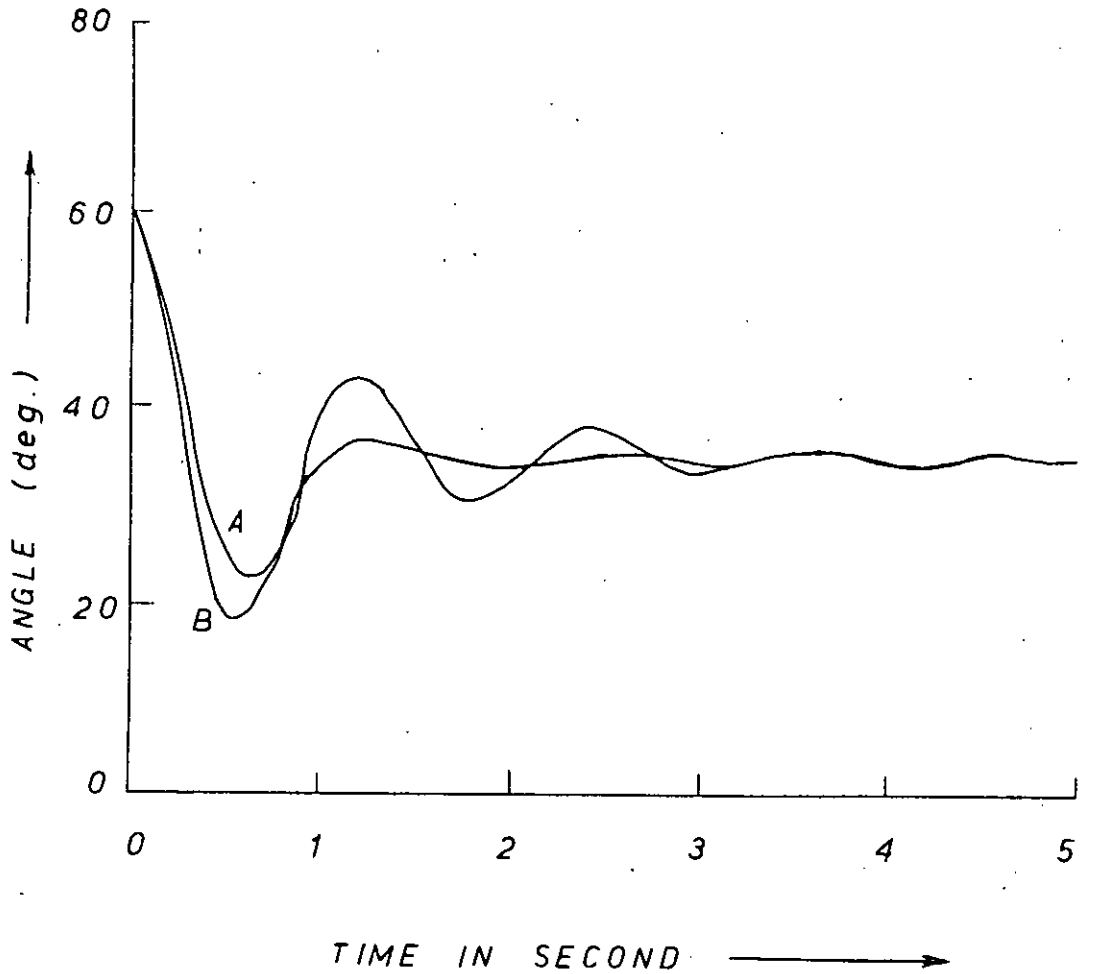

FIG. 5.18. ROTOR ANGLE VS. TIME FOR SWITCHING-ON OF A PARALLEL TRANSMISSION LINE.

A — WITH VELOCITY ONLY

B — WITH VELOCITY AND FIELD CURRENT SIGNAL

5.5 Armature Current

Auxiliary stabilizing signal proportional to the deviation of armature current from steady state value was fed to the exciter of the synchronous generator. The armature current deviation signal alone showed no improvement of transient stability. But some improvement in transient stability was observed when the magnitude of the armature current signal was combined with velocity feedback signal for a 3-ϕ short circuit at the generator terminals. Fig. 5.19 shows the swing curve and phase plane trajectories ~~respectively~~ for this case. A gain of -0.6 was employed in the armature current feedback loop. For other types of disturbances such as torque step, pulse etc. this combination of armature current and velocity gives rise to unstable situation.

A different combination + 0.4 times the armature current deviation with 20 times the speed deviation results in sufficient improvement of transient stability for all disturbances like step, pulse etc. Different states and trajectories are plotted in Fig. 5.20 - 5.23. For a three phase fault at machine terminals this combination of armature current and velocity makes the system unstable. Thus the armature current deviation signal results in improvement of transient stability for some types of disturbances and worsens response for others. Since the type of disturbance in a power system is unpredictable a general armature current deviation feedback scheme can not be used for power system stabilization.

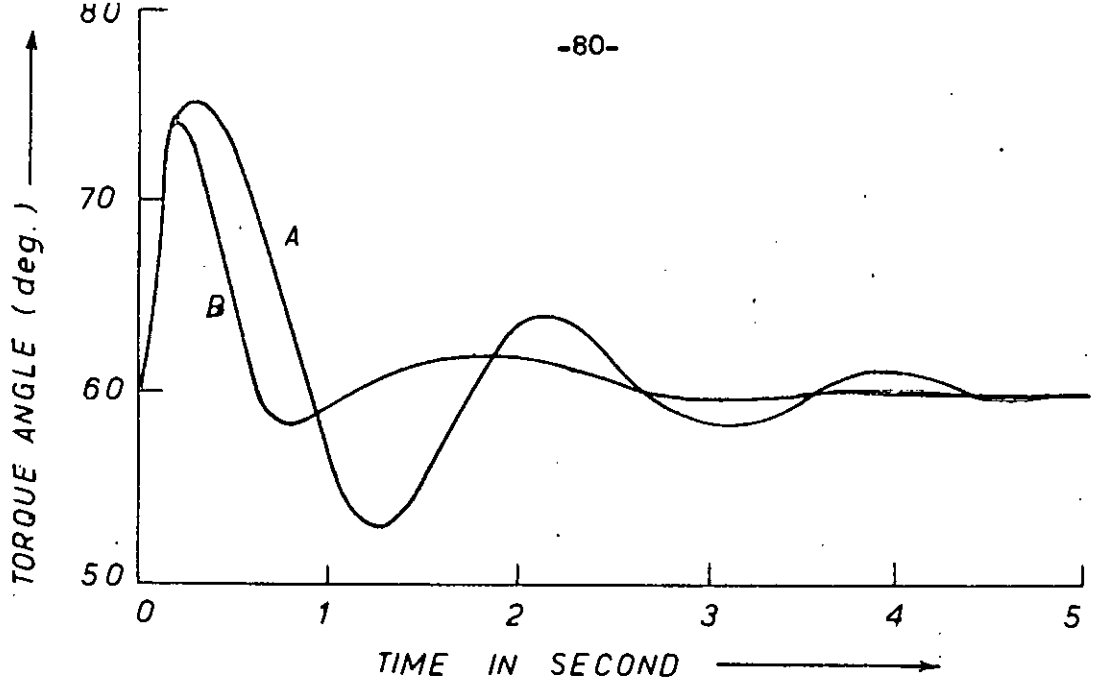

FIG. 5 19(A). SWING CURVES SHOWING EFFECT OF ARMATURE CURRENT DEVIATION SIGNAL 3Ø FAULT.

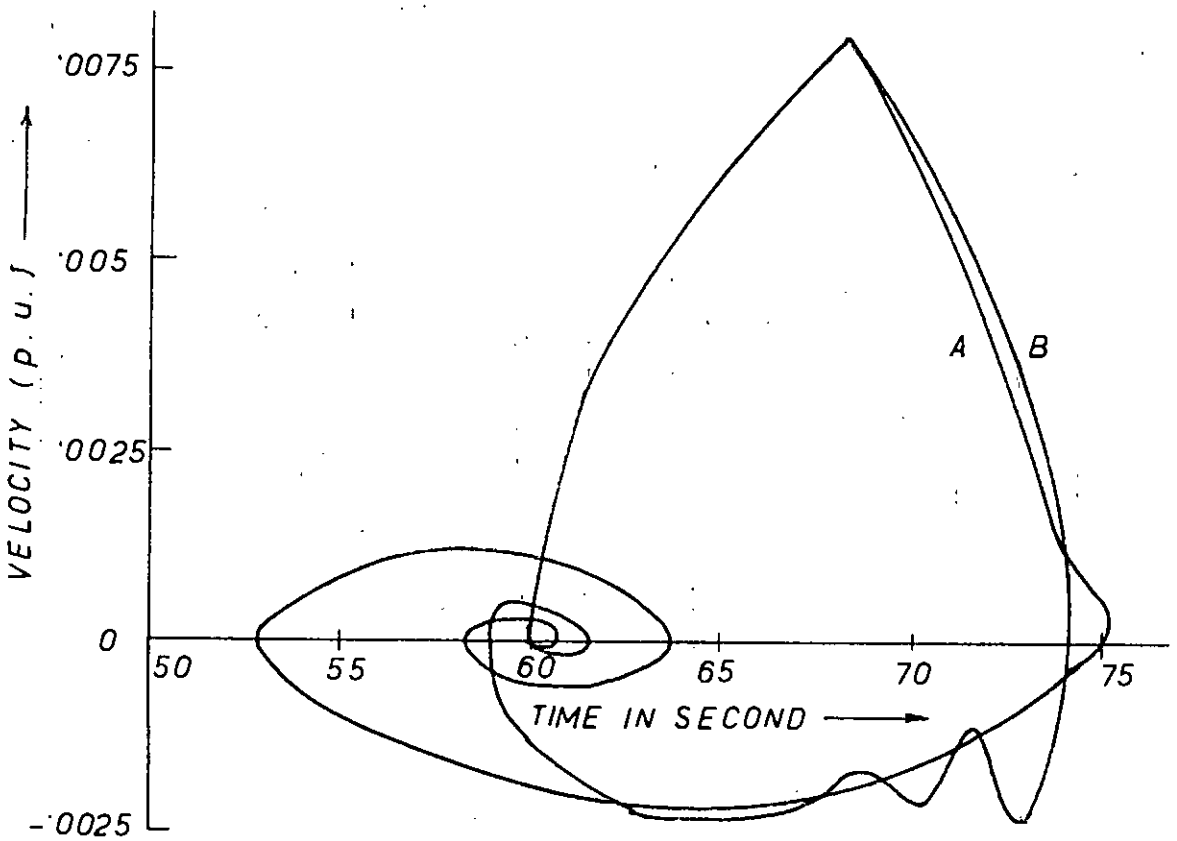

FIG. 5 19(B). VELOCITY ANGLE DIAGRAM FOR 3Ø FAULT.

A — WITH VELOCITY SIGNAL

B — WITH VELOCITY AND $|\Delta i_a|$ SIGNAL.

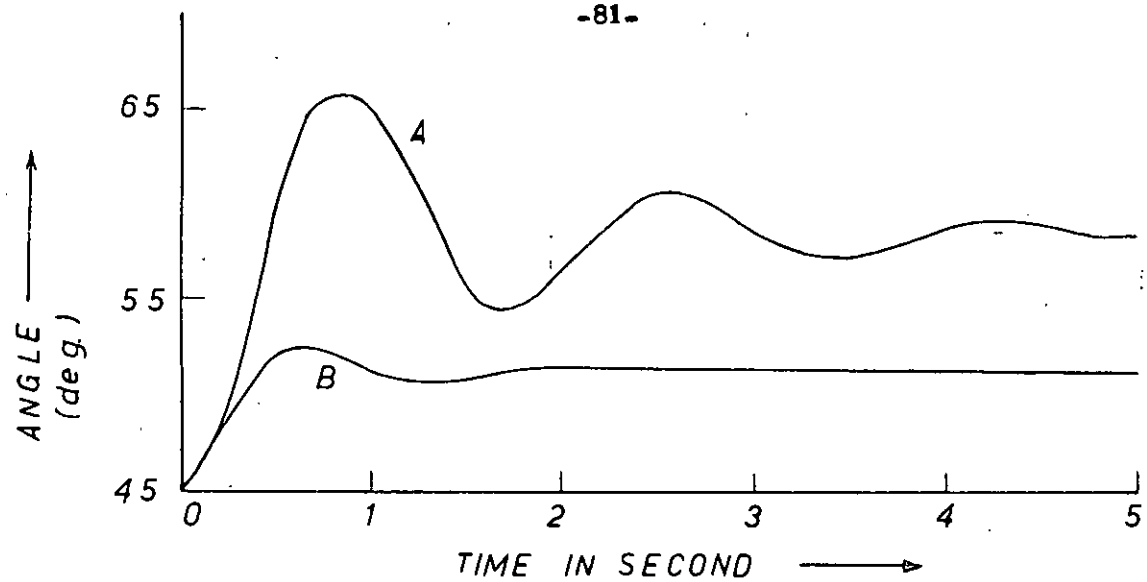

FIG. 5·20 TORQUE ANGLE CHARACTERISTICS FOR 25% TORQUE STEP.

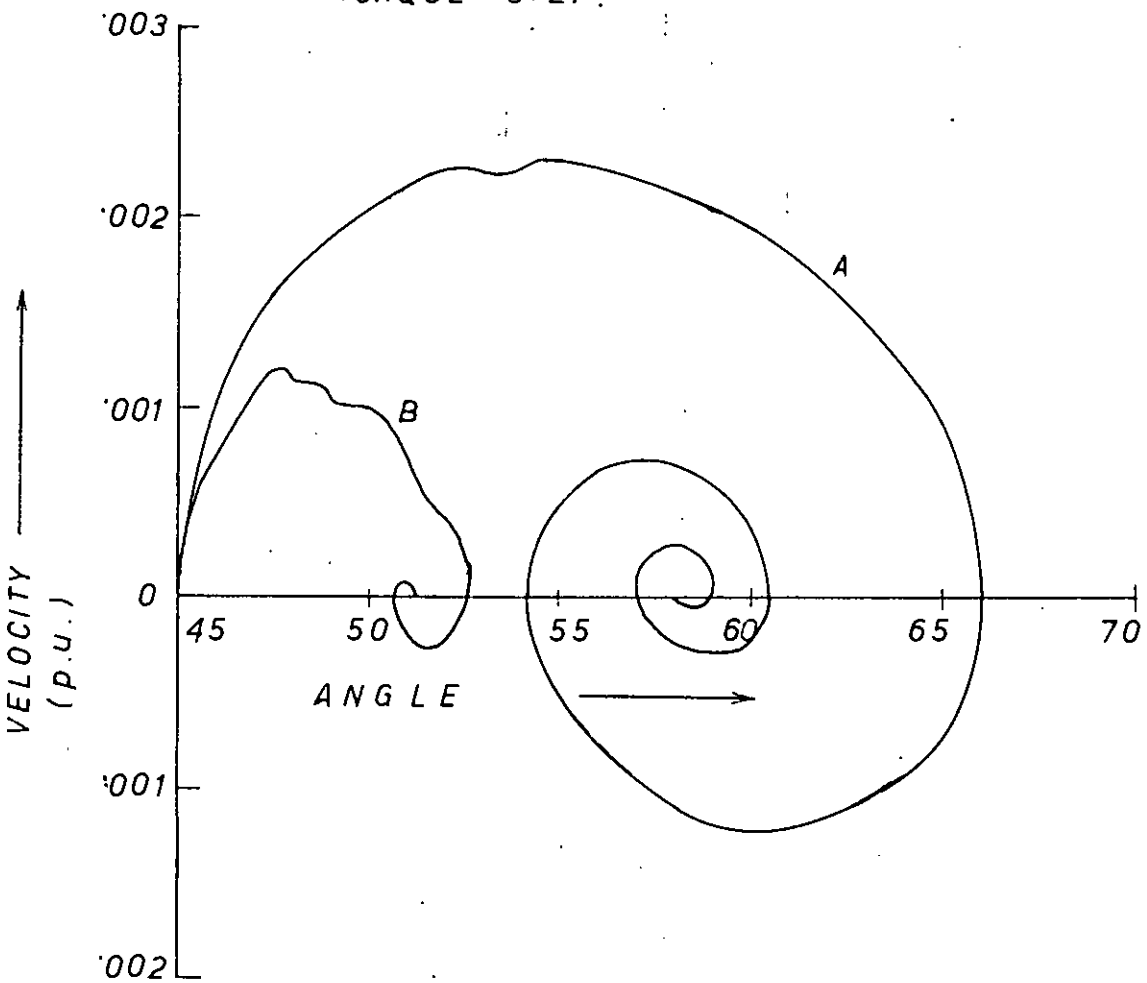

FIG. 5·21. VELOCITY ANGLE DIAGRAM FOR 25% TORQUE STEP.

A — WITH VELOCITY SIGNAL ONLY
B — WITH VELOCITY AND ARMATURE CURRENT SIGNAL.

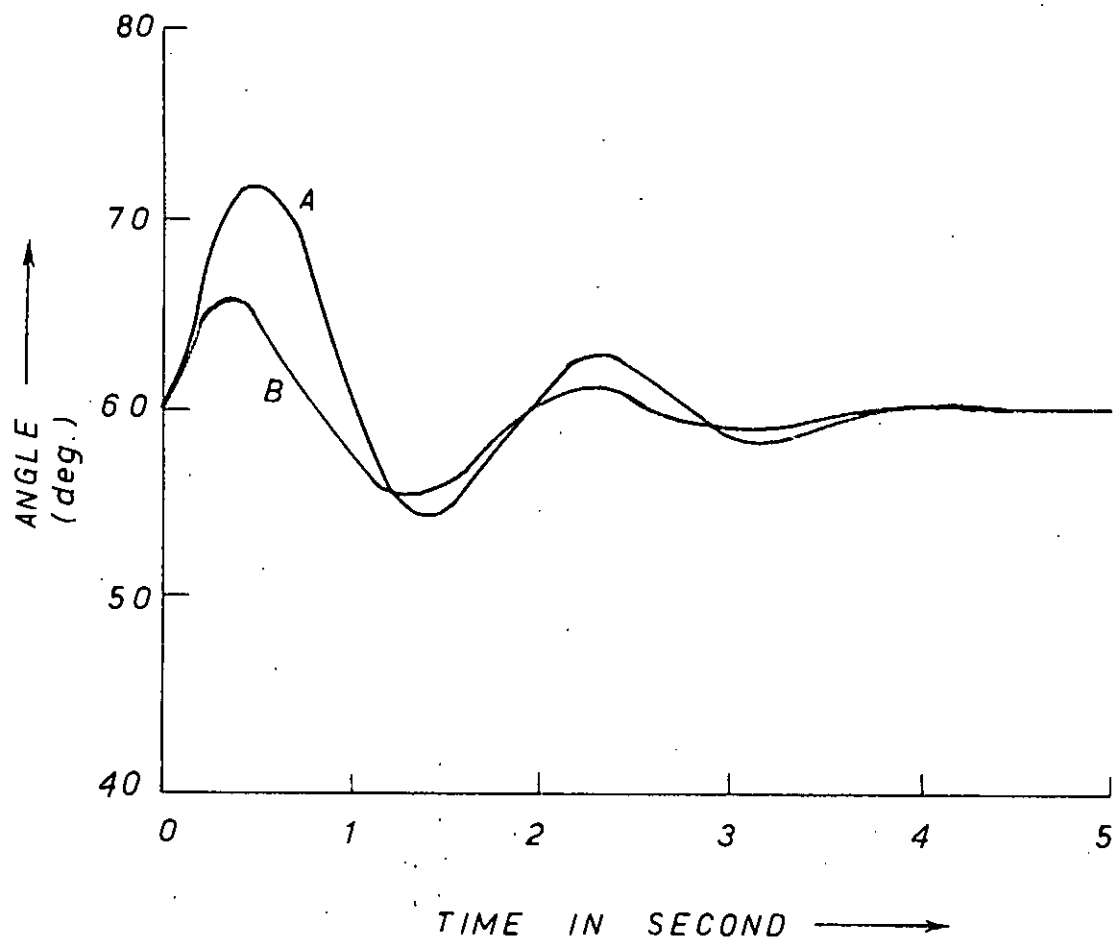

FIG. 5·22 ROTOR ANGLE VS. TIME FOR 50% TORQUE PULSE.

A — WITH VELOCITY SIGNAL
B — WITH VELOCITY AND $|\Delta i_a|$ SIGNAL.

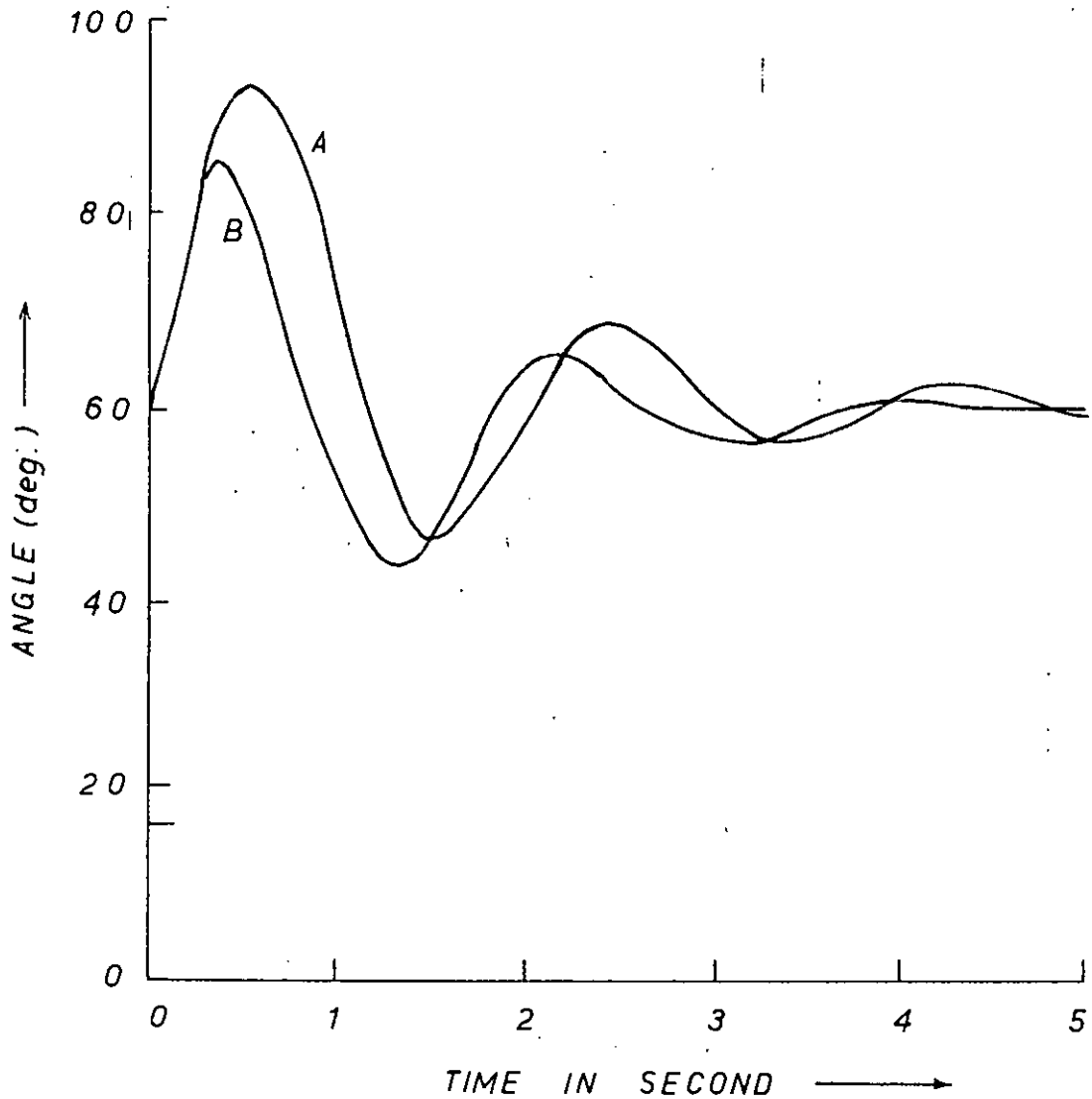

FIG. 5.23 ROTOR ANGLE OSCILLATION FOR THREE PHASE FAULT AT MIDDLE OF TRANSMISSION LINE.

A — WITH VELOCITY SIGNAL

B — WITH VELOCITY AND $|\Delta i_a|$ SIGNAL.

5.6 Torque Angle

A control derived from the change of torque angle (δ) from the steady operating value was fed to the exciter in combination with velocity signal. Swing curves and phase portraits for a number of test cases have been presented in Figures 5.24 - 5.29. Various combinations of velocity and rotor angle signals were attempted. It has been observed that best response is obtained when the gain factor with rotor angle deviation is 1.00.

As can be seen from the figures, the rotor angle feedback signal is most effective in controlling the transients. The settling time is significantly small compared to that for velocity feedback only. For a 25% torque step (Fig. 5.25) the rotor angle deviation and velocity combination brings the system to a stable equilibrium point with simply one overshoot and an undershoot where as with velocity signal only, the system returns to the equilibrium point with a number of oscillations.

As in the case of field current feedback, the rotor angle deviation signal changes the nominal excitation voltage, thus changing the output power level. So for various disturbances like torque steps, pulses, switching-in and out of transmission lines etc. the steady operating point gets shifted from the desired equilibrium points.

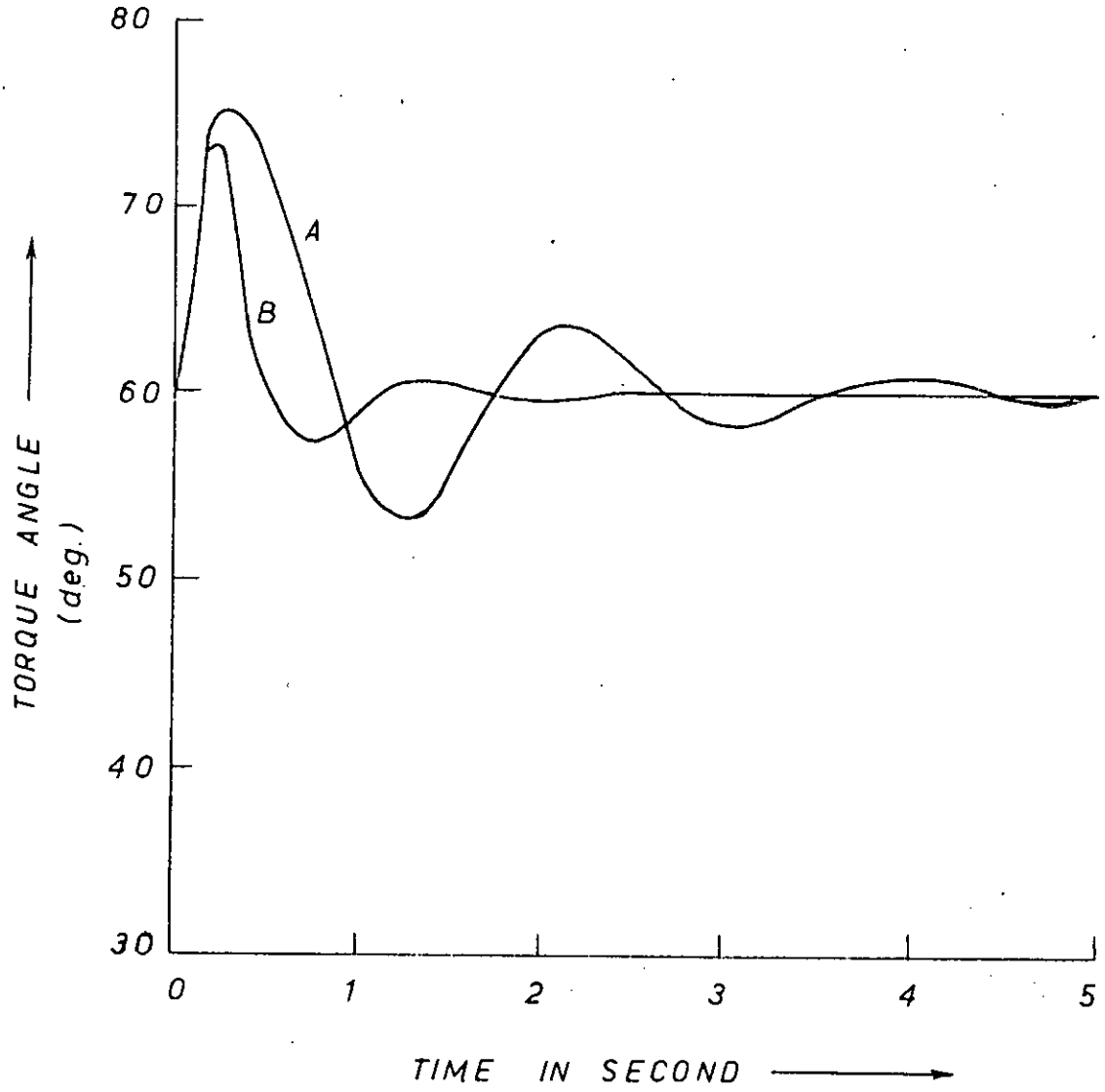

FIG. 5·24 SWING CURVES SHOWING EFFECT OF TORQUE ANGLE DEVIATION SIGNAL FOR 3Ø FAULT.

A — VELOCITY ONLY.

B — VELOCITY AND ANGLE DEVIATION SIGNAL.

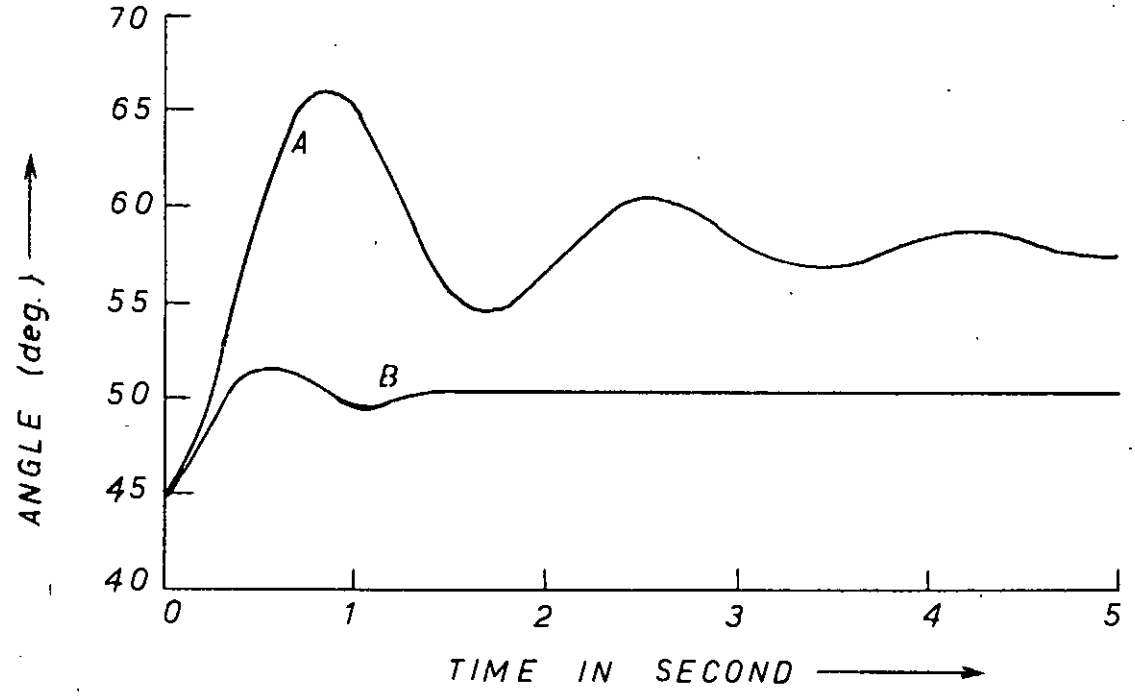

FIG. 5·25 TORQUE ANGLE CHARACTERISTICS FOR 25% TORQUE STEP.

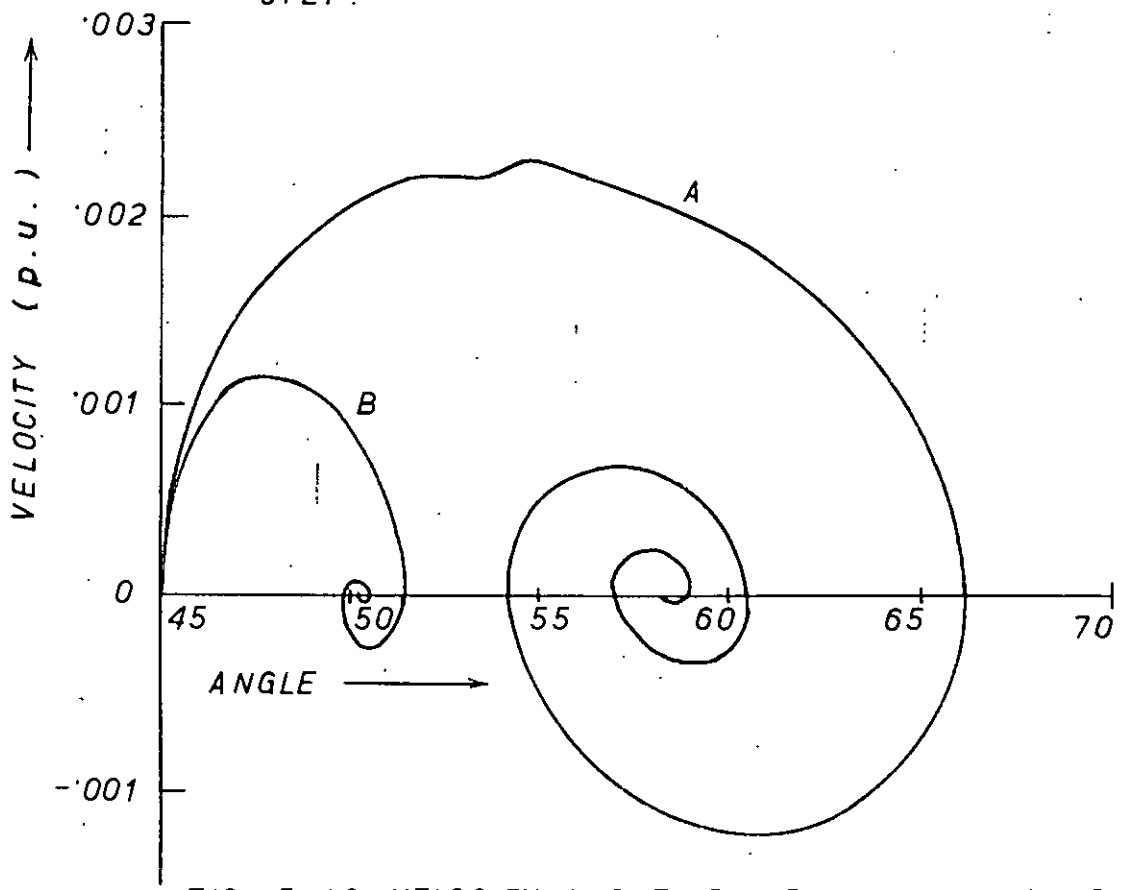

FIG. 5·26 VELOCITY ANGLE DIAGRAM FOR A STEP (25%) INPUT.

A —— WITH VELOCITY SIGNAL ONLY.

B —— WITH VELOCITY & $\Delta\delta$ SIGNAL.

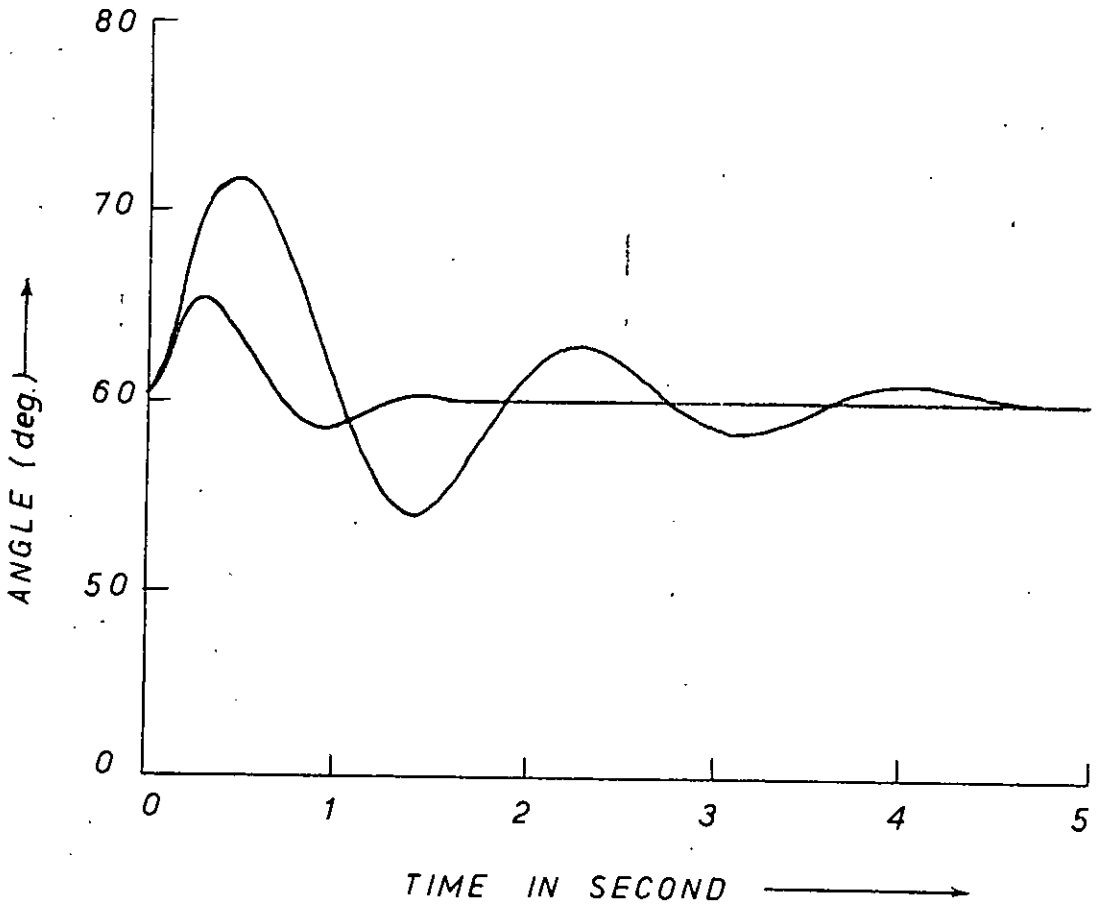

FIG. 5·27 ROTOR ANGLE VS. TIME FOR 50% TOROUE PULSE.

A — WITH VELOCITY SIGNAL.
B — WITH VELOCITY AND $\Delta\delta$ SIGNAL.

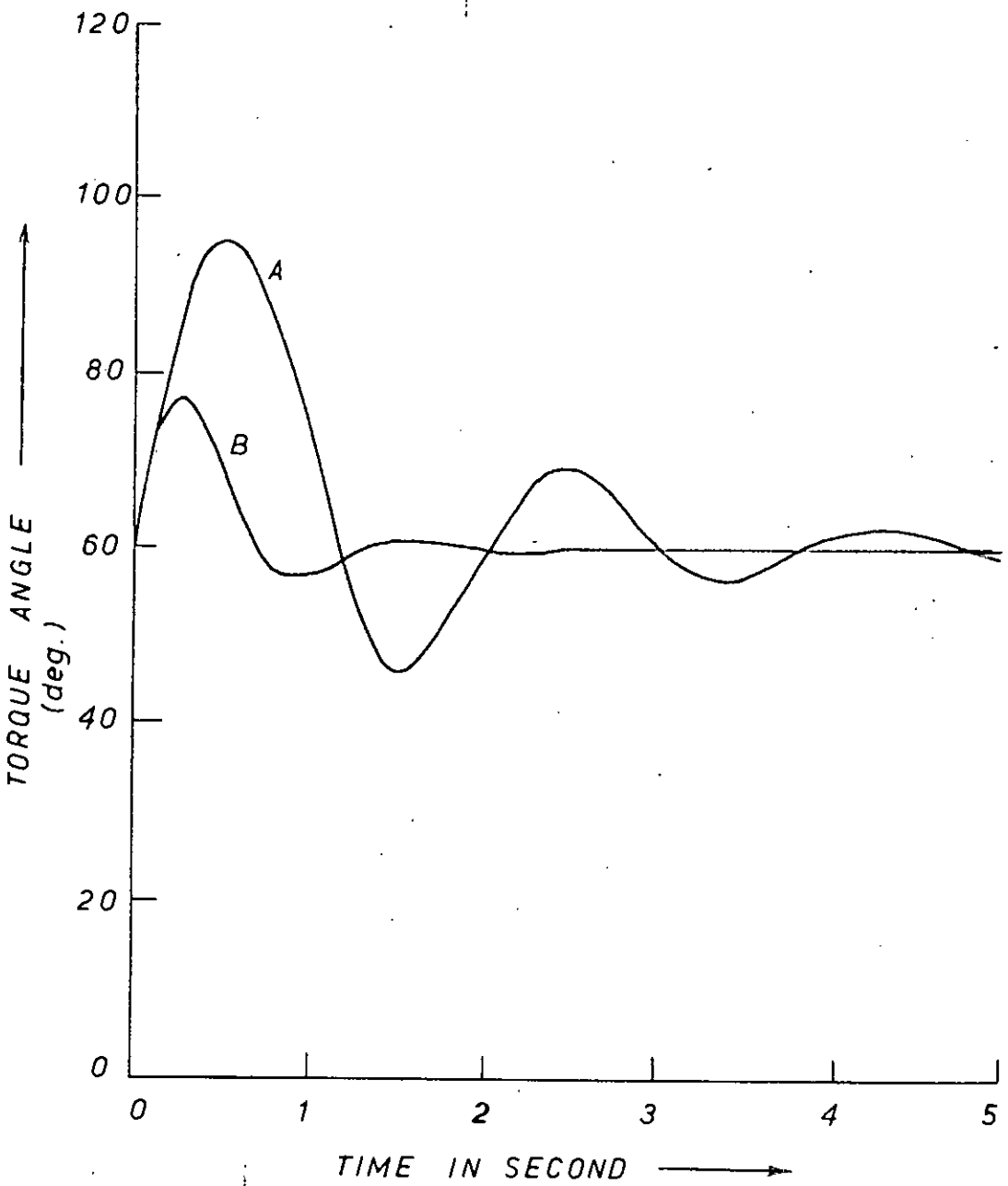

FIG. 5·28 ROTOR ANGLE OSCILLATION FOR THREE PHASE FAULT AT MIDDLE OF TRANSMISSION LINE.

A — WITH VELOCITY SIGNAL.
B — WITH VELOCITY AND $\Delta\delta$ SIGNAL.

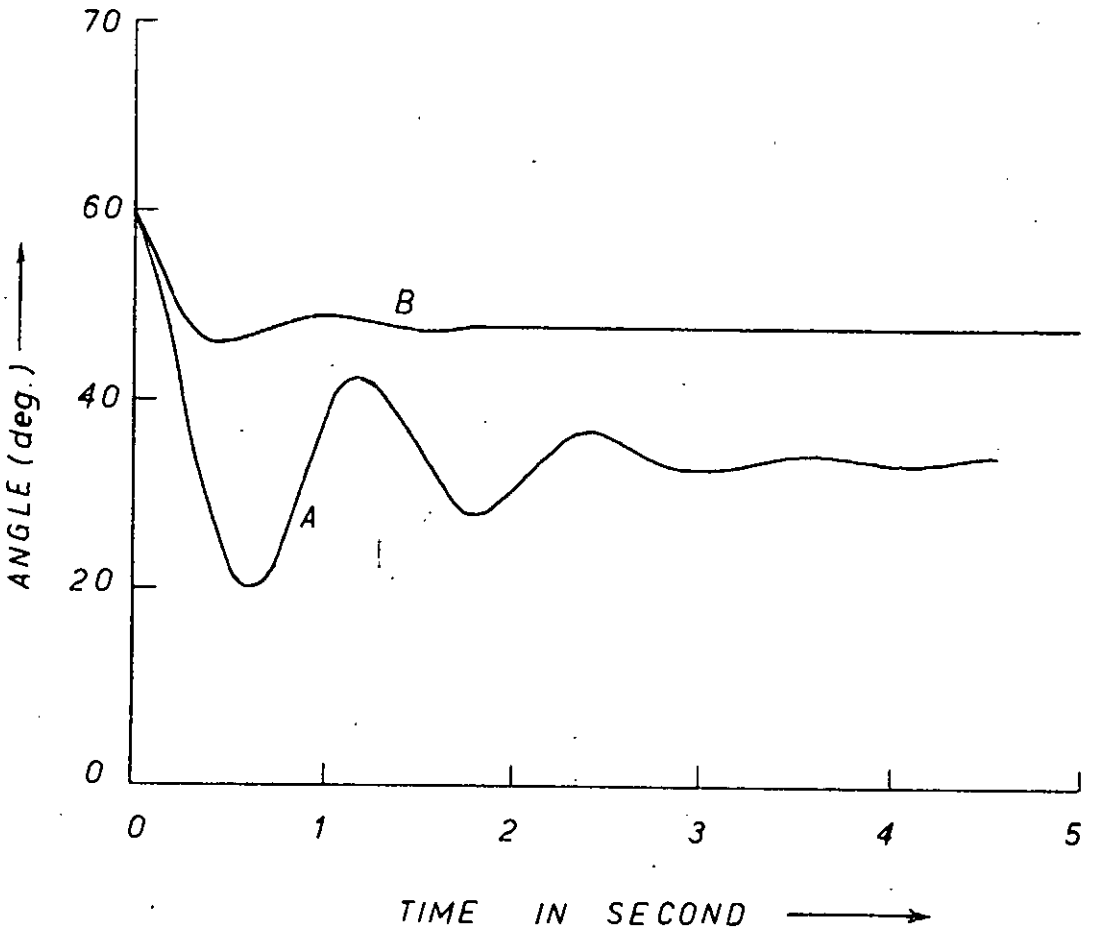

FIG. 5·29 ROTOR ANGLE VS. TIME FOR SWITCHING-ON A PARALLEL TRANSMISSION LINE.

A — WITH VELOCITY SIGNAL

B — WITH VELOCITY AND $\Delta\delta$ SIGNAL

5.7 Comparative Study of Different Stabilizing Signals

The effects of various stabilizing signals on different types of system disturbances have been discussed in the preceeding sections. The different figures of merit such as maximum swing, settling time are given in Table 5.1. Swing curves for different types of disturbances for all the stabilizing signals attempted are shown in Fig. 5.30 - 5.34. It is obvious that addition of a stabilizing signal derived from rotor velocity effects sufficient improvement in transient performance over voltage regulator action alone. Further improvement can be obtained with a suitable combination of velocity signal and magnitude of field current deviation signal and also with a suitable combination of velocity signal and torque angle deviation signal. In both cases the steady state operating point shift from the expected operating point for disturbances like torque steps etc. This is of no problem since steady state operating point can be adjusted easily.

From an inspection of the swing curves for different faults and disturbances on the system it can be seen that a velocity and rotor angle feedback signal combination removes the transients most effectively in comparison to any other stabilizing signal. However, the change in steady operating point is maximum with this combination. Though for disturbances like torque steps etc, the next best combination is velocity and armature current deviation, this can not be used as a stabilizing signal in general since it provides positive damping for some type of disturbances and negative damping for others. Though the settling time increases with the field current and velocity combination signal it is quite satisfactory in terms of shift of the steady operating point.

Type of disturbance	Stabilizing signal	First rotor excursion (deg.)	Settling time (Sec.)	Final rotor angle (deg.)
1. 3-Ø fault at 60°	a) Voltage reg.only	75.0	10.5	60
	b) n	75.1	3.35	60
	c) $n + pn^2$	74.5	3.3	60
	d) $n + \lvert\Delta i_{fd}\rvert$	79.8	2.4	60
	e) $n + \lvert\Delta i_a\rvert$	unstable	-	-
	f) $n + \Delta\partial$	73	1.1	59.9
2. 3-Ø fault at 45°	a) Voltage reg.only	56.5	10.0	45
	b) n	56.3	4.3	45
	c) $n + pn^2$	56.3	4.3	45
	d) $n + \lvert\Delta i_{fd}\rvert$	62.5	3.2	45.2
	e) $n + \lvert\Delta i_a\rvert$	unstable	-	-
	f) $n + \Delta\partial$	55.4	1.3	44.9
3. 25% step at 45°	a) Voltage reg.only	71.3	12.0	58
	b) n	66.1	3.85	58
	c) $n + pn^2$	66.0	3.75	58
	d) $n + \lvert\Delta i_{fd}\rvert$	55.6	0.9	53.6
	e) $n + \lvert\Delta i_a\rvert$	52.4	0.8	51.1
	f) $n + \Delta\partial$	51.4	1.1	50.2
4. 40% step at 45°	a) Voltage reg.only	88.7	12.8	65.8
	b) n	78.3	3.15	65.8
	c) $n + pn^2$	78.3	3.1	65.8
	d) $n + \lvert\Delta i_{fd}\rvert$	60.6	1.15	57.8
	e) $n + \lvert\Delta i_a\rvert$	55.8	0.9	53.9
	f) $n + \Delta\partial$	54.9	0.65	52.7
5. 15% Torque pulse at 60° for 6 c/s	a) Voltage reg.only	64.9	9.0	60
	b) n	63.4	1.65	60
	c) $n + pn^2$	63.4	1.60	60
	d) $n + \lvert\Delta i_{fd}\rvert$	61.6	0.6	60
	e) $n + \lvert\Delta i_a\rvert$	61.8	1.55	60
	f) $n + \Delta\partial$	61.6	0.45	59.9

Type of disturbance	Stabilizing signal	First rotor excursion (deg.)	Settling time (Sec.)	Final rotor angle (deg.)
6. 50% torque pulse at 60° for 6 c/s	a) Voltage reg.only	77.9	11.0	60
	b) n	72.1	3.45	60
	c) $n + pn^2$	71.8	3.45	60
	d) $n + \lvert\Delta i_{fd}\rvert$	65.4	1.65	60
	e) $n + \lvert\Delta i_a\rvert$	66.0	2.1	60
	f) $n + \Delta\partial$	65.7	0.6	59.9
7. 100% torque pulse at 60° for 6 c/s	a) Voltage reg. only	99.0	12.2	60
	b) n	85.1	4.3	60
	c) $n + pn^2$	83.7	4.3	60
	d) $n + \lvert\Delta i_{fd}\rvert$	71.6	1.75	60
	e) $n + \lvert\Delta i_a\rvert$	69.8	3.35	60
	f) $n + \Delta\partial$	71.2	1.1	59.8
8. 3-Ø fault at middle of line	a) Voltage reg.only	109.3	12.0	60
	b) n	95.1	4.5	60
	c) $n + pn^2$	95.4	4.5	60
	d) $n + \lvert\Delta i_{fd}\rvert$	81.7	3.35	60
	e) $n + \lvert\Delta i_a\rvert$	86.5	3.55	60
	f) $n + \Delta\partial$	77.8	1.2	59.9
9. Parallel transmission line switched on	a) Voltage reg.only	8.1	11.0	33.5
	b) n	19.5	3.75	33.5
	c) $n + pn^2$	19.4	3.7	33.5
	d) $n + \lvert\Delta i_{fd}\rvert$	15.6	3.25	33.6
	e) $n + \lvert\Delta i_a\rvert$	8.2	1.75	33.4
	f) $n + \Delta\partial$	45.6	0.65	47.9

Table 5.1 Results in Brief.

Gains:
Regulator = -20
Velocity = 20
Acceleration = 10
Field current = 0.5
Armature current = 0.4
Torque angle = 1.0

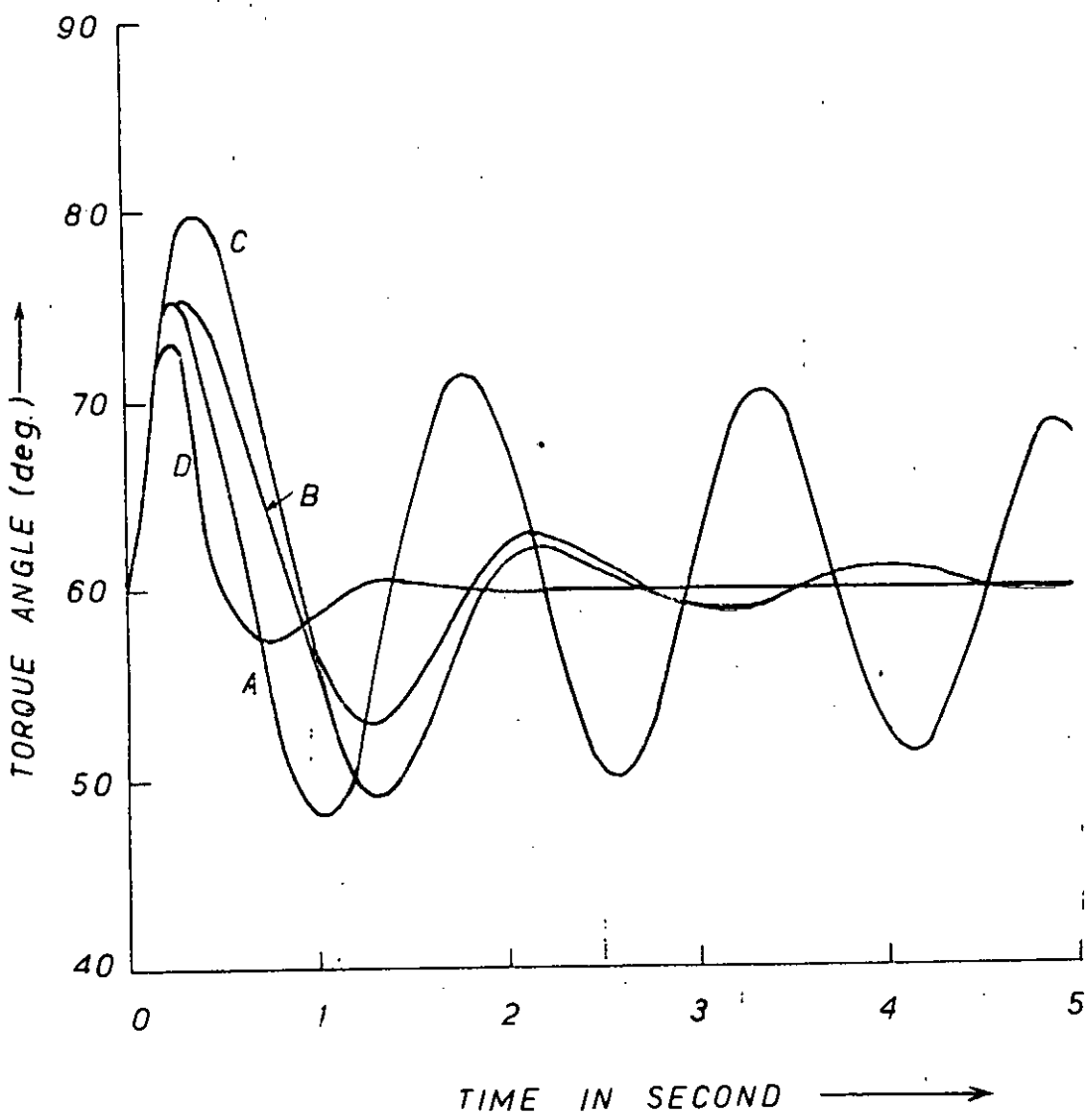

FIG. 5·30 SWING CURVES SHOWING EFFECT OF DIFFERENT STABILIZING SIGNALS FOR THREE PHASE FAULT.

A — VOLTAGE FEEDBACK ONLY

B — WITH VELOCITY SIGNAL.

C — WITH VELOCITY AND FIELD CURRENT DEVIATION SIGNAL.

D — WITH VELOCITY AND TORQUE ANGLE DEVIATION SIGNAL.

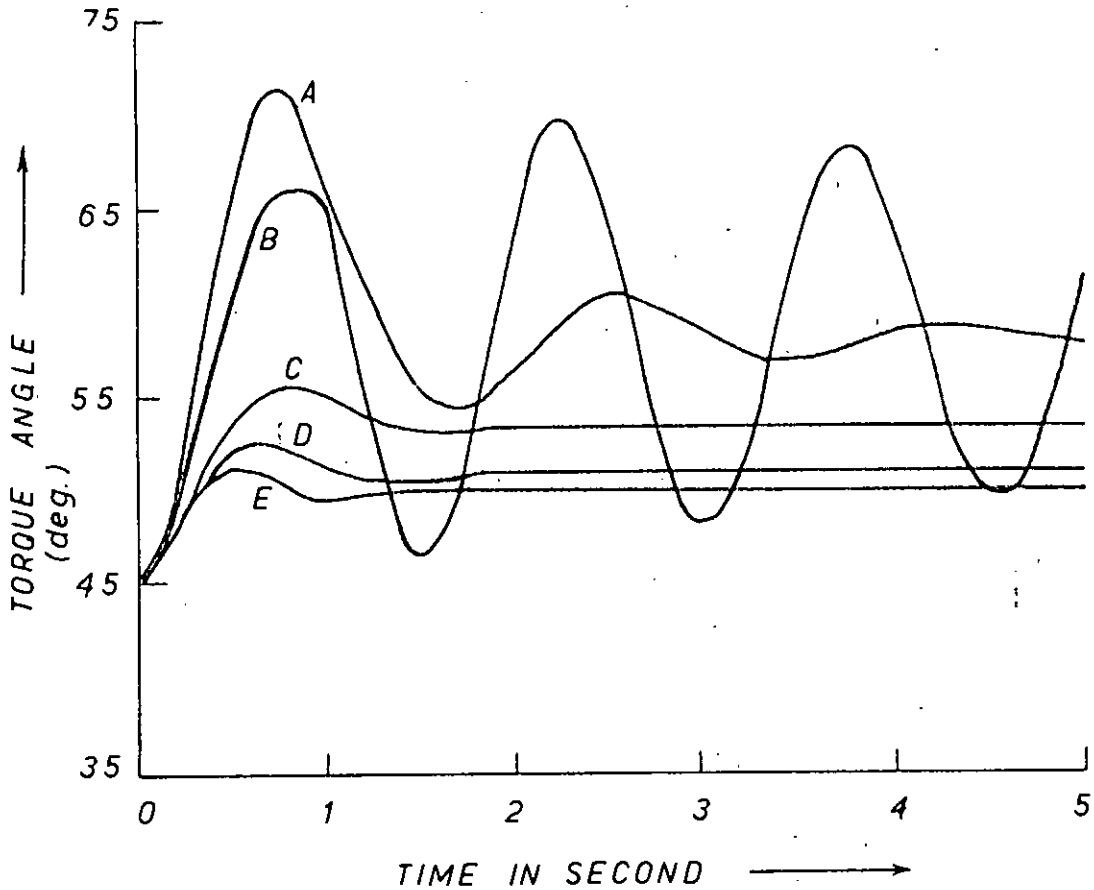

FIG. 5·31 TORQUE ANGLE CHARACTERISTICS FOR 25 % TORQUE STEP.

A — VOLTAGE FEEDBACK ONLY

B — WITH VELOCITY SIGNAL.

C — WITH VELOCITY AND FIELD CURRENT DEVIATION SIGNAL.

D — WITH VELOCITY AND ARMATURE CURRENT DEVIATION SIGNAL.

E — WITH VELOCITY AND TORQUE ANGLE DEVIATION SIGNAL.

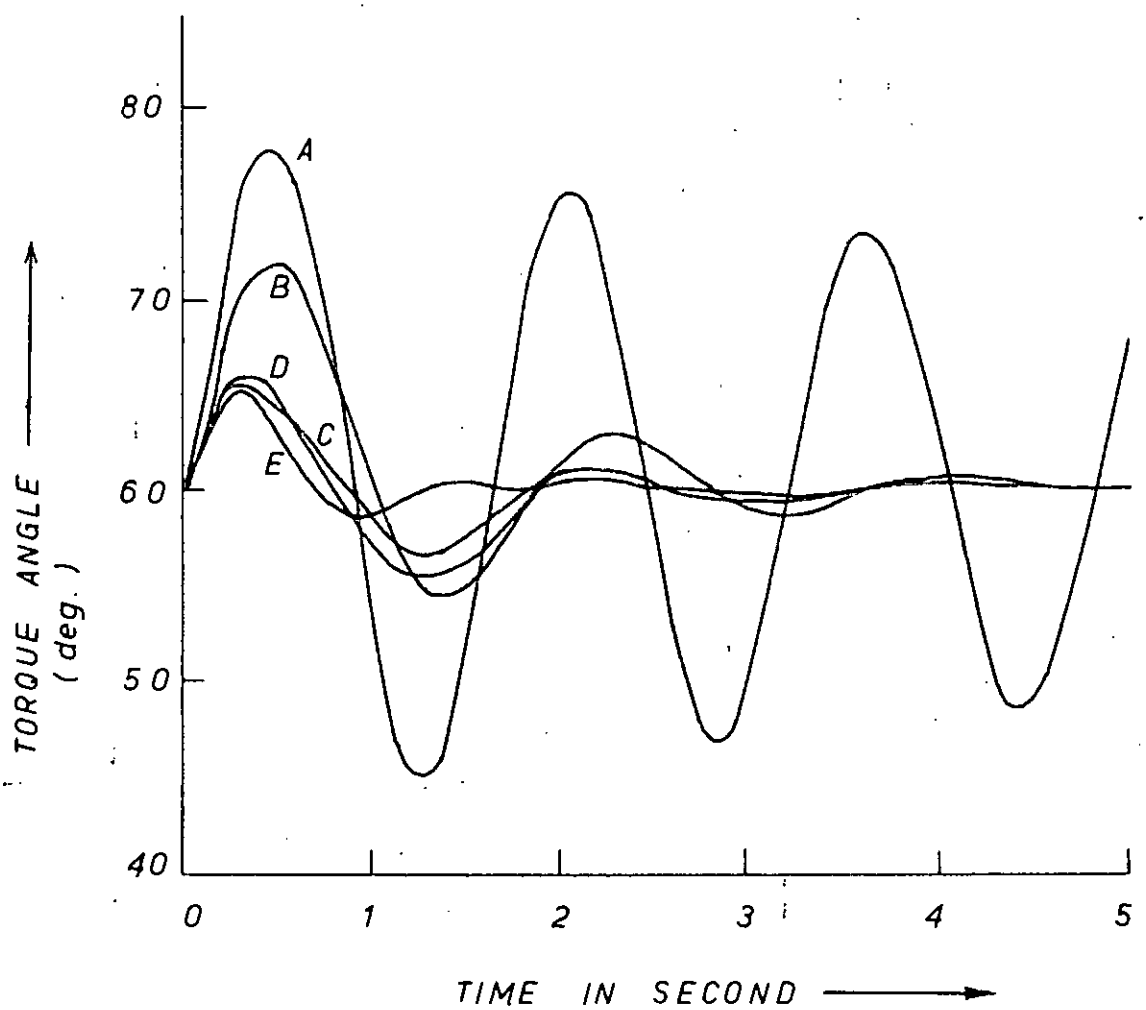

FIG. 5 · 32 ROTOR ANGLE VS. TIME FOR 50% TORQUE PULSE.

A — VOLTAGE REGULATOR ONLY
B — WITH VELOCITY SIGNAL
C — WITH VELOCITY AND FIELD CURRENT DEVIATION SIGNAL.
D — WITH VELOCITY AND ARMATURE CURRENT DEVIATION SIGNAL.
E — WITH VELOCITY AND TORQUE ANGLE OEVIATION SIGNAL

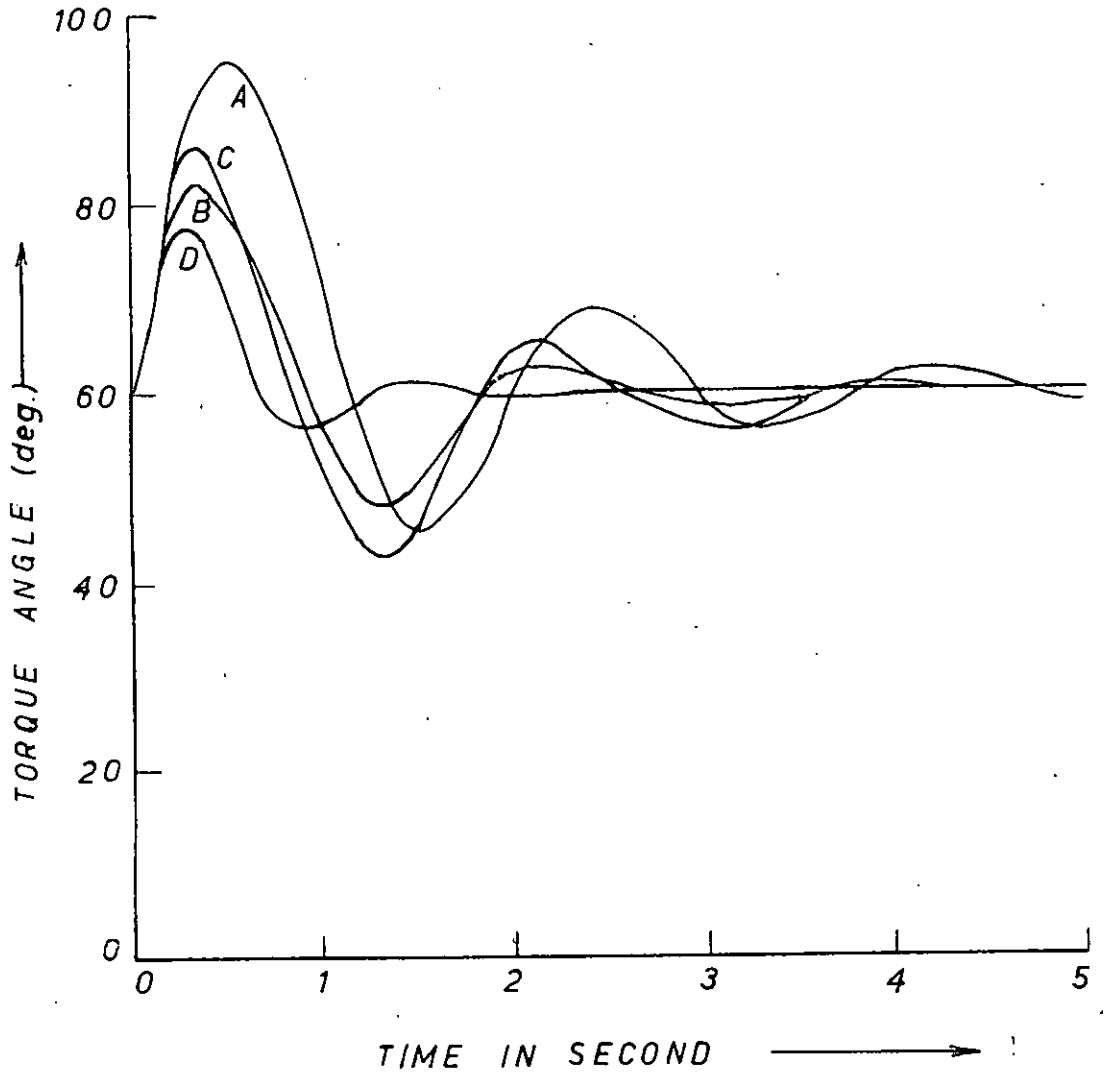

FIG. 5·33 ROTOR ANGLE OSCILLATION FOR THREE PHASE FAULT AT MIDDLE OF TRANSMISSION LINE.

A — VELOCITY SIGNAL ONLY

B — WITH VELOCITY AND FIELD CURRENT DEVIATION SIGNAL.

C — WITH VELOCITY AND ARMATURE CURRENT DEVIATION SIGNAL.

D — WITH VELOCITY AND TORQUE ANGLE DEVIATION SIGNAL.

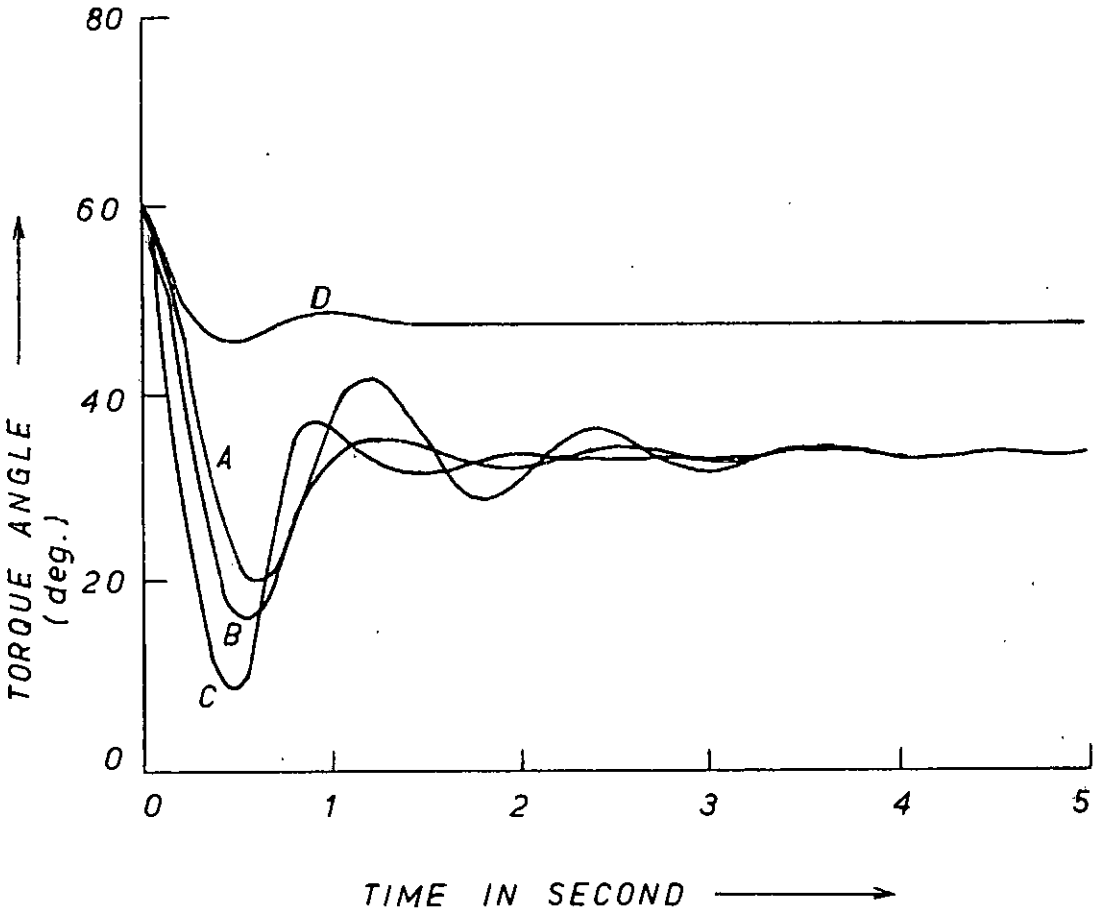

FIG. 5·34 ROTOR ANGLE VS. TIME FOR SWITCHING-ON OF PARALLEL TRANSMISSION LINE.

A — WITH VELOCITY SIGNAL.

B — WITH VELOCITY AND FIELD CURRENT DEVIATION SIGNAL.

C — WITH VELOCITY AND ARMATURE CURRENT DEVIATION SIGNAL.

D — WITH VELOCITY AND TORQUE ANGLE DEVIATION SIGNAL.

5.8 Effect of Time Constants and Ceiling Voltage

To study the effect of exciter time constant and the ceiling voltage on transient performance of the power system a six cycle three phase fault at the machine terminals was considered. Fig. 5.35 shows the swing curves for different exciter time constant. A larger time constant of exciter deteriorates the transient response and in absence of adequate stabilizing signal the system may become unstable. However an auxiliary stabilizing signal may offset the detrication of response due to introduction of large time constant in the exciter. Though the system may remain stable in such cases, the first rotor excursion increases and settling time may also become larger.

A small time lag is inherent in terminal voltage feedback circuit of the rectifier excitation system. A larger time constant in the voltage deviation sensing although shows some improvement in the case of a three phase fault at machine terminals, it deteriorates transient stability for other types of disturbances on the system.

The exciter ceiling voltage is of significance under conditions of large disturbances where the gain and time constant permit the ceiling voltage to be reached. The transients due to a disturbance would be controlled more effectively if the exciter voltage could be increased to a large value. But due to physical constraints, the exciter voltage can not be increased indefinitely. Fig. 5.36 shows the swing curves for two different ceiling

voltages viz. 2 p.u. and 4 p.u. A higher ceiling voltage gives a smaller first rotor excursion and an improved damping. A negative exciter ceiling voltage shows no significant improvement in this case.

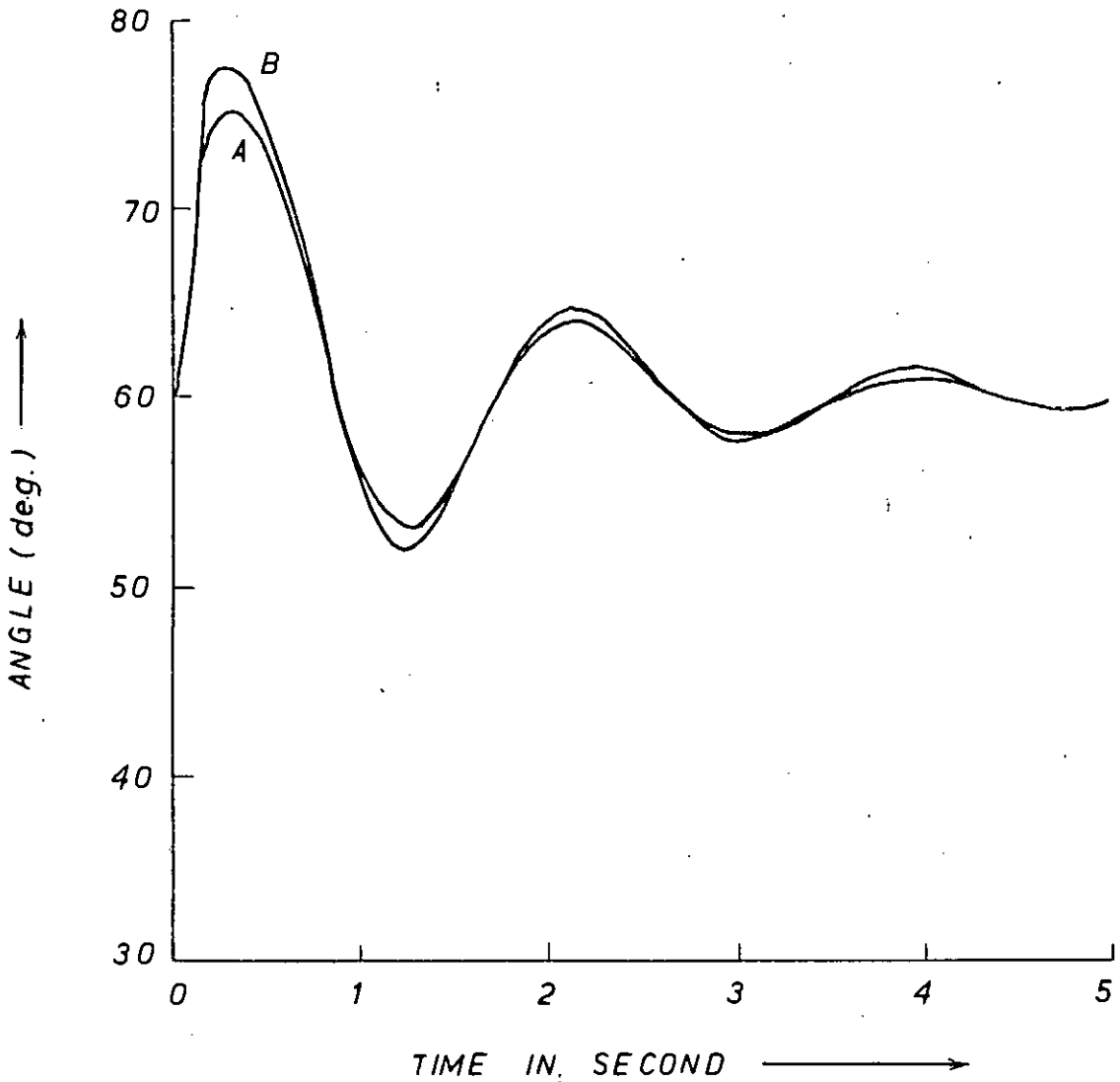

FIG. 5 35(A) TORQUE ANGLE CHARACTERISTICS SHOWING EFFECT OF TIME CONSTANT ON THREE PHASE FAULT (WITH VOLTAGE AND VELOCITY FEEDBACK).

A — TIME CONSTANT 20 m Sec.

B — TIME CONSTANT 100 m Sec.

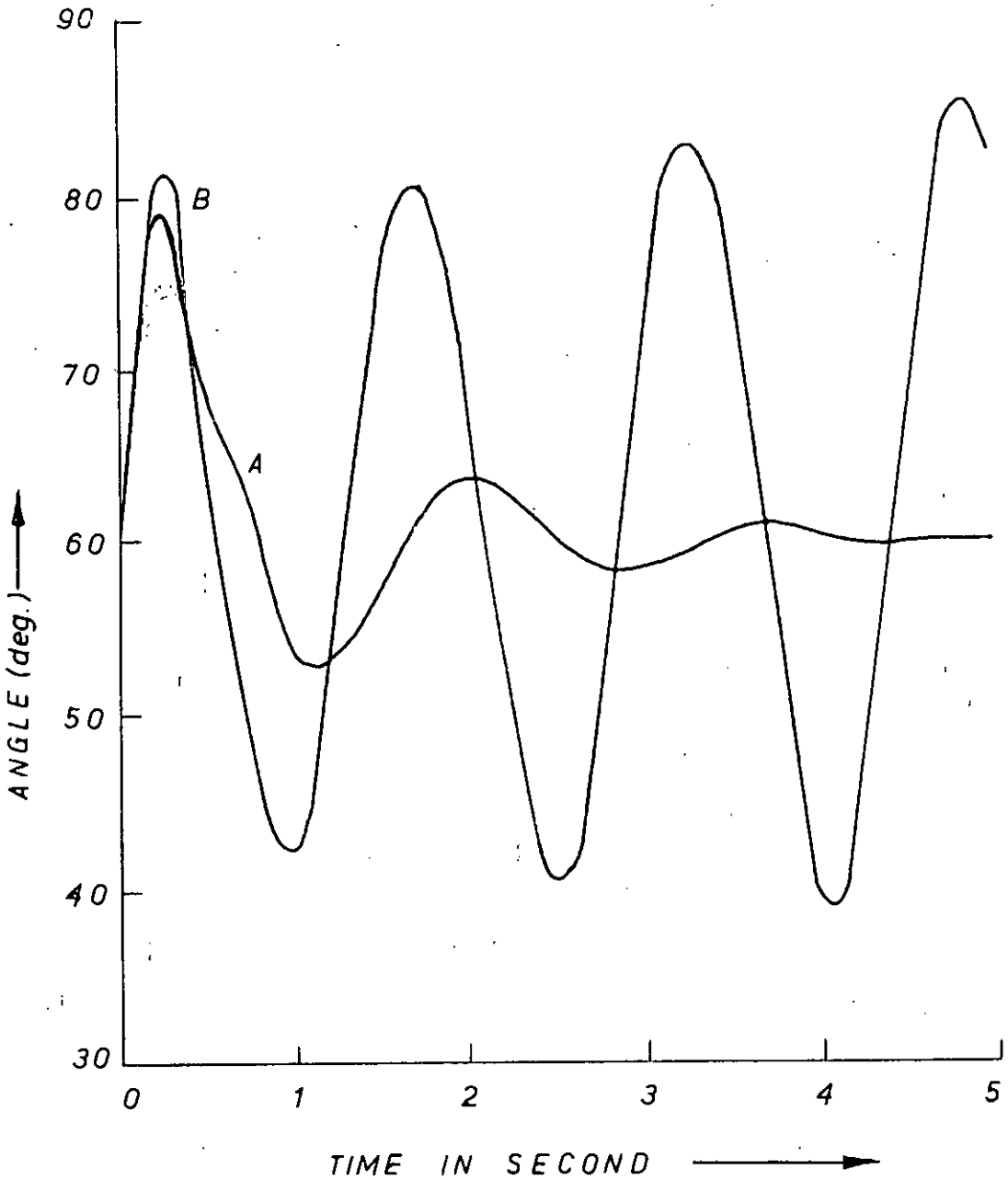

FIG. 5·35 (B). TORQUE ANGLE CHARACTERISTICS FOR 3 PHASE FAULT WITH EXCITER TIME CONSTANT 500 m Sec.

A — VOLTAGE AND VELOCITY FEEDBACK

B — WITH VOLTAGE FEEDBACK ONLY.

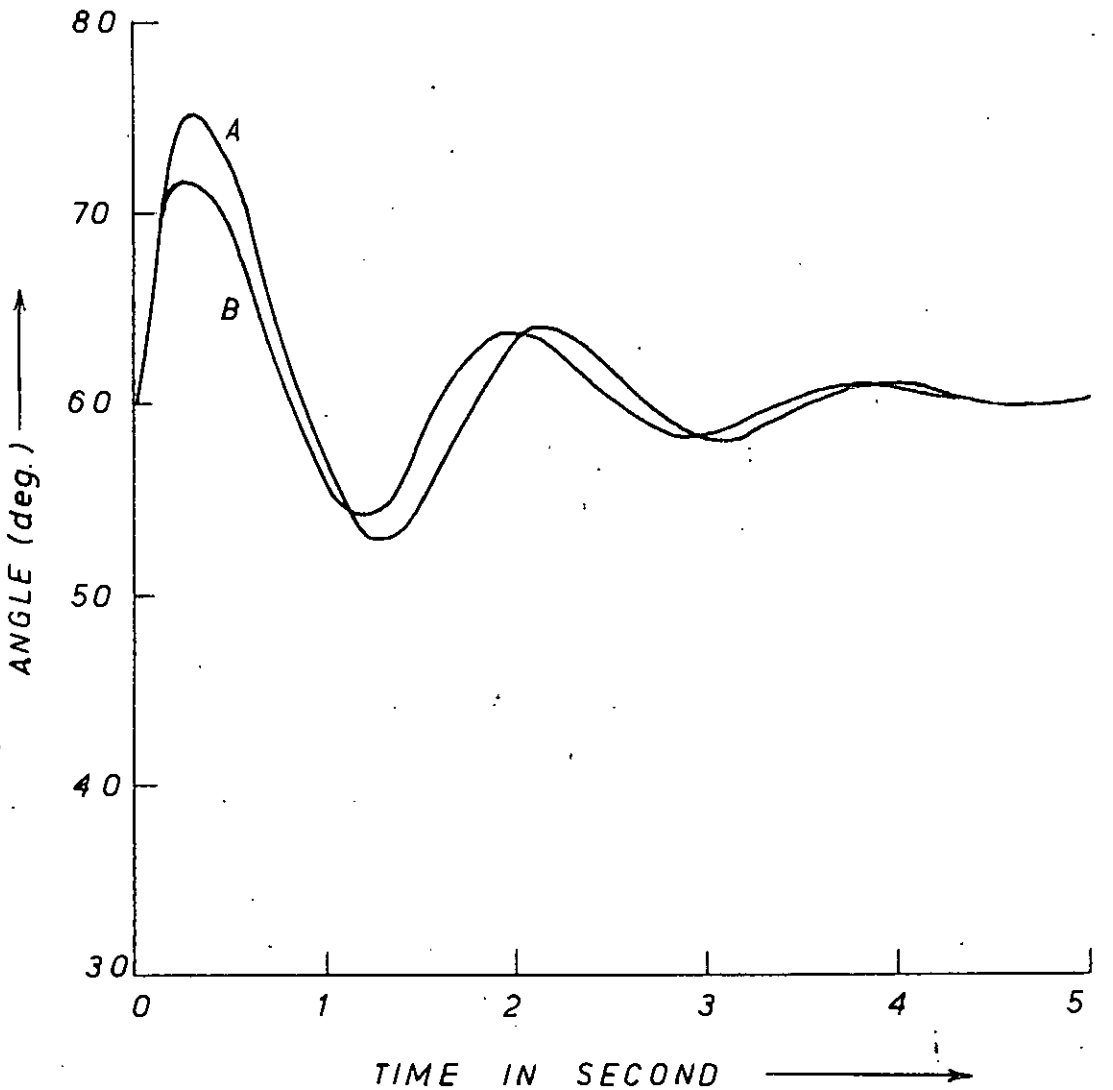

FIG. 5·36. ROTOR ANGLE OSCILLATION WITH DIFFE — RENT CEILING VOLTAGE (3 PHASE FAULT).
A — CEILING VOLTAGE 2·0
B — CEILING VOLTAGE 4·0

CHAPTER 6

CONCLUSIONS

6.1 Summary and Conclusions

A synchronous generator connected to infinite bus through a transmission line have been represented by a set of first order non linear differential equations. These equations represent the system completely under any conditions - steady state and transient under balanced three phase operation. These equations contain coefficients which depend on parameters such as inertia constant, resistance, self and mutual inductances of different circuits of the synchronous machine, resistance and reactance of transmission line etc.

Various tests were performed on a laboratory machine to find the different synchronous machine parameters. D.c. measurement of inductances was prefered to conventional a.c. bridge method since, as discussed in section 4.1, the inductance which govern the machine behaviour is that to direct current. For measurement of large inductances such as self inductance of field coil, mutual inductance between stator and field a storage oscilloscope can be used as the detector in the d.c. inductance bridge. For small inductances such as direct and quadrature axis synchronous inductance a ballistic galvanometer or a flux meter should be used as detector. Due to nonavailability of these instruments direct and quadrature axis synchronous inductances were measured by slip test. The inertia constant of the synchronous machine was measured by retardation test which is more precise than the usual dynamometer method of measurement.

Power system computations are generally done in per unit. As discussed, there is no unique system for per unit conversion of quantities in the case of rotating machines. A comparative study of different per unit systems have been carried out and the unit voltage base system was found to be suitable. This system of conversion was employed in this study.

A mathematical model of the electrinic excitation system is developed. The transfer function of each block of the excitation system was found from circuit configuration and compared with experimental results. A simplified representation and an overall transfer function of the excitation system was derived. The effectiveness of the exciter for power system stabilization have been studied.

Excitation control offers one of the best methods of reducing transients in a power system. But a high speed voltage regulator deteriorates system stability. To improve transient performance with such an excitation system additional stabilizing signals are required. Search for different stabilizing signals have been carried out for a number of disturbances in the system. A signal proportional to shaft speed deviation stabilizes the transient disturbances quickly. This is in agreement with the results obtained experimentaly in a previous study. Additional damping may be obtained if signals proportional to field current deviation or torque angle deviation is used in conjunction with velocity signal. Considering all the figures of merit such as peak overshoot, peak time, settling time etc. The torque angle

deviation signal in combination with rotor velocity signal exhibited best transient improvement. The field current deviation and torque angle deviation signal alone showed poor damping characteristics. Application of acceleration signal showed slight improvement of transient stability. It was observed that for disturbances like torque step, line switching etc, the additional stabilizing signals has the effect of shifting the operating point to a new value after the disturbance has ceased. This is quite obvious because of the fact that the addition of torque angle and field current deviation signal in the exciter change the excitation level of the system causing a permanent shift of operating point. Maximum shift of operating point occurs with the torque angle deviation signal. The armature current deviation signal can not be used for stabilization because it provides positive damping for some disturbances and negative damping for others. The combination of various feedback signals for best transient improvement for different disturbances were obtained by a number of trials.

The effect of change of various parameters of the exciter have also been studied. The exciter gain has a very significant effect on first rotor excursion. For a particular type of disturbance, an optimum value of exciter gain can be determined from first rotor excursion and transient elimination viewpoint. Deviation of exciter gain from optimum value results in deterioration of transient stability. The exciter time constant has significant effect on transient stability in absence of additional

stabilizing signal. If the exciter time constant is large, the system may even lose synchronism for some type of disturbances. Additional stabilizing signal offsets this deterioration introduced by large time constants. The exciter ceiling voltage is of significance under conditions of large disturbance. First rotor excursion can be minimized by driving the exciter to a higher ceiling voltage resulting in improved overall transient performance of the system.

6.2 Suggestions for Further Research

Further areas of investigation include the search for suitable stabilizing signal considering governor and prime mover dynamics and damper winding in the system representation. Transmission line representation should include distributed capacitance.

Stability study of multimachine system is of major importance. It is obvious that the amount of work in such a study will be tremendous. Realization of different stabilizing signals for "on line" application should be attempted.

APPENDIX-I

The data for the single machine infinite bus system was found from experimental study. The system configuration is given in Fig. 5.1.

Machine rating 1.5 KVA, 230 Volts

$x_{afd} = 1.0$	$H = 2.4$
$x_d = 1.05$	$r_a = 0.1134$
$x_q = 0.558$	$x_e = 1.56$
$r_{fd} = 0.01542$	$r_e = 0.0425$
$x_{ffd} = 1.195$	$\tau_r = 0.02$ Sec.

The operating points considered are

1)

$i_{fdo} = 1.2$	$V = 0.74$
$i_{do} = 0.2986207$	$E_{fdo} = 1.2$
$i_{qo} = 0.324558$	$e_{to} = 0.862307$
$\delta_o = 60^o$	$P_o = 0.315751$

2)

$i_{fdo} = 1.2$	$V = 0.74$
$i_{do} = 0.24346$	$E_{fdo} = 1.2$
$i_{qo} = 0.264974$	$e_{to} = 0.922192$
$\delta_o = 45^o$	$P_o = 0.264947$

APPENDIX-II

PROGRAMS

1. LINEARISATION OF SCR CHARACTERISTICS
2. CALCULATION OF STEADY STATE OPERATING POINTS
3. TRANSIENT STABILITY STUDY BY RUNGE KUTTA INTEGRATION

```
// JCB UET91306 SAROJ BISWAS STABILITY PROBLEM
// OPTION LINK,LIST
// EXEC FFORTRAN
C     STRAIGHT LINE APPROXIMATION OF SCR CHARACTERISTICS
C
      DIMENSION SCR(38),ALPHA(37),EFD(37)
      READ(1,20) C1,C2,C4,D1,D2
   20 FORMAT(5F10.5)
      SCR(1)=0.0
      DO 10 I=1,37
      SCR(I+1)=SCR(I)+5.0
      ALPHA(I)=SCR(I)*3.141592/180.0
      C2=C2+ALPHA(I)
   10 C4=C4+ALPHA(I)**2
      DO 11 I=1,13
      EFD(I)=1.885*(1.0+COS(ALPHA(I)))
      C1=C1+EFD(I)
   11 C2=C2+EFD(I)*ALPHA(I)
      DO 12 I=14,36
      EFD(I)=3.504*(1.0+COS(ALPHA(I)))/(3.141592-ALPHA(I))
      C1=C1+EFD(I)
   12 C2=C2+EFD(I)*ALPHA(I)
      EFD(37)=0.0
      DENOM=C1*C4-C2*C2
      A0=(C1*C4-C2*C2)/DENOM
      A1=(C1*C2-C1*C2)/DENOM
      WRITE(3,18) (SCR(I),EFD(I),I=1,37)
   18 FORMAT(2F15.5)
      WRITE(3,19) A0,A1
   19 FORMAT(2F10.5)
      CALL EXIT
      END
/*
// EXEC LNKEDT
// EXEC
  37.0       0.0        0.0        0.0        0.0
/*
/&
```

```
// JOB UET91306 SAROJ BISWAS STABILITY PROBLEM
// OPTION LINK,LIST
// EXEC FFORTRAN
C      JOB 91306 SAROJ KANTI BISWAS,BUET,DACCA
C      POWER ANGLE CURVE
C      SYSTEM PARAMETERS IN THEIR USUAL NOTATIONS
C
   11 READ(1,21) XD,XQ,RA,RE,XE,XAFD,XFFD,RFD,V,TM,EFD
   21 FORMAT(1)F7.5)
      W=314.1592
      CC=((XAFD*XAFD)-(XFFD*(XD+XE)))/W
      GG=(XQ+XE)/W
      A7=(RE+RA)*XFFD/DD
      A8=-XFFD*(XE+XQ)/DD
      A9=XFFD*V/CC
      A11=XAFD/QQ
      A12=-(XQ+XE)/QQ
      A13=-(RE+RA)/QQ
      A14=-V/QQ
      A15=-XAFD/TM
      A16=(XD-XQ)/TM
      A19=(XE*RFD*XAFD)/(W*DD)
      A20=RE+(XE*XFFD*(RE+RA))/(W*DD)
      A21=-((XE*XFFD*(XE+XQ))/(W*DD)+XE)
      A22=-(XE*RFD)/(W*CD)
      A23=V+((XE*XFFD*V)/(W*DD))
      A24=(XE*XAFD)/(W*QQ)
      A25=XE-((XD+XE)*XE/(W*QQ))
      A26=RE-(XE*(RE+RA)/(W*QQ))
      A27=V-(XE*V/(W*QQ))
      A28=V/(XD+XE)
      A29=V*V*(XD-XQ)/((XD+XE)*(XQ+XE))
      FI=EFD/XAFD
      DENOM=A7*A13-A8*A12
      DELTA=-180.0
   53 DEL=DELTA/180.0*3.141592
      CS=COS(DEL)
      SN=SIN(DEL)
      DI=(FI*A8*A11+A8*A14*CS-A9*A13*SN)/DENOM
      QI=(A9*A12*SN-FI*A7*A11-A7*A14*CS)/DENOM
      ED=A19*FI+A20*DI+A21*QI+A22*EFD+A23*SN
      EQ=A24*FI+A25*DI+A26*QI+A27*CS
      EDG=ED**2+EQ**2
      ET=SQRT(EDQ)
      POUT=(FI*A15+A16*DI)*QI*(-TM)
      P=DI*V*SN+QI*V*CS
      QO=EQ*DI-ED*QI
      Q=DI*V*CS-QI*V*SN
      POWER=(A28*EFD*SN+A29*SN*CS)
      WRITE(3,80)DI,QI,ED,EQ,ET,POUT,POWER,DELTA,QO,Q,P
   80 FORMAT(7F13.8,F8.1,3F11.6)
      DELTA=DELTA+5.0
      IF(DELTA-180.0) 53,53,11
      END
/*
// EXEC LNKEDT
```

```
N IV 36CN-FO-475 3-6          MAINPGM          DATE  16/05/77     TIME  12.C
C       JOB 91306 SAROJ KANTI BISWAS,BUET,DACCA
C       TRANSIENT ANALYSIS OF POWER SYSTEM
C       SOLUTION BY RUNGA KUTTA METHOD OF INTEGRATION
C       STEP SIZE IS C.CC5 SECONDS
C
        DIMENSION YO(7),AF(29),AFC(29),Y(7),A(29),YY(7),RKC(7,5),DY(7)
        DO 67 N=1,7
        DO 67 L=1,5
     67 RKC(N,L)=C.C
C
C       INITIAL OPERATING CONDITIONS
C       Y'S REPRESENT SYSTEM STATES &DY'S ARE INCREMENTS
C
     22 READ(1,59) EO,E10,DT,(YC(I),I=1,7)
     59 FORMAT(3F1C.6/7F1C.6)
        TIO=SQRT(YO(2)*YO(2)+YO(3)*YO(3))
C
C       SYSTEM PARAMETERS IN THEIR USUAL NOTATIONS
C
     34 READ(1,24) XD,XQ,RA,RE,XE,XAFD,XFFD,RFD,VBUS,TM,TIN,K
     24 FORMAT(11F7.5,I2)
C
C       CALCULATION OF CONSTANTS OF DYNAMIC EQUATIONS FOR FAULTED AND
C       FAULT CLEARED CONDITIONS
C       AF'SAND AFC'S REPRESENT CONSTANTS AT FAULTED &FAULT CLEARED CONDITIONS
C
        W=314.1592
        DD=((XAFD*XAFD)-(XFFD*(XD+XE)))/W
        QQ=(XQ+XE)/W
        AF(1)=RFD*(XD+XE)/DD
        AF(2)=(RE+RA)*XAFD/DD
        AF(3)=-(XE+XQ)*XAFD/DD
        AF(4)=XAFD*VBUS/DD
        AF(5)=(-RFD*(XD+XE))/(XAFD*DD)
        AF(6)=RFD*XAFD/DD
        AF(7)=(RE+RA)*XFFD/DD
        AF(8)=-XFFD*(XE+XQ)/DD
        AF(9)=XFFD*VBUS/DD
        AF(10)=-RFD/DD
        AF(11)=XAFD/QQ
        AF(12)=-(XD+XE)/QQ
        AF(13)=-(RE+RA)/QQ
        AF(14)=-VBUS/QQ
        AF(15)=-XAFD/TM
        AF(16)=(XD-XQ)/TM
        AF(17)=TIN/TM
        AF(18)=314.1592
        AF(19)=(XE*RFD*XAFD)/(W*DD)
        AF(20)=RE+(XE*XFFD*(RE+RA))/(W*DD)
        AF(21)=-((XE*XFFD*(XE+XQ))/(W*DD)+XE)
        AF(22)=-(XE*RFD)/(W*DD)
        AF(23)=VBUS+((XE*XFFD*VBUS)/(W*DD))
        AF(24)=(XE*XAFD)/(W*QQ)
        AF(25)=XE-((XD+XE)*XE/(W*QQ))
```

```
      AF(26)=RE-(XE*(RE+RA)/(M*GG))
      AF(27)=VBLS-(XE*VBLS/(M*GG))
      AF(28)=-VBLS/(TM*(XD+XE))
      AF(29)=-VBLS*VBLS*(XD-XG)/((XD+XE)*(XG+XE)*TM)
      IF(K.EQ. 2) GO TO 21
      DO 18 I=1,29
   18 AFC(I)=AF(I)
      GO TO 34
C
C     GAINS AND TIME CONSTANTS ARE GIVEN
C
   21 READ(1,63) GVOL,GVEL,GACL,GFLD,GCUR,GREG,T1,T2,EFDMX,NN
   63 FORMAT(5F8.4,I8)
      IF(NN .EQ. 5 ) GO TO 22
      IF(NN .EQ. 0) CALL EXIT
      WRITE(3,48)
   48 FORMAT(1H1,5X,'FI',7X,'DI',7X,'GI',7X,'ED',7X,'EQ',7X,'ET',6X,
     2'ET1',8X'AN',8X,'EFD',8X,'VDEV',7X,'ACCL',5X,'DELTA',6X,'TT'/)
      I=0
      M=0
      TT=0.0
      DO 64 N=1,7
   64 Y(N)=YO(N)
      DO 65 N=1,29
   65 A(N)=AF(N)
      GO TO 80
   33 DO 76 N=1,29
   76 A(N)=AFC(N)
C
C     LIMITS OF CEILING VOLTAGE
C
   80 IF(Y(6) .GE. EFDMX) Y(6)=EFDMX
      IF(Y(6) .LE.0.0) Y(6)=0.0
      Y4=1.0+Y(4)
      ED=A(19)*Y(1)+A(20)*Y(2)+A(21)*Y(3)*Y4+A(22)*Y(6)+A(23)*SIN(Y(5))
      EQ= (A(24)*Y(1)+A(25)*Y(2))*Y4+A(26)*Y(3)+A(27)*COS(Y(5))
      EDQ= ED**2+EQ**2
      ET=SQRT(EDQ)
      ACCL=A(17)+(A(28)*Y(6)+A(29)*COS(Y(5)))*SIN(Y(5))
      VERROR=ET0-Y(7)
      DDEL=(Y(5)-YO(5))/YO(5)
      TI=SQRT(Y(2)*Y(2)+Y(3)*Y(3))
      CLRR=(TI-TIO)/TIO
      FCLR=(Y(1)-YO(1))/YO(1)
      IF(I .LT. 24) VERRCR=0.0
C
C     STABILIZING SIGNALS ARE APPLIED
C
      EE=VERROR+GVEL*Y(4)+GACL*ACCL*ACCL
      IF(I-M) 15,20,15
   20 M=M+20
      IF(I .LT. 80) M=M-120
      VDEV=(ET-ET0)/ET0
      DELTA=Y(5)*180.0/3.141592
```

```
V 1V 36CN-FO-475 3-6          MAINPGM          DATE   16/05/77      TIME     13.C(

      WRITE(3,88) Y(1),Y(2),Y(3),ED,EQ,ET,Y(7),Y(4),Y(6),VCEV,ACCL,
     2DELTA,TT
   88 FORMAT(7F5.3,5F11.4,F7.2)
C
C      INTEGRATION LOOP STARTS
C
   15 DO 6C L=2,5
      DDT=DT/2.
      IF(L .EQ. 5 ) DDT=DT
   12 DO 17 N=1,7
   17 YY(N)=Y(N)+RKC(N,(L-1))*DDT
      YY4=1.C+YY(4)
C
C      CALCLLATION OF RLNGE COEFFICIENTS
C
      RKC(1,L)=A(1)*YY(1)+A(2)*YY(2)+A(3)*YY(3)*YY4+A(4)*SIN(YY(5))+
     2A(5)*YY(6)
      RKC(2,L)=A(6)*YY(1)+A(7)*YY(2)+A(8)*YY(3)*YY4+A(9)*SIN(YY(5))
     2+A(10)*YY(6)
      RKC(3,L)=(A(11)*YY(1)+A(12)*YY(2))*YY4+A(13)*YY(3)+
     2A(14)*COS(YY(5))
      RKC(4,L)=A(17)+A(28)*YY(6)*SIN(YY(5))+A(29)*SIN(YY(5))*COS(YY(5))
      RKC(5,L)=A(18)*YY(4)
      RKC(6,L)=(GREG*EE-YY(6)+EC)/T1
   6C RKC(7,L)=(GVOL*ET-YY(7))/T2
      DO 16 N=1,7
      DY(N)=(RKC(N,2)+2.*RKC(N,3)+2.*RKC(N,4)+RKC(N,5))*DT/6.0
C
C      NEW VALUES OF SYSTEM STATES
C
   16 Y(N)=Y(N)+DY(N)
      TT=TT+DT
      I=I+1
C
C      TRANSIENT BEHAVIOLR IS STLDIED FCR FIVE SECCNDS
C
      IF(TT-5.) 85,21,21
   85 IF(ABS(Y(5))-1C.C) 100,1CC,66
C
C      A S1> CYCLE FALLT IS APPLIED
C
  1CC IF(I-24) 6C,33,6C
   66 WRITE(3,77)
   77 FORMAT(//2C>,3CHTHE MACHINE LCSSES SYNCHFCNISM)
      GO TO 21
      END
```

REFERENCES

1. E.W. Kimbark, " Power system stability", Vol. 1 and III John Willey and Sons.

2. C. Concordia "Synchronous machines" John Wiley, NY 1951.

3. A.E.Fitzerald and C. Kingsley "Electric machinary" Mc.GrawHill Book Company.

4. A.W. Rankin "Per unit impedance of synchronous machines" Part I AIEE Trans. Vol. 64 April 1945.

5. A.W. Rankin "Per unit impedance of synchronous machines" Part II AIEE Trans. Vol. 64 Dec. 1945.

6. F.P.DeMello and C. Concordia "Concept of synchronous machine stability as affected by excitation control" IEEE Trans. on power apparatus and systems Vol. PAS-88 pp. 316-329, April 1969.

7. P.L. Dandeno et al. "Effects of high speed rectifier excitation systems on generator stability limits" IEEE trans on power apparatus and system Vol. PAS-87, pp. 190-201, Jan. 1968.

8. H.M. Ellis, J.E. Hardy, A.L. Blythe and J.W. Skooglund "Dynamic stability of the Peace River transmission system" IEEE Trans. on Power apparatus and system vol. PAS 85, pp. 586-600, June 1966.

9. F.R. Schleif, G.E. Martin, R.R. Angell, "Damping of system oscillations with a hydrogenerating unit" IEEE Trans. on power apparatus and system, Vol. PAS-86, pp. 438-442, Apr. 1967.

10. O.W. Hanson, C.J. Goodwin, P.L. Dandeno, "Influence of excitation and speed control parameters in stabilizing inter system oscillations" IEEE Trans. on power apparatus and systems, Vol. PAS -87, pp. 1306-1313, May, 1968.

11. J.L. Dineley, A.J. Morris and C. Preele. "Optimized Transient stability from Excitation control of synchronous generators" IEEE Trans. on power apparatus and systems Vol. PAS 87, No. 8, pp. 1696-1705, Aug. 1968.

12. R.T. Byerly, F.W. Keay, J.W. Skooglund. "Damping of power oscillations in salient pole machine with static exciters" vol. PAS-89, July/Aug. 1970, pp. 1009-1020.

13. G.A. Jones "Transient stability of synchronous generators under conditions of Bangbang excitation scheduling" IEEE Trans. on power appratus and system Vol. PAS-84, pp. 114-121, Feb. 1965.

14. O.J.M. Smith "Optimal transient removal in a power system" IEEF Trans. on power apparatus and systems vol. PAS-84, pp. 361-374, May 1965.

15. A.H.M. Abdur Rahim. "A quasi optimal excitation control for power system stability" Ph.D. Thesis, Department of Electrical Engineering, University of Alberta, Canada 1972.

16. M.M.A. Safa "Design and performance of a solid state exciter for power system stabilization" M.Sc. Thesis BUET.

17. S.B. Carry "Power system stability" Vol. I and II John Wiley and Sons.

18. C.V. Jones "The unified theory of electric machines" Butterworths U.K.

19. C.D. White and H.H. Woodson, "Electromechanical energy conversion" John Wiley and Sons, NY.

20. A.F. Puchstein, T.C. Lloyd, A.G. Conrad "Alternating current machines" John Wiley and Sons. NY.

21. F.R. Schleif, H.D. Hunkins, G.E. Martin, E.E. Hattan "Excitation control to improve power line stability" IEEE trans. on power apparatus and system" Vol. PAS-87, No.6, pp. 1426-1434, June 1968.

22. J.M. Undrill. "The effects of regulating elements on the dynamic behaviour of power system Ph.D. Thesis, University of Canterbury, Newzealand 1965.

23. F.R. Schleif, J.H. White."Damping for the Northwest and Southwest tie line oscillations - an analog study" IEEE Trans. on power apparatus and systems, Vol. PAS 85, pp. 1239-1247,Dec.1966.

24. G. Shackshaft. "General purpose turbo alternator model" Proc. IEE, Vol. 110, No.4, pp. 703-713, April 1963.

25. J.C. Prescott, A.K. El-Karashi 'A method of measuring self inductance applicable to large electrical machine" Proc. IEE Vol. 106, Part A, April.

26. J.L. Dineley and M.W. Kennedy. 'Concept of synchronous generator stability" Proc. IEE Vol. III, No. 1, Jan. 1964.

27. H.K. Messerle and R.W. Bruck, "Steady state stability of synchronous generator as effected by regulators and governors" Proc. I.E.E., Vol.102 C, 1955, pp-24.

28. H.K. Messerle; "Relative dynamic stability of large synchronous generators" Proc. I.E.E. Vol. 103 C, pp- 234, 1956.

29. M.V. Merrov "Introduction to the dynamics of Automatic regulating of Electrical Machines" Butterworths, London 1951.